# Analyzing FLUENT CFD Models and Data to Develop Fundamental Codes to Assess the Effects of Graphite Oxidation in an HTGR Air Ingress Accident

by

Caroline A. Cochran

B.S., Mechanical Engineering, with honors (2007)
B.A., Economics (2007)
University of Oklahoma



SUBMITTED TO THE DEPARTMENT OF NUCLEAR SCIENCE AND ENGINEERING

IN PARTIAL FULFILLMENT OF THE REQUIREMENTS FOR THE DEGREE OF MASTER OF SCIENCE IN NUCLEAR SCIENCE AND ENGINEERING

AT THE

MASSACHUSETTS INSTITUTE OF TECHNOLOGY

FEBRUARY, 2010



Author.....
Department of Nuclear Science and Engineering
January 15, 2010

Certified by.....
Professor of the Practice of Nuclear Engineering Andrew C. Kadak
Thesis Supervisor

Certified by.....
Professor Emeritus Michael Driscoll
Thesis Reader

Accepted by.....
Professor Jacquelyn Yanch
Chairman, Department Committee on Graduate Students

**Analyzing FLUENT CFD Models and Data to Develop Fundamental Codes to Assess the Effects of Graphite Oxidation in an HTGR Air Ingress Accident**

by

Caroline A. Cochran

Submitted to the Department of Nuclear Engineering on January 15, 2010,
in partial fulfillment of the requirements for the degree of
Master of Science in Nuclear Engineering

## Abstract

The primary product of this thesis is a faster running computer code to model air ingress events in high temperature gas reactors as a potential subroutine for nodal codes such as MELCOR to model air ingress events. Because of limitations found in FLUENT, and the limitations of the data set, a simple model of the effects of graphite oxidation reactions and structures was built in MATLAB code and is described. This code is based on the fundamental understanding of the physical phenomena at work along with common assumptions. The code is subject to typical instabilities inherent in the physical phenomena as well as uncertainties introduced in the numerical methods themselves. Sample results of the code are presented, which show remarkable similarities to the NACOK data considering the simplistic formulas used. The code structure is described in detail. A simplistic MELCOR model is described, which was built to inform the structure of the code, although the source code for MELCOR was not provided to allow integration of the code into MELCOR.

As part of the code development process, the previous MIT work to model air ingress experiments were reviewed to understand the reasons for the portions of apparently non-physical results obtained through past FLUENT models. In addition, a 2-D FLUENT model was created to perform transient analysis which was previously limited to steady state conditions due to the longer computational time required for the 3-D modeling. This model was also created in an effort to compare the results of the previous models using porous media assumptions versus explicitly modeled geometry. Finally, the 2-D model showed valuable steady state results in a much shorter time period than the 3-D model.

Additionally, the data provided by the NACOK experiments is reviewed and assessed with respect to data mining for correlations for potential use in a code or correlations characterizing the effects of graphite oxidation on the HTGR air ingress accident. Attempts were made to use the output of the FLUENT code as "data" for mining since the limited amount of NACOK data made developing correlations difficult. Simple correlations between the data were found. The difficulties for data mining in this project are presented, along with some reflections on the potential for data mining in general, to inform analyses of the graphite oxidation process in air ingress accidents.

# ACKNOWLEDGEMENTS

I gratefully acknowledge Professor Andrew Kadak, who mentored me and provided much of his time to guide this project. Professor Kadak has invaluable intuition in this field, along with incredible patience and consideration when personal or other difficulties arise. This project also owes gratitude to Prof. Buongiorno and Dr. Chang Oh of INL for reading and offering advice. Last, I thank my family for their never-ending support.

# TABLE OF CONTENTS

# LIST OF FIGURES

# LIST OF TABLES

# 1. INTRODUCTION

At a recent Next Generation Nuclear Power Conference (1), the state of air ingress analysis was reviewed. This review illustrated the difficulty of accurate analysis of the effects of air ingress on temperature, graphite corrosion, its effects on the structural integrity of any reactor using graphite as a reflector, and the lack of studies tying these aspects together. High Temperature Gas Reactors (HTGRs) especially require understanding of the effects of a Loss of Coolant Accident (LOCA), since the potential ingress of air could chemically react with the graphite resulting in corrosion and generally exothermic reactions raising the temperature further. The NRC is developing a modified version of MELCOR to analyze accidents in high temperature gas reactors but as yet, comprehensive modeling of air ingress analyses are not available, especially not in any benchmarked industrially applicable or time un-intensive form. Moreover, outside of computation, there is little experimental work and data specific for these accident scenarios to take into account the combined effects of a LOCA in HTGRs. The tests conducted at the Julich Research Institute at the NACOK test facility (2) are two of very few large-scale tests with realistic geometry conditions.

While limited data is available from these tests, the successful implementation of the complex factors affecting the behavior chemical reactions in high temperature gas reactors in any finite-element, multi-physics simulation requires specialized knowledge and intricate model development of a system along with prohibitively high computational requirements.

One of the most advanced computational fluid dynamics/multi-physics code, FLUENT (3), requires transient analysis—as opposed to the simpler steady state analysis-- for any natural convection problems that involve large changes in temperature. Moreover, the maximum allowable time step is dictated by the geometrical constraints of the system and the initial parameters. These geometrical constraints and parameters include the complex geometries of HTGRs, including fuel and reflector zones with long and narrow geometries along with natural convection and complicated species transport parameters and chemical reactions with the graphite. This typically means a maximum time step on the order of 0.001 s, each requiring 5-10

iterations per time step. Thus, any computation of air ingress in a reactor situation is excessively long and not very useful for safety analyses which require many such simulations.

The potential development of benchmarked correlations that can be used in safety analysis software such as MELCOR presents a valuable and significantly more efficient method for reactor analysis, especially for HTGRs.

## 1.1. THESIS OBJECTIVES

The objective of this thesis is first to review the previous MIT work to model air ingress experiments and to understand the reasons for the portions of apparently non-physical results obtained through past FLUENT models. In addition, a 2-D FLUENT model was created to perform transient analysis which was previously limited to steady state conditions due to the longer computational time required for the 3-D modeling. This model was also created in an effort to compare the results of the previous models using porous media assumptions versus explicitly modeled geometry.

Next, the data provided by the NACOK experiments is reviewed and assessed with respect to data mining for correlations for potential use in a code or correlations characterizing the effects of graphite oxidation on the HTGR air ingress accident. Attempts were made to use the output of the FLUENT code as "data" for mining since the limited amount of NACOK data made developing correlations difficult. Simple correlations between the data were found. The difficulties for data mining in this project are presented, along with some reflections on the potential for data mining in general, to inform analyses of the graphite oxidation process in air ingress accidents.

The primary product of this work is a faster running code to model air ingress events as a potential subroutine for nodal codes such as MELCOR. Because of described limitations found in FLUENT, and the limitations of the data set, a simple model of the effects of graphite oxidation reactions and structures was built in MATLAB code and is described. The model code is based on the fundamental understanding of the physical phenomena at work along with common assumptions. The code is subject to the instabilities inherent in the physical phenomena

as well as uncertainties introduced in the numerical methods themselves, although these uncertainties were attempted to be minimized through various improvements on the code iterations and structure. Sample results of the code are presented, which show remarkable similarities to the NACOK data considering the simplistic formulas used. The code structure is described in detail. A simplistic MELCOR model is described, which was built to inform the structure of the code, although the source code for MELCOR was not provided to allow integration of the code into MELCOR.

# 2. Background and General Theory

## 2.1. The Pebble Bed Reactor

The pebble bed modular reactor (PBMR) is a small reactor which utilizes fuel in the form of "pebbles," or spheres, and the Brayton gas cycle as opposed to the steam cycle in order to produce electricity. The reactor is operated at higher temperatures than light water reactors, at design temperatures ranging from 540C in the cold leg to 900C in the hot leg. The design is known for high cycle efficiencies at greater than 41% (4), producing 400 MWth and greater than 165 MWe. The advantages of the reactor and fuel type include increased proliferation resistance, higher efficiencies and burnup, and "passive safety." Figure 2-1 shows a cross-section of the PBMR core.

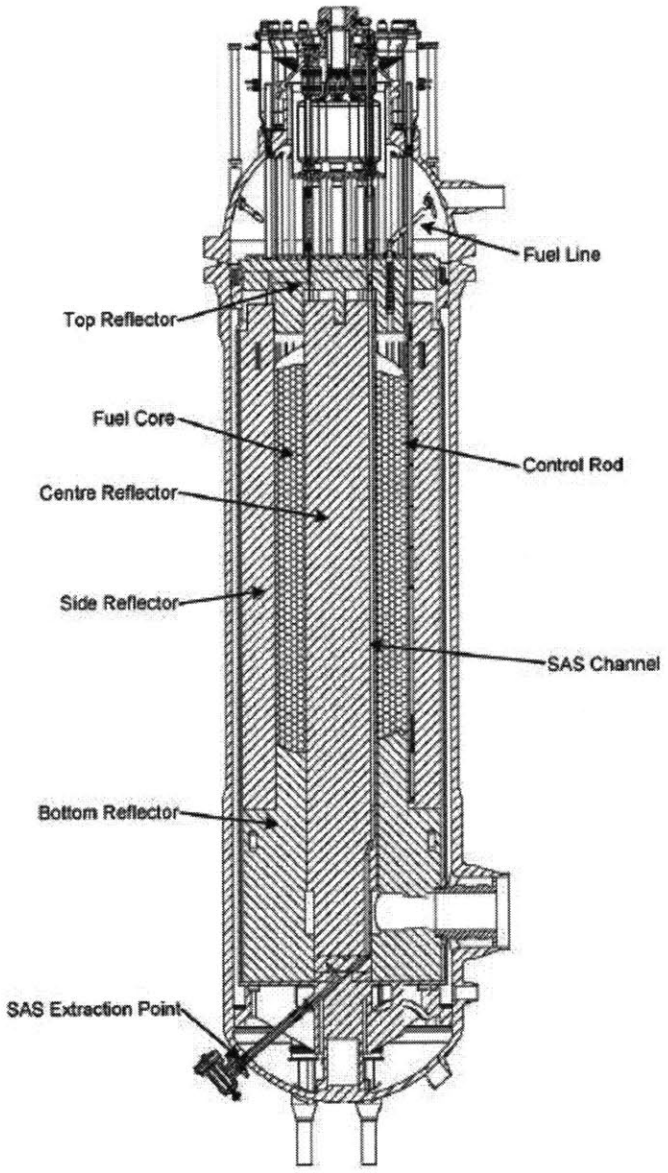


FIGURE 2-1: PBMR REACTOR CORE CROSS-SECTION (5)

The fuel for the PBMR is the TRISO-coated particle fuel, shown in Figure 2-2.

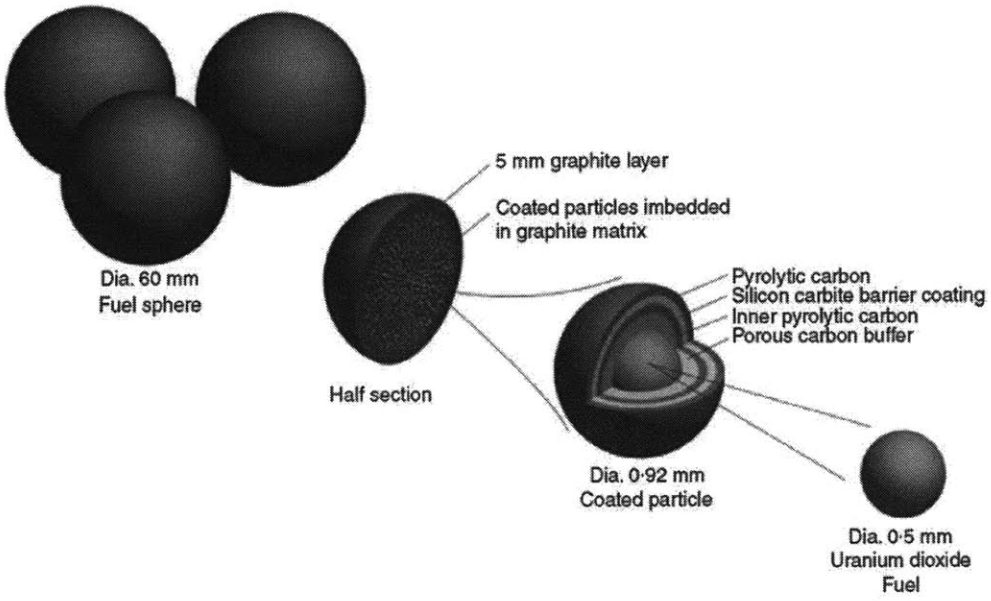


FIGURE 2-2: TRISO-COATED FUEL SPHERE LAYERS (6)

## 2.2. THE AIR INGRESS ACCIDENT IN THE PBMR

The air ingress problem is a complicated phenomenon, with many co-dependent variables and geometrical considerations affecting accident progression. For instance, diffusion, followed by buoyancy and natural convection are the drivers for flow. However, buoyancy depends directly on temperatures, specifically temperature differences with height. Once air reaches the graphite, there are several chemical reactions possible which depend on temperature. The chemical reactions themselves then generate heat which in turn can create complicated flow and temperature differences from the surface to the bulk of the air. These flow and temperature differences both depend on and affect the natural convection, buoyancy, and therefore the bulk mass flow rate of air. The amount of air flow can both limit the reactions, by bringing cooling air, as well as increase the reactions by supplying more air to react with the graphite. The properties of air, such as heat capacity, density, and viscosity, also depend highly on temperature. Humidity complicates the reactions even further. Additionally, the properties of graphite are highly variable depending on the type of graphite used which significantly affects the corrosion rate and resulting temperature impacts (7). There are also significant uncertainties and variations of graphite corrosion rates.

Changes in viscosity have been shown to significantly slow the potential velocity of air with increasing temperature in these experiments. Radiative heat transfer in the core becomes more significant the higher the temperature. Radiative heat transfer is generally neglected in most models because of its geometry dependence and the narrow absorption frequency bands in case of gases, which make blackbody or even "grey" assumptions difficult. Treatment of radiative heat transfer does not lend itself to the porous assumption generally required to make pebble bed calculations reasonable. Moreover, radiation heat transfer within air and from solids to air are complicated by the fact that air is not transparent or a solid, but rather has complicated spectrums of absorption for each of its components.

All of these factors point to the impossibility of a non-iterative calculation of outcome for air ingress accidents without significant amounts of benchmarked data. These complications also highlight the previously mentioned requirement of very small time steps for any model, as well as the need for a very well designed mesh to avoid divergence in results. The demands on the mesh are heightened for modeling an experiment performed at large scale such as the NACOK experiments- with overall geometries spanning 0.3m by 0.3m and on the order of 5m high, while having channels with radii as small as 0.008m. The net effect is that complicated computational fluid dynamics models will require large computational capabilities and long computational times. The motivation of this thesis is to develop benchmarked simpler algorithms allowing for a more useful tool for accident and transient analysis.

## 2.3. THEORY GOVERNING THE OVERALL AIR INGRESS ACCIDENT

According to German research, the air ingress loss of coolant accident has several stages (2). First, there is a rapid depressurization characterized by the helium coolant exiting the pressure vessel into the containment until the pressure equalizes with that of the containment. Second, the air in the containment begins to slowly diffuse into the reactor, which can be characterized by well-established information on multi-component diffusion. This process from diffusion before the onset of natural convection is estimated by different research to take between hours and many days (2)(8). The time required for diffusion of air into the reactor is highly dependent on the location and orientation of the break (9). Angled breaks at the top of the

vessel are the most dangerous for allowing air ingress, compared to the best case of a purely horizontal break at the bottom of the vessel. Generally, a worst case scenario of a double-guillotine break is assumed in either an inlet or outlet pipe which would cause a true chimney effect by creating a hot leg and cold leg configuration. Third, the pressure vessel goes through periodic "breathing" episodes, wherein the helium contracts due to cooling of the air, drawing air in, and expands back out upon being reheated by the hot pressure vessel materials and decay heat. At some point, the air comes in contact with the graphite and reacts, creating more heat and therefore buoyancy. Fourth, onset of natural convection is reached, which is the flow of air through the reactor. Lastly, this process can reach a steady state should the amount of heat generated by the chemical reactions and decay heat match that removed by the reactor vessel due to either air entering or reactor vessel heat transfer. Over the long term such as weeks, the reactor will cool down as a result of the reduced decay heat from the core.

Most theories regarding stages of air ingress accidents include the depressurization, followed by diffusion, and onset of natural circulation. However, studies done at INL have shown that the process can occur much faster than assumed when considering diffusion alone, due to stratified flow(8). Stratified flow is the concept that some air may be entering in one direction, on a lower layer, while hotter air may be exiting on another, higher layer. This was likewise confirmed by the 2D FLUENT model, discussed in Section 6.2.

## 2.4. Diffusion, Buoyancy and Natural Circulation

The flow in an air ingress accident is first dominated by pressure differences between the reactor primary system and the containment, but is afterwards dominated by a combination of diffusion and buoyancy, which lead to an overall flow condition called natural circulation.

Gaseous diffusion is a slow process which takes place through the random motion of particles of two or more species through a concentration difference. Diffusion is well characterized by experimentally determined diffusion coefficients and is generally modeled using Fick's laws. The one-dimensional form of Fick's law is given below in Equation 2-1 (10).

$$J = -D \cdot \frac{\delta c}{\delta x}$$

2-1

Where

$J$ = the total flux of the species over an area

$D$ = the diffusion coefficient

$\frac{\delta c}{\delta x}$ = the change in concentration, c, with the change in distance, x.

Buoyancy and natural circulation are driven by density differences in a fluid. The effects of buoyancy can be derived using the concepts of conservation of momentum together with the force of gravity. The fundamental equations used for momentum are the Navier-Stokes equations:

$$\rho \cdot \frac{d\vec{u}}{dt} = -\nabla p + \rho \cdot \vec{g} + \mu \cdot \nabla^2 \vec{u}$$

2-2

Where $\rho$ is the density of the fluid in question, $\vec{u}$ is the velocity, $p$ is the pressure, $\vec{g}$ is the gravitational acceleration, and $\mu$ is the molecular viscosity, which is assumed constant in this formulation. Neglecting the molecular viscosity term, this equation becomes the Euler equations of motion (11). These are frequently written using $\rho = \rho_o + \rho'$ and $p = p_o + p'$, so that the Eulerian equations of motion become:

$$\rho \cdot \frac{d\vec{u}}{dt} = -\nabla p' + \rho' \cdot \vec{g}$$

2-3

The Boussinesq approximation is then frequently made in the case of a non-compressible flow with low velocity, which asserts that the change in density within a small layer is negligible, such

that $\rho = \rho_o$ for the left side of the equation. The Eulerian equation with the Boussinesq approximation then becomes:

$$\frac{d\vec{u}}{dt} = -\frac{\nabla p'}{\rho_o} + \frac{\rho'}{\rho_o} \cdot \vec{g}$$

2-4

## 2.5. CHEMICAL REACTIONS

Rate constants for chemical reactions are commonly formulated in the Arrhenius form:

$$k = A \cdot e^{-\frac{E}{R \cdot T}}$$

2-5

where k is the reaction rate coefficient and A is the rate constant, which have consistent units depending on the order of the reaction, E is the activation energy, R is the gas constant, and T is the temperature in Kelvin.

The order of a reaction is the power to which a reactant is raised in the rate equation. For instance, for the reaction of oxygen with graphite to produce carbon dioxide, the reaction could be given as

$$2 \cdot C + O_2 \rightarrow 2 \cdot CO$$

2-6

And the rate equation would take the form

$$r = k \cdot [C]^m \cdot [O_2]^n$$

2-7

where m represents the order of reaction with respect to C and n represents the order of reaction with respect to O2. Primarily, the order of reaction is determined experimentally. While it frequently takes an integer value, the value can take on a range of values. For the graphite oxidation reaction, the order of reaction with respect to oxygen ranges between 0 and 1 (12)(13)

The order of reaction determines the units taken by k, and requires particular attention. Reaction rates are generally given in units of mol/L and rate constants "k" must have units consistent with the units for the other terms in the rate equation. For a zero order reaction, the reaction k takes the units mol/L*time; for a first order reaction, the units of k are 1/time; and for a second-order reaction the units of k are L/mol*time (14). The literal meaning of a zero-order reaction with respect to an element is that the reaction is independent of the concentration of that element. For a first order reaction with respect to an element, the reaction is dependent only on the concentration of the element. It follows that the graphite oxidation reaction would be zero order with respect to carbon because the graphite is plentiful compared to the amount of oxygen. In this case, the order of reaction would depend primarily on the concentration of oxygen since it is the primary reactant. However, it also makes sense that the concentrations of other species in air could prevent unobstructed diffusion of oxygen to the graphite surface. Also CO and $CO_2$ present competing reactions with graphite oxidation in the form of carbon monoxide oxidation and the Boudouard reactions. Thus, the graphite oxidation reaction is typically found to be between 0 and 1 with respect to oxygen.

The chemical reactions occurring in the air ingress accident include the graphite oxidation to either carbon monoxide or carbon dioxide, the Boudouard reaction converting $CO_2$ to C and CO or vice versa, and the reaction of CO with $O_2$ to produce $CO_2$. While the Boudouard and graphite oxidation reactions are dependent on surface area of the graphite, the reaction of CO and $O_2$ is a volumetric reaction.

The fundamental reaction mechanisms for the reaction of carbon with oxygen are still being established, with differing theories for whether oxygen first reacts to form CO or CO2, with the other being a secondary reaction, or if each is a separate primary reaction (15). In the literature, and as used in previous studies, the graphite oxidation reaction is grouped as one reaction, and the ratio of CO to CO2 produced is given a separate temperature dependent formula. Please see Equation 9-7 in Section 9.1 for discussion on this ratio.

Table 2-1 lists some of the reaction constants for the reactions involved in the air ingress accident. Figure 2-3 and Figure 2-4 show the absolute value of the heat generated by reactions in

absolute value on a log scale, given a sample reflector surface area and air volume. The reflector used was the same as used on the 2nd and 3rd levels of the NACOK experiments, and the values used for the reactions are the same as shown in Table 2-1 and discussed in more detail in Section 9.1 for the use in the nodal code. These figures show how dramatically more important the carbon oxidation reaction is as compared to the other reactions, and why the water reaction can be safely neglected for our analysis purposes.

TABLE 2-1: REACTIONS AND CHEMICAL RATE CONSTANTS AND ENERGIES

| Reaction | Rate constant (A) | Activation energy (E) |
|---|---|---|
| O + C | 7,943 | 78,300 |
| CO2+C | 2,220 | 30,635 |
| CO+O2 | 1.3*10^8 | 126,000 |

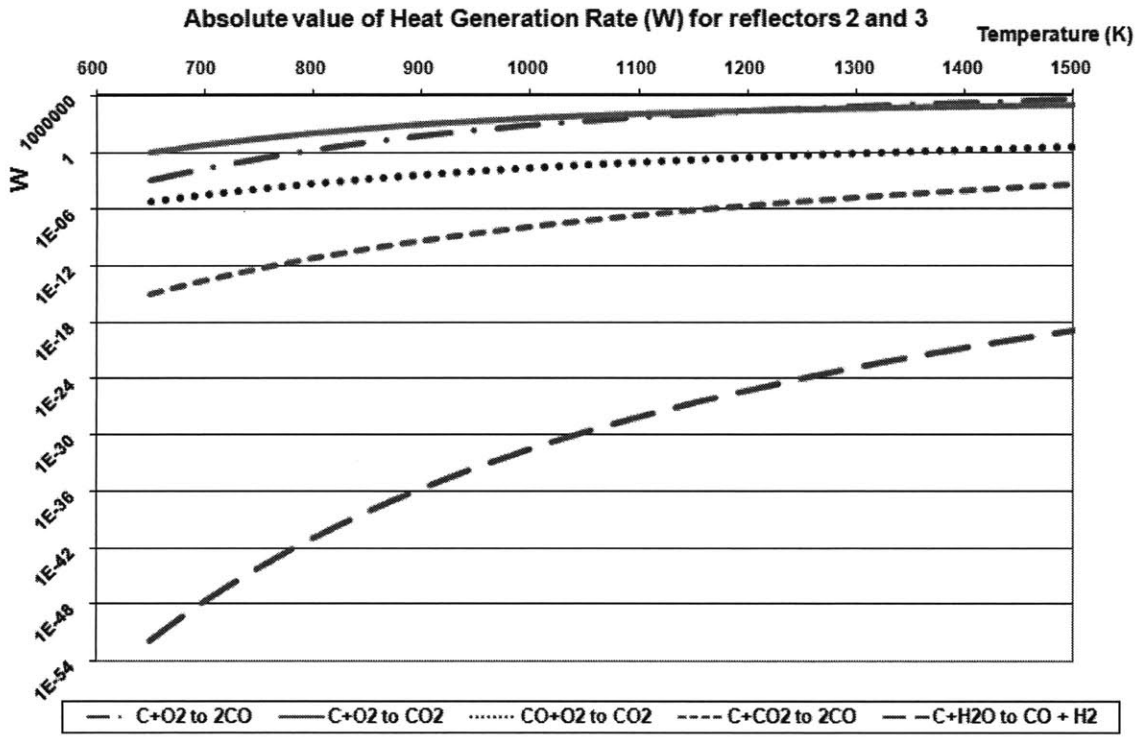


FIGURE 2-3: ABSOLUTE VALUE OF HEAT GENERATION BY CHEMICAL REACTION FOR A SAMPLE REFLECTOR GEOMETRY, INCLUDING THE WATER REACTION

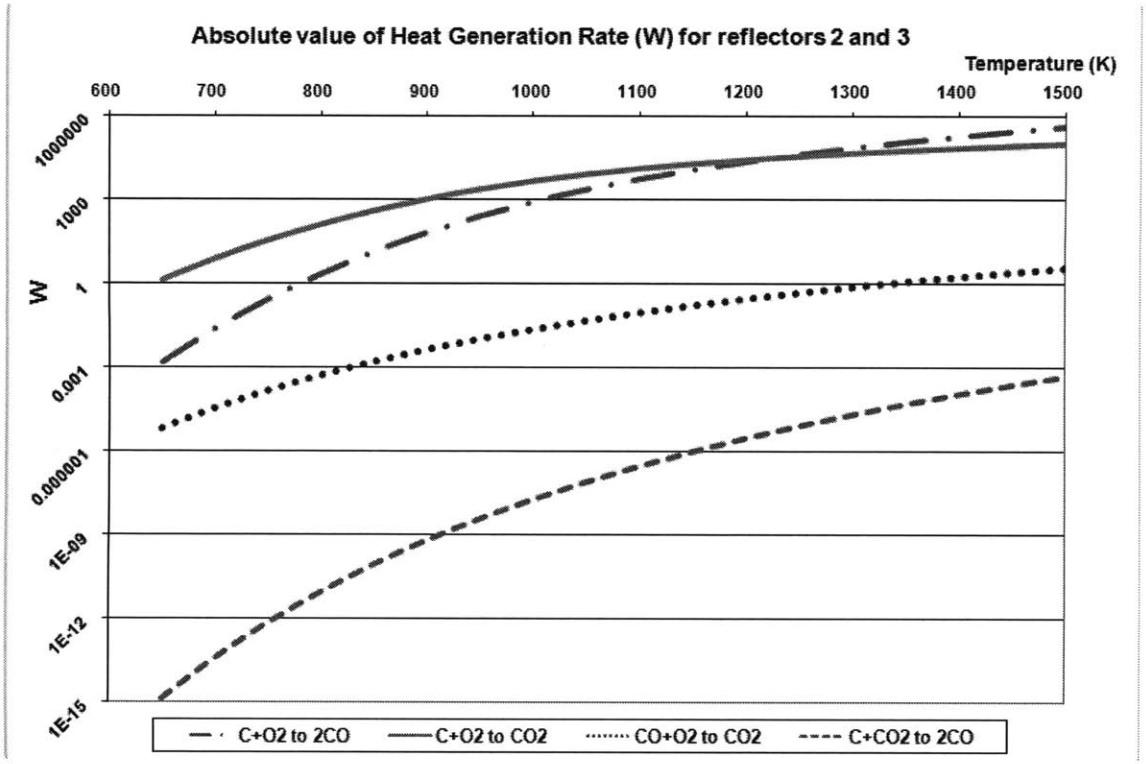


FIGURE 2-4: ABSOLUTE VALUE OF HEAT GENERATION BY CHEMICAL REACTION FOR A SAMPLE REFLECTOR GEOMETRY, NOT INCLUDING THE WATER REACTION

Finally, the kinetics of graphite corrosion follow different regimes depending primarily on temperature. Three primary regimes have been outlined clearly by Moormann et al (16) (17) and are shown graphically in Figure 2-5.

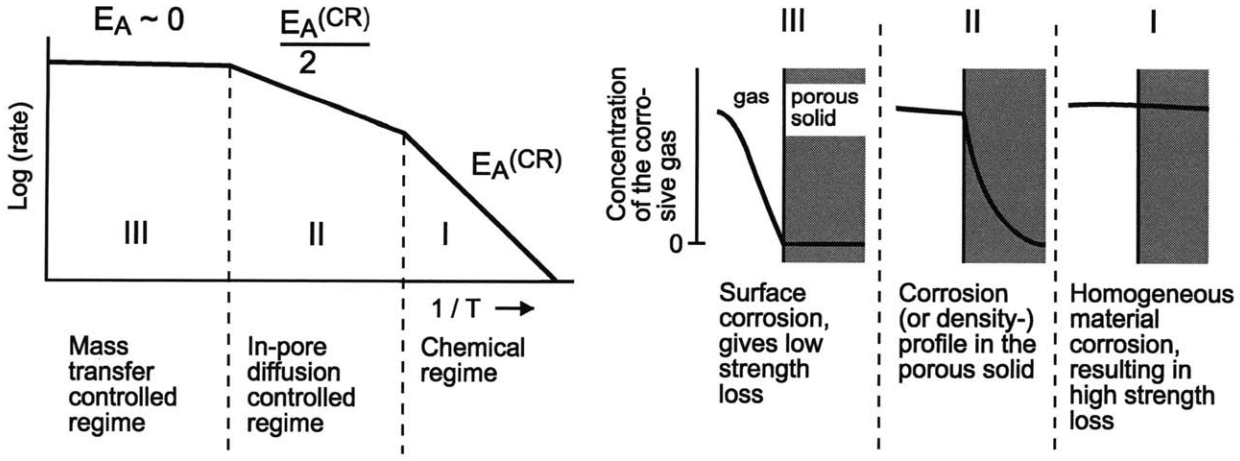


FIGURE 2-5: GRAPHITE CORROSION REGIMES AND EFFECTS ON REACTION RATES (17)

The regime at the lowest temperature corresponds to the chemical regime. While the reaction rates are lowest in this regime, the oxygen is able to diffuse through the graphite and corrode, causing high strength loss. The limiting factor is the chemical reaction kinetics alone. At higher temperatures, the reaction takes place more quickly, corresponding to an activation energy of roughly half that in regime I. The amount of diffusion is limited by the higher rate of reaction, so it is said to be in-pore diffusion limited. In regime III, the reaction has an effective activation energy of zero and the reaction occurs as quickly as the oxygen comes in contact with the graphite. Thus, regime III is mass transfer controlled.

### 2.6. COMPLICATING FACTORS

Common assumptions such as neglecting heat transfer by radiation, assuming ideal gases, bulk temperatures, assuming constant values such as reaction parameters and material properties or neglecting graphite corrosion regimes may strongly affect accurate modeling of the air ingress experiment. In addition, attention must be paid to the graphite corrosion regime and the effect of burnoff on reaction rates. In the case of the FLUENT modeling, the effects of water vapor, radiation, and burnoff have been neglected. However, as described in Section 5, the FLUENT models' results matched closely to the data with these assumptions. The 1-D MATLAB code includes simple accommodations for effects of water vapor on air properties, including: density and specific heat, as well as increase in surface area due to burnoff, and radiative heat transfer, described in section 0.

## 3. OVERVIEW OF AIR INGRESS EXPERIMENTS

### 3.1. JAERI EXPERIMENTS OF EARLY 1990'S AND KUHLMANN NACOK EXPERIMENTS OF 1999

Several key experiments in recent decades have impacted understanding of the air ingress accident for high temperature gas reactors. Among these are the experiments done by Takeda and Hishida at JAERI (13), and those performed at the NACOK (Naturzug im Core mit

Korrosion) facility in Germany. MIT began work on CFD modeling of air ingress experiments with the work by Tieliang Zhai and Andrew Kadak characterizing the JAERI experiments of the early 1990s and the NACOK experiments by Kuhlmann in 1999 (16). The JAERI experiments were small scale U-tube experiments which included an experiment examining diffusion and onset of natural convection using two components of nitrogen and helium, and then assessed multicomponent effects of air ingress including diffusion, natural circulation, and chemical reactions as a result of adding a graphite column portion to the first experimental setup (17)(13). Figure 3-1 and Figure 3-2 show the JAERI experimental setups. These experiments were focused on a prismatic geometry, characterized by flow through fuel channels, while the NACOK experiments were oriented toward the pebble bed reactors setup, which is characterized by flow through fuel pebbles. However, both utilized double-guillotine break assumptions and approximations of upside down U geometry with experimental "hot-" and "cold-leg" flow paths representing the hot reactor interior and the outlet, respectively. Kuhlmann's work similarly addressed air ingress through experiments on the effect of helium on air ingress, the onset of natural convection and the rates of mass flow in a heated column, and the impact of different amounts of helium on mass flow (16). Kuhlmann then performed large scale experiments at NACOK with an experimental setup closer to an actual possible air ingress event as shown in Figure 3-3. The first of the two main experiments performed involved varying temperatures of the hot leg and cold leg and assessing the effects of temperature and geometry on mass flow through ceramic pebbles. Kuhlmann finally applied these results to a second experiment incorporating chemical reactions in a graphite pebble bed.

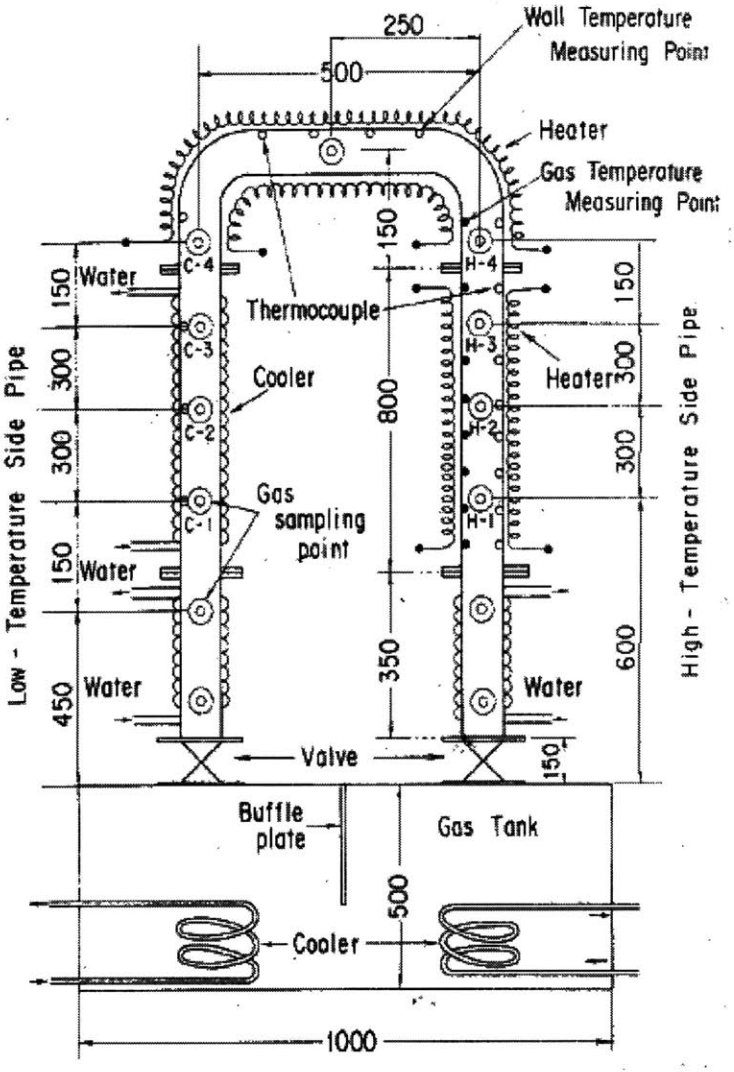


FIGURE 3-1: JAERI N-HE DIFFUSION EXPERIMENTAL SETUP (DIMENSIONS IN MM)

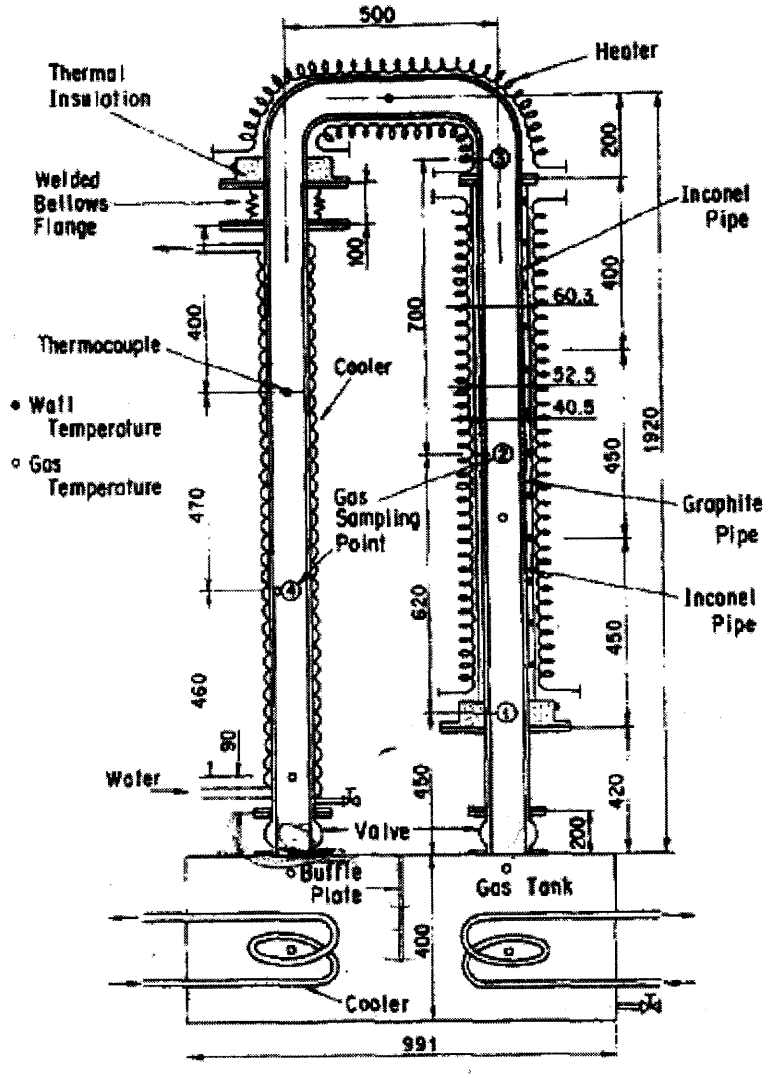


FIGURE 3-2: JAERI MULTI-COMPONENT EXPERIMENTAL SETUP (DIMENSIONS IN MM)

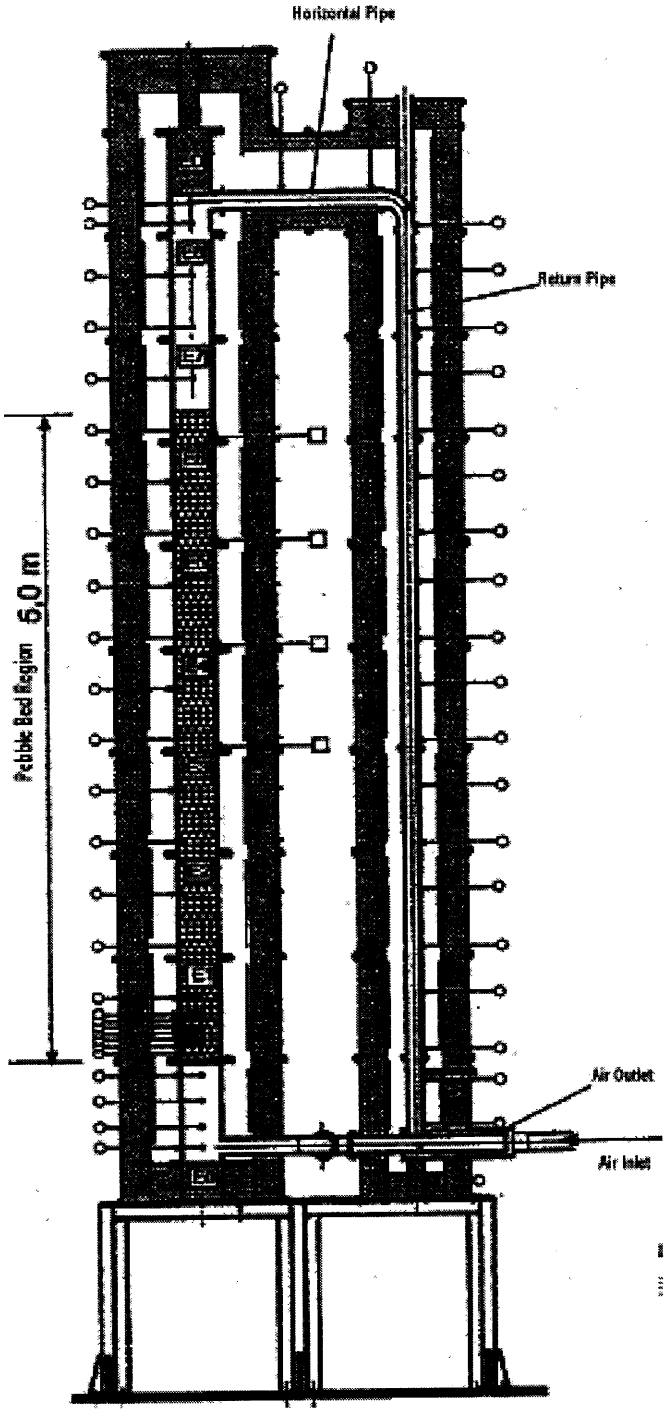


FIGURE 3-3: NACOK EXPERIMENTAL SETUP

Zhai (7) utilized three 3D FLUENT models to benchmark the JAERI He-N diffusion test, the JAERI multi-component test, and the NACOK ceramic pebble test. The first two were run as

transient simulations, with the second as a multicomponent model with chemical reactions in the graphite tube portion. The NACOK model was run as a steady state simulation with porous media approximations for the large ceramic pebble area. These models proved to have good agreement to the experimental data as measured by certain parameters such as time for diffusion of nitrogen in the JAERI tests and ceramic pebble bed temperature versus mass flow rate in the NACOK test. FLUENT has been proven to be extremely accurate especially for use of two component diffusion and for flow and heat transfer scenarios which can be assumed to show steady state behavior. In addition, the FLUENT porous media approximation shows excellent agreement when applied appropriately, e.g. where there are not significant time-dependent effects and disparities in temperature of the fluid and solid in question.

## 3.2. NACOK Experiments of 2004

Based on the previous experiments, additional experiments at NACOK were performed in 2004 to gain better understanding of the air ingress processes in pebble bed reactors by utilizing more realistic pebble bed geometries, including multiple levels of graphite reflectors with different channel dimensions and multiple layers of pebbles. Experiments were performed with a simple open chimney and including a return cold leg.

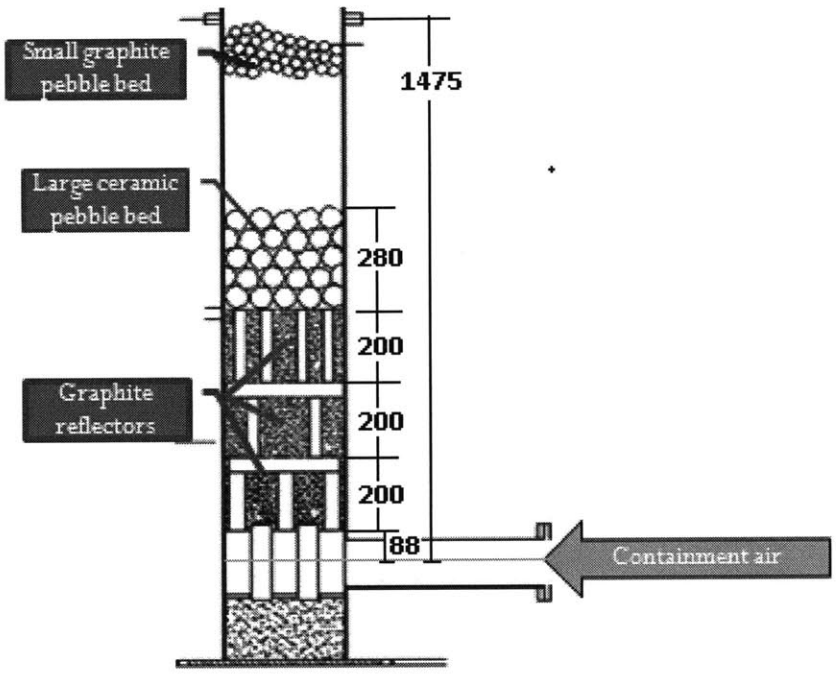


FIGURE 3-4: NACOK OPEN AND RETURN CHIMNEY HOT LEG SCHEMATIC (DIMENSIONS IN MM)

Figure 3-4 shows a simplified schematic of the open and return chimney set up, which were similar. In the actual set up, the chimney extends upwards past the topmost pebble bed at 1.2m by about 5m. The return leg drawing is far more complex as the chimney not only extends many meters above the pebble bed but also connects horizontally to the equally tall return leg. Figure 3-6 shows a cutout of the drawing for the NACOK return leg experiment.

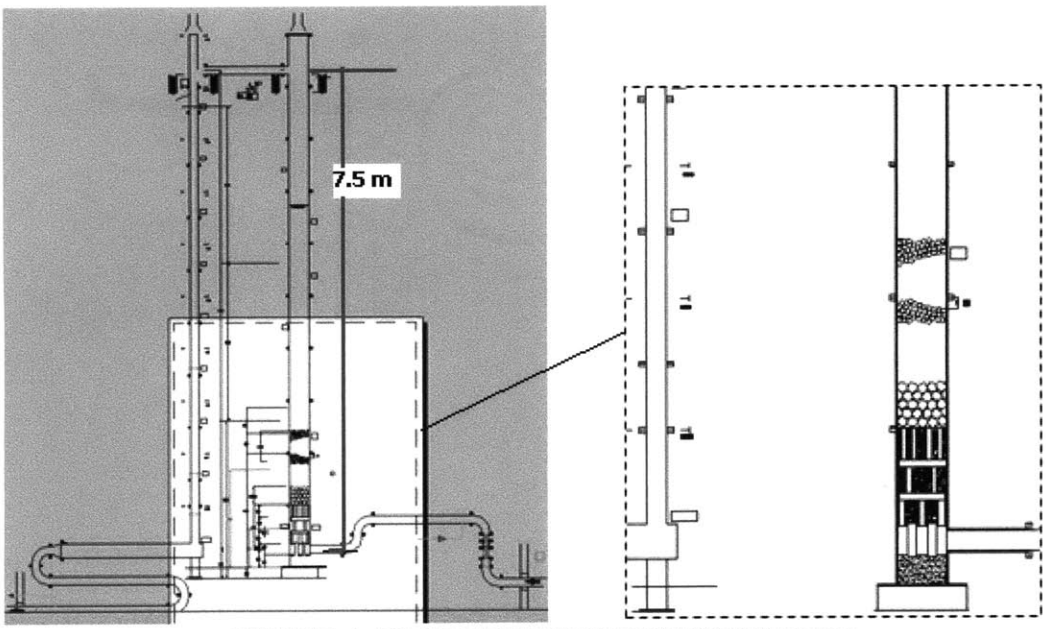

FIGURE 3-5: NACOK RETURN CHIMNEY SCHEMATIC

For both the open chimney and hot and cold leg experiments, the interior was flushed with hot nitrogen and the walls were electrically heated to a set temperature through the experiment. Air at atmospheric pressure and ambient temperature then flowed through the experimental setup and then reacted with the graphite to heat up the air and graphite. Species and temperature data were taken at certain points in the experiment apparatus over time. The open chimney experiment was run for approximately 8 hours. The return chimney was run for approximately 20 hours, however after about 4 hours, the reactions and heat produced became out of control and the initial set wall temperatures had to be lowered. Both the open and the return chimney had the same plan for gas sensors, shown in Figure 3-7.

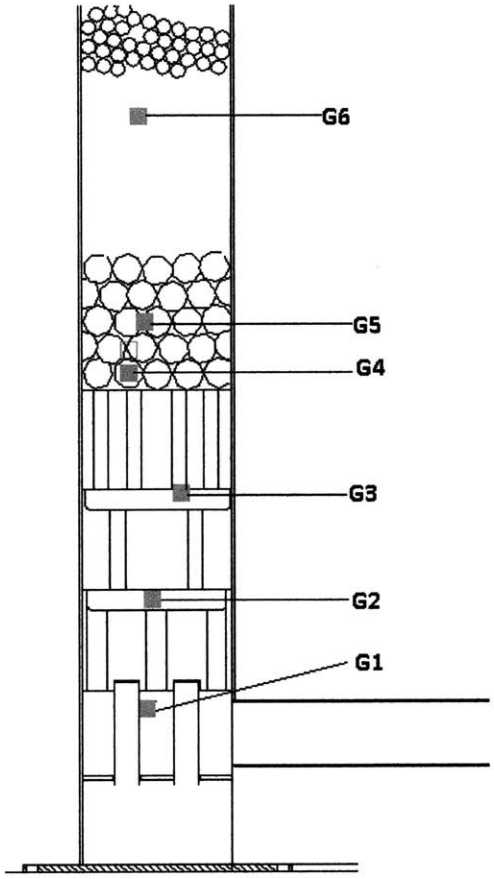


FIGURE 3-7: GAS SENSOR LOCATIONS IN OPEN AND RETURN CHIMNEY EXPERIMENTS

### 3.2.1. OPEN CHIMNEY EXPERIMENT

For the open chimney experiment, as described above, the walls were electrically heated to 650C and the chamber was flushed with hot nitrogen. Then the valve was opened, and atmospheric air began to flow through the chimney reflectors and pebbles. Temperature sensors, denoted with the prefix "R," were used for the outer walls to monitor the temperature to be sure the heaters maintained the minimum 650C through the experiment. The thermocouple locations are given in Figure 3-8, which shows both the regulatory temperature sensors and regular thermocouples.

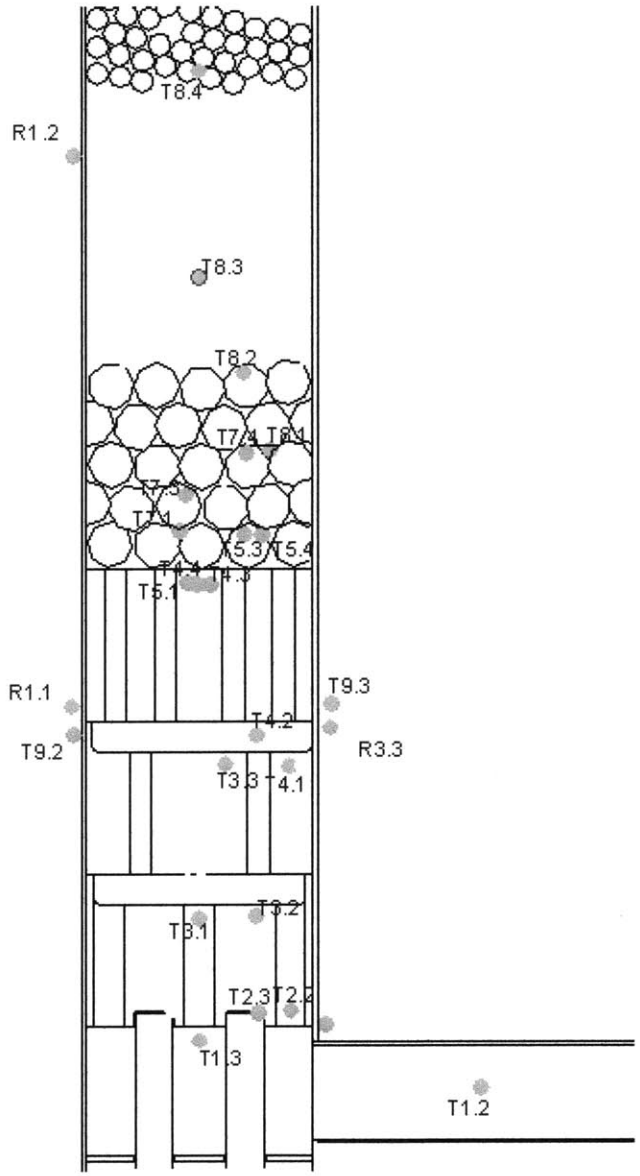


FIGURE 3-8: OPEN CHIMNEY THERMOCOUPLE LOCATIONS

The lowest interior portions are composed of three layers of reflector blocks, supported by four graphite columns. These reflectors are made of ASR-1RS graphite, which has similar properties to IG-110 graphite used in Japan (18). The first layer of graphite blocks is composed of two blocks, shown in Figure 3-9, each with six cross-drilled channels of 40mm diameter each. The second and third layers each have two blocks, shown in Figure 3-10. The third layer blocks

are placed with an orientation 90 degrees rotated about the vertical axis relative to the blocks of the second layer. Each block has 48 channels of 16mm diameter each.

FIGURE 3-9: ONE OF TWO FIRST LAYER GRAPHITE BLOCKS

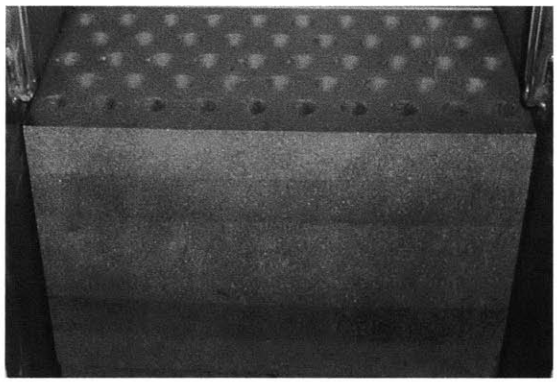

FIGURE 3-10: ONE OF FOUR SECOND AND THIRD LAYER GRAPHITE BLOCKS

Above the reflectors are two pebble regions. The lowest is directly above the third layer of reflectors, and the highest is separated from the first by an empty space. Both pebbles are made of A3-3 graphite (18). The lower pebble bed is made of larger diameter pebbles at 60mm, and the higher pebble bed is made of smaller diameter pebbles at 10mm diameter.

### 2.2.2 RETURN CHIMNEY EXPERIMENT

This experiment is analogous to the open chimney experiment, except that instead of venting the air directly above the pebble bed, the vent at the top is closed and the air passes through the connecting pipe to the cold leg. The connecting pipe at the top of the cold leg was held to a cooler temperature of between 175C and 200C (18).

In the experimental procedure, the heating elements heat the hot leg to a minimum 850C and instead of nitrogen, the chamber is filled with helium. The air flow was then initiated with an equalized pressure to atmospheric. The flow rate was at a lower constant value than the open chimney as shown in Figure 4-11 versus Figure 4-13 for the open chimney.

# 4. THE 2004 NACOK EXPERIMENTS- REVIEW OF DATA RECEIVED

## 4.1. THE OPEN CHIMNEY DATA RECEIVED

The data received for the open chimney experiment included gas species data for helium, oxygen, carbon monoxide and carbon dioxide with time at 9 different vertical locations. The 650 degree C open chimney experiment was run for approximately 8 hours, between 13:09 and 21:09 on 3/10/2004. However, the available data was apparently not taken consistently over this time period. The times of data available at a location may be only for a few hours, while the data on another location may be available in spotty intervals through the full duration of the experiment. Moreover, the data points taken for one species at a location may not start at a similar time or last for a similar duration as the data points taken for another species at the same location. Figure 3-7 illustrates the 6 lower gas sensor locations for the open chimney experiment with respect to the geometry. Figure 4-1, Figure 4-2, and Figure 4-3 show data for the species volume fractions for the 7 most useful gas detector locations. In an ideal gas, the volume fraction is equivalent to a molar fraction and is given by the following:

$$Volume\ fraction = molar\ fraction = \frac{number\ of\ moles\ of\ species\ i}{total\ number\ of\ moles\ of\ all\ species} \qquad 4\text{-}1$$

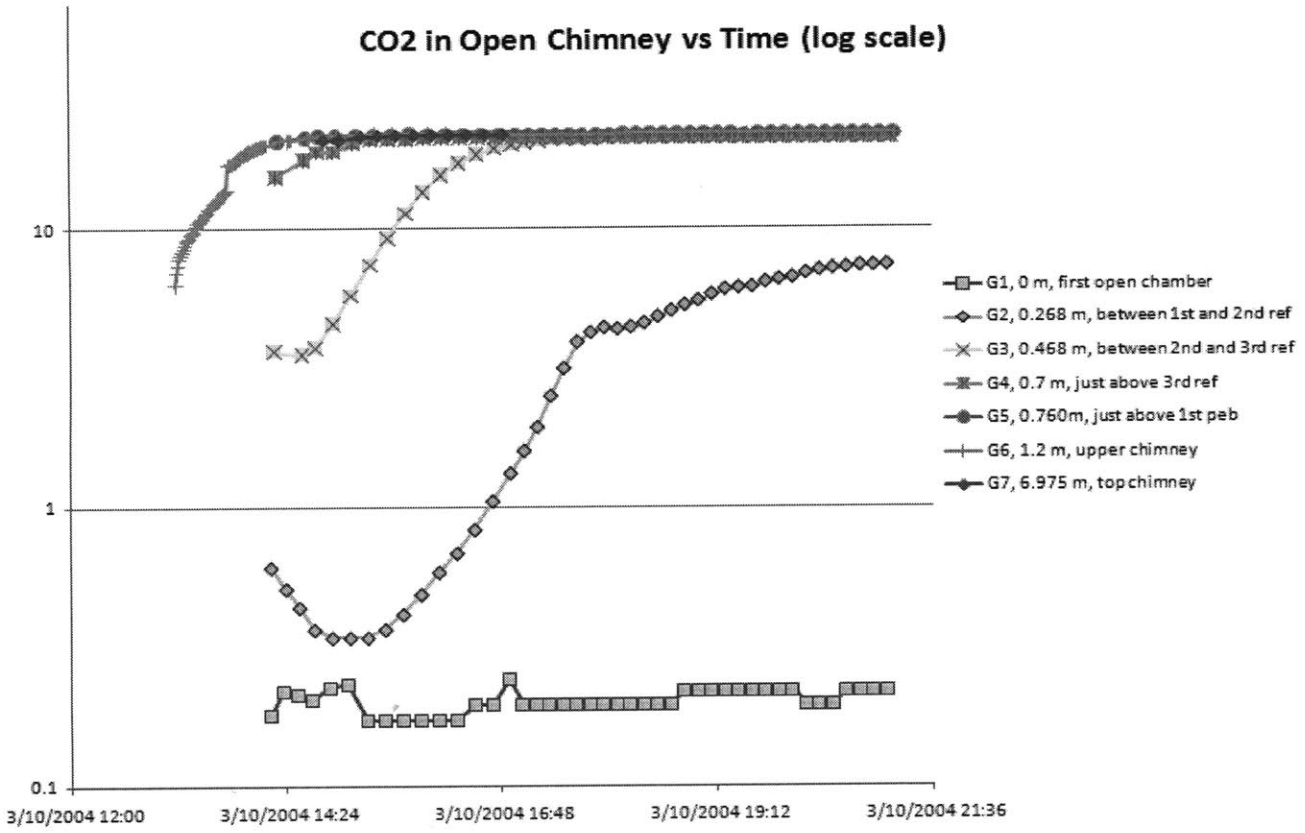


FIGURE 4-1: $CO_2$ VOLUME FRACTION IN OPEN CHIMNEY EXPERIMENT

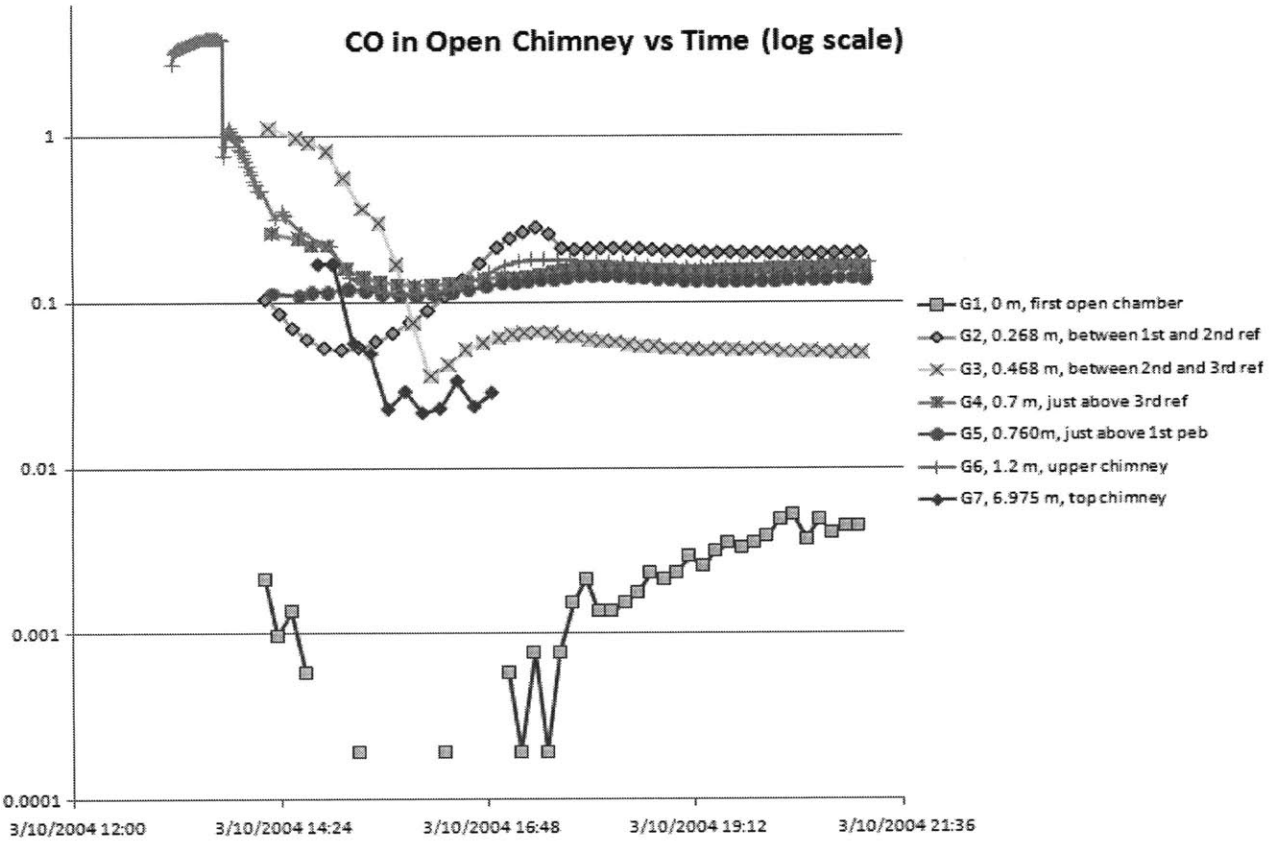


FIGURE 4-2: CO VOLUME FRACTION IN OPEN CHIMNEY EXPERIMENT

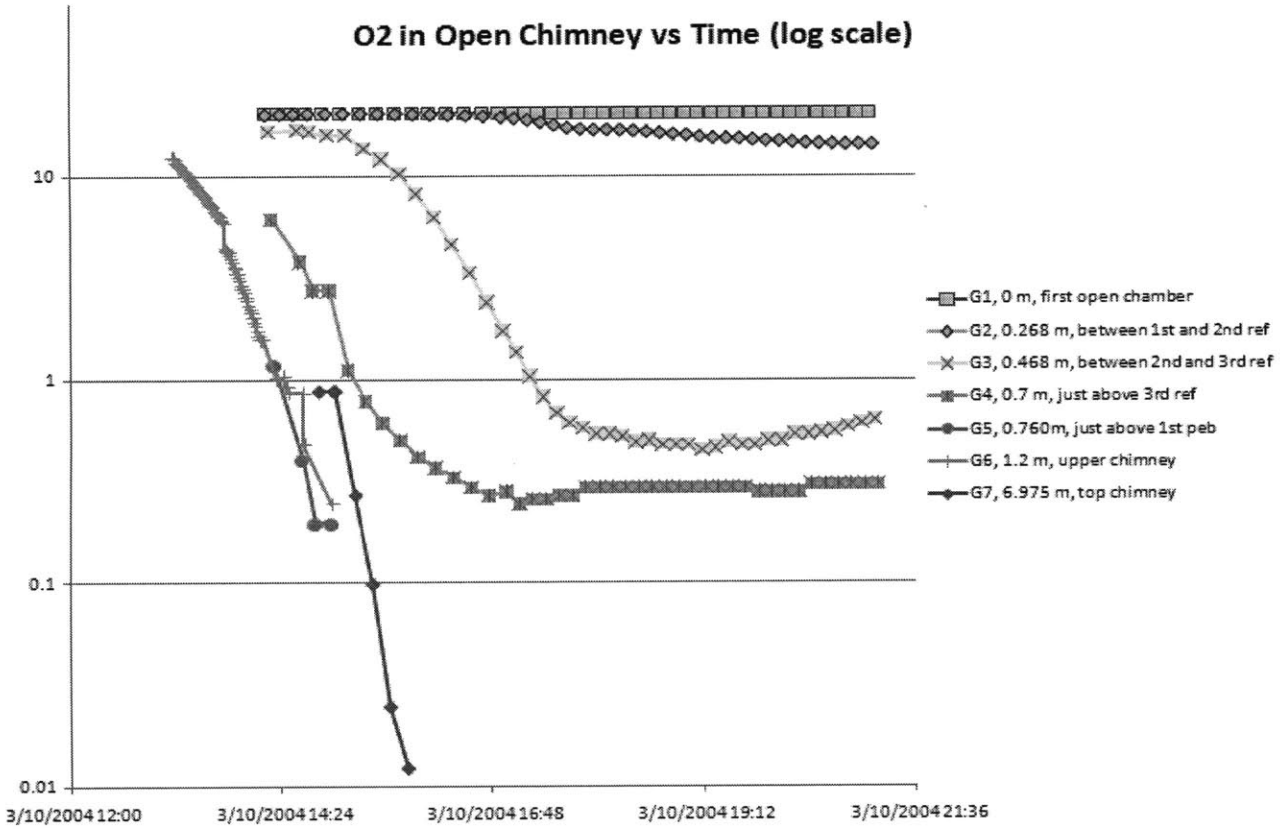


FIGURE 4-3: $O_2$ VOLUME FRACTION IN OPEN CHIMNEY EXPERIMENT

In Figure 4-1 and Figure 4-3, CO2 clearly increases while O2 clearly decreases, respectively, for the duration of the experiment in all locations. This is evidence of the graphite oxidation taking place. The amount of carbon monoxide, shown in Figure 4-2, is less clearly demonstrative of graphite oxidation because the relative amount of carbon monoxide produced in the graphite oxidation reaction is much smaller than for carbon dioxide for the temperatures experienced in the experiment. Moreover, the Boudouard reaction favors consumption of CO and CO2 production under about 850C, while above this temperature, the reaction produces CO. Only above about 1000C does the much more significant graphite oxidation reaction favor the production of carbon monoxide over carbon dioxide (as shown in Figure 2-4), which is significantly higher than the maximum temperature reached in this experiment.

For the open chimney, the temperatures with time were never acquired, and were apparently lost due to an error in the experiment computers. Likewise, mass flow and density data were lost for

the open chimney experiment. However, an operator's log taken during the experiment was provided, which includes the German operator's abbreviated notes and occasional screen captures of the computer's readings at random points in the experiment. Thus replicating these experiments using computer simulations based on the available data is difficult. Ultimately, temperatures from these log screen captures were used to compare temperatures. The following chart shows the data from the control temperature sensors.

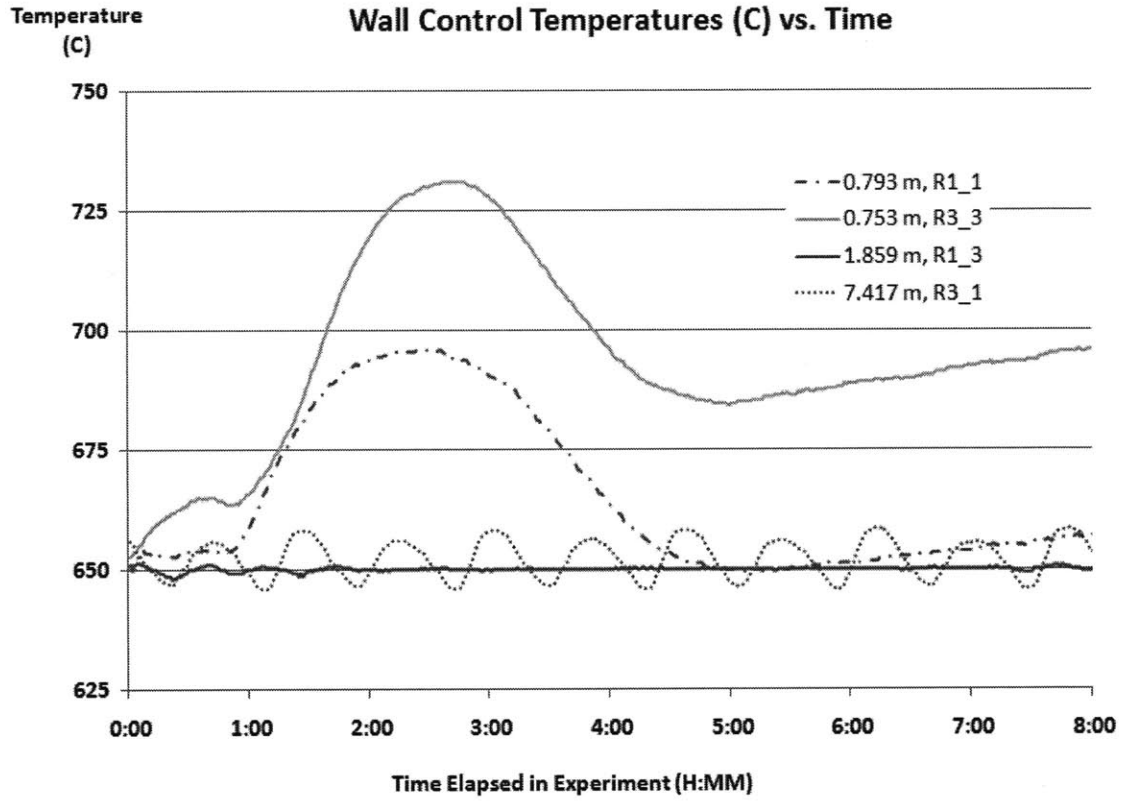


FIGURE 4-4: OPEN CHIMNEY WALL CONTROL TEMPERATURE SENSORS

As can be seen in Figure 4-4, the lower sensors around 0.75-0.80 m. heights, R1_1 and R3_3, experienced enough heat to increase the temperature of the walls significantly above the 650C minimum set temperature. Figure 3-8 shows the locations of the temperature sensors in the open chimney experiment with respect to geometry.

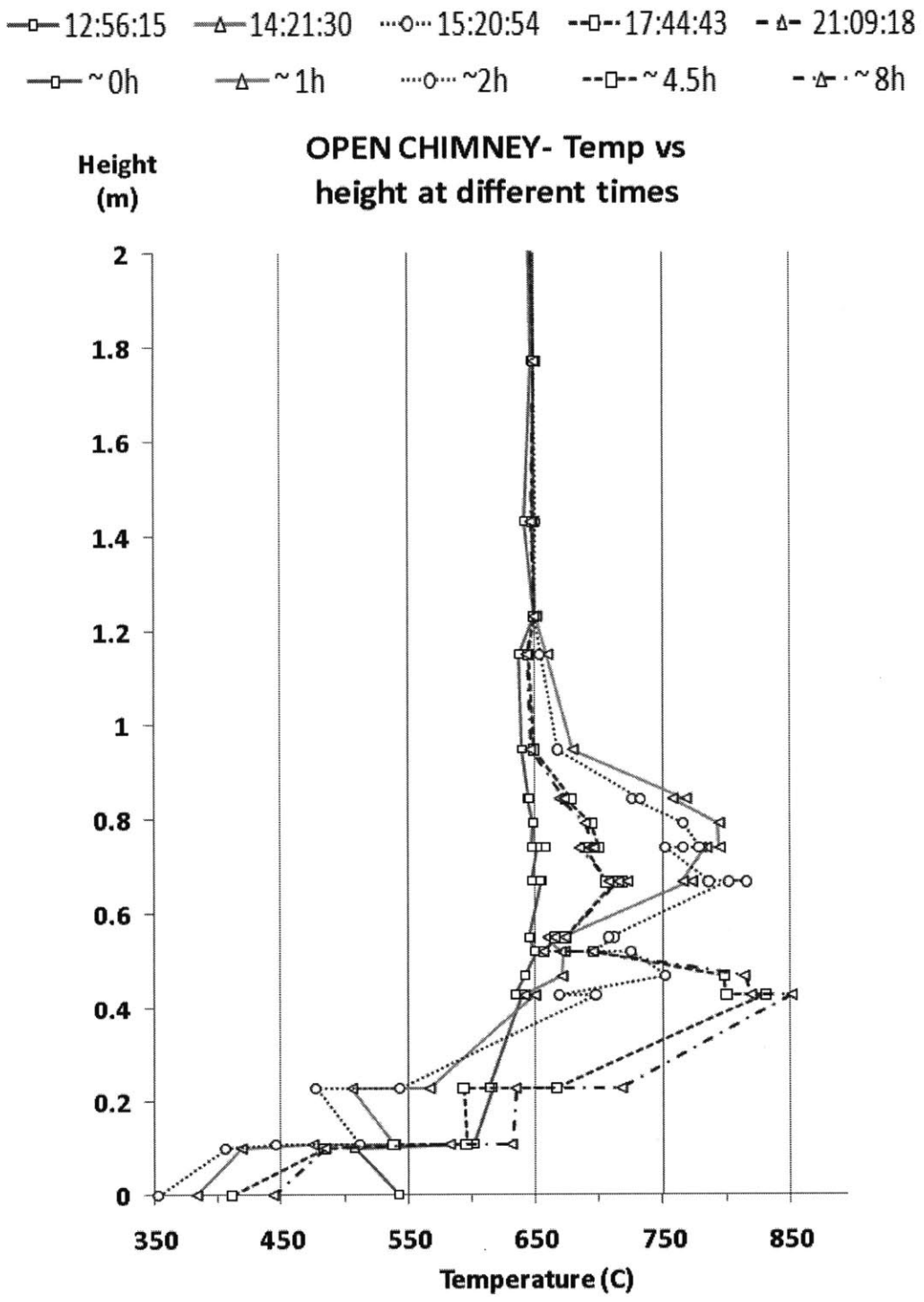


FIGURE 4-5: TEMPERATURE VALUES FOR OPEN CHIMNEY COPIED FROM OPERATOR LOG SCREEN CAPTURES

## 4.2. THE RETURN CHIMNEY DATA RECEIVED

For the return chimney experiment, unlike the open chimney, temperature data with time was not lost and was provided. However, the only species data provided was for oxygen and at two locations, just below the topmost graphitic pebble bed, G6, and measuring the inlet species. The return chimney experiment was conducted over approximately 25 hours between 06:47 on 07/27/2004 and 07:37 on 07/28/2004. Volumetric flow was given throughout the experiment and was shown to be practically constant for 20 of the 25 hours. Figure 4-6, Figure 4-7, and Figure 4-8 show the mass flow rate over the full experiment, the first 5 hours, and compared with the set temperature changes, respectively.

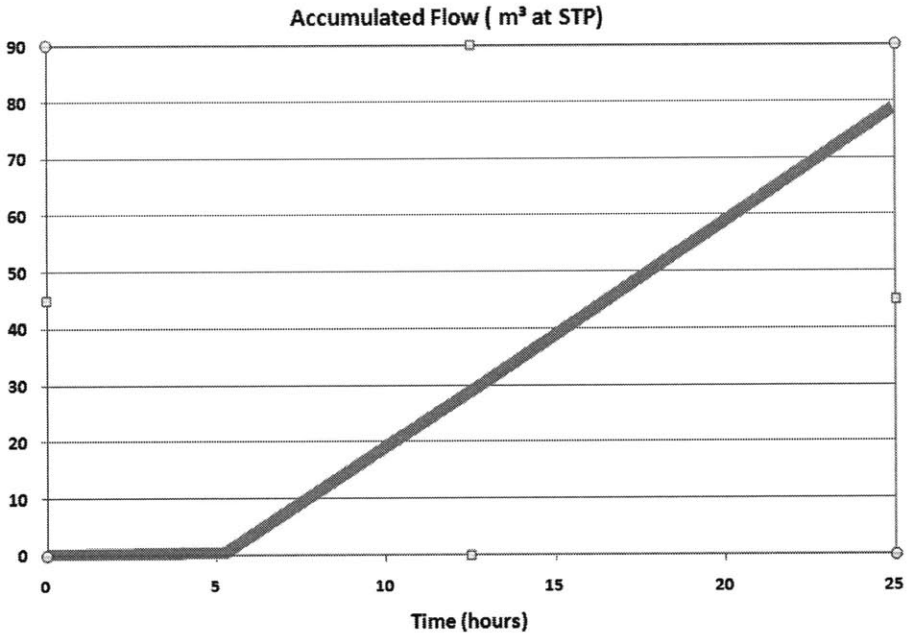


FIGURE 4-6: TOTAL ACCUMULATED AIRFLOW IN RETURN CHIMNEY EXPERIMENT OVER 25 HOURS

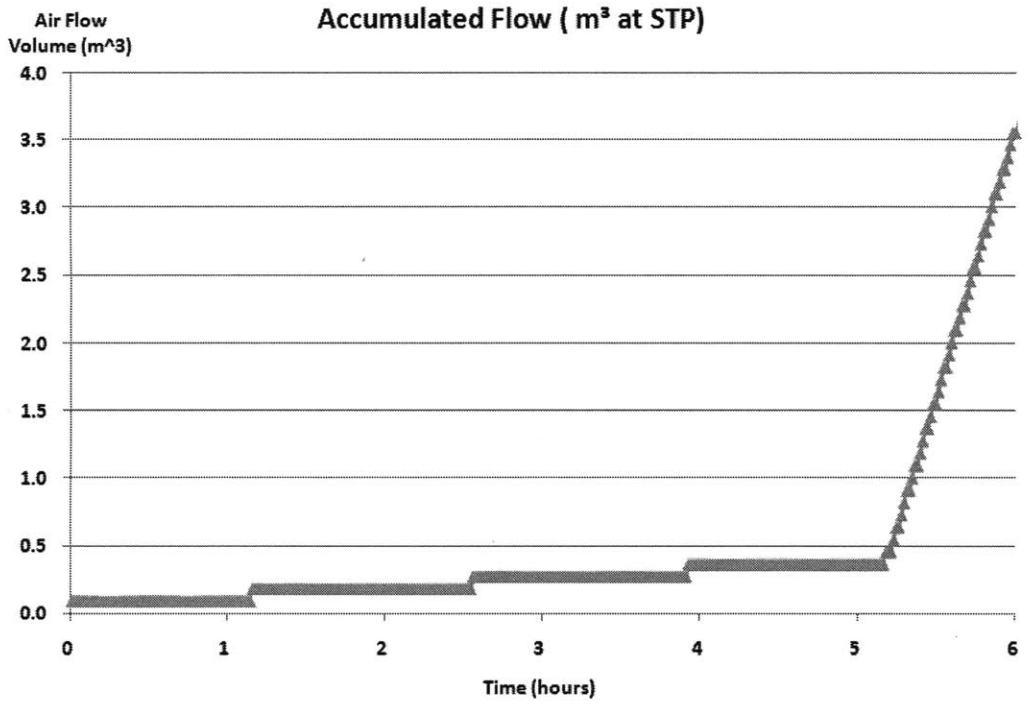


FIGURE 4-7: TOTAL ACCUMULATED AIRFLOW IN RETURN CHIMNEY EXPERIMENT OVER FIRST FEW HOURS

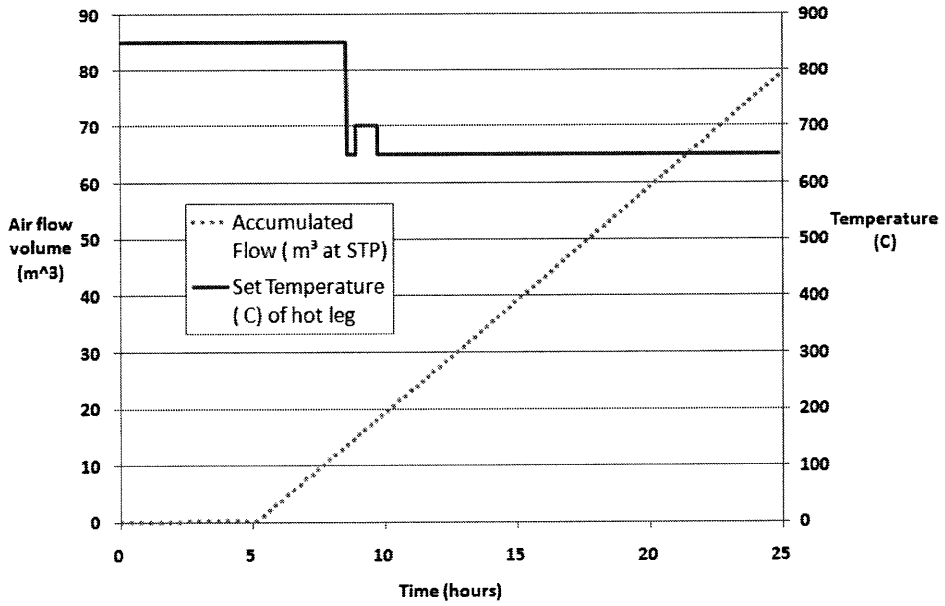


FIGURE 4-8: SET HOT LEG TEMPERATURE COMPARED WITH VOLUMETRIC FLOW IN RETURN CHIMNEY OVER TIME

Figure 4-8 shows that while the air ingress flow rate is relatively constant, the control temperatures for the return chimney experiment varied significantly through the experiment. The overall effect of these changes of the hot leg temperature on the rest of the temperatures in the experiment is shown in Figure 4-9.

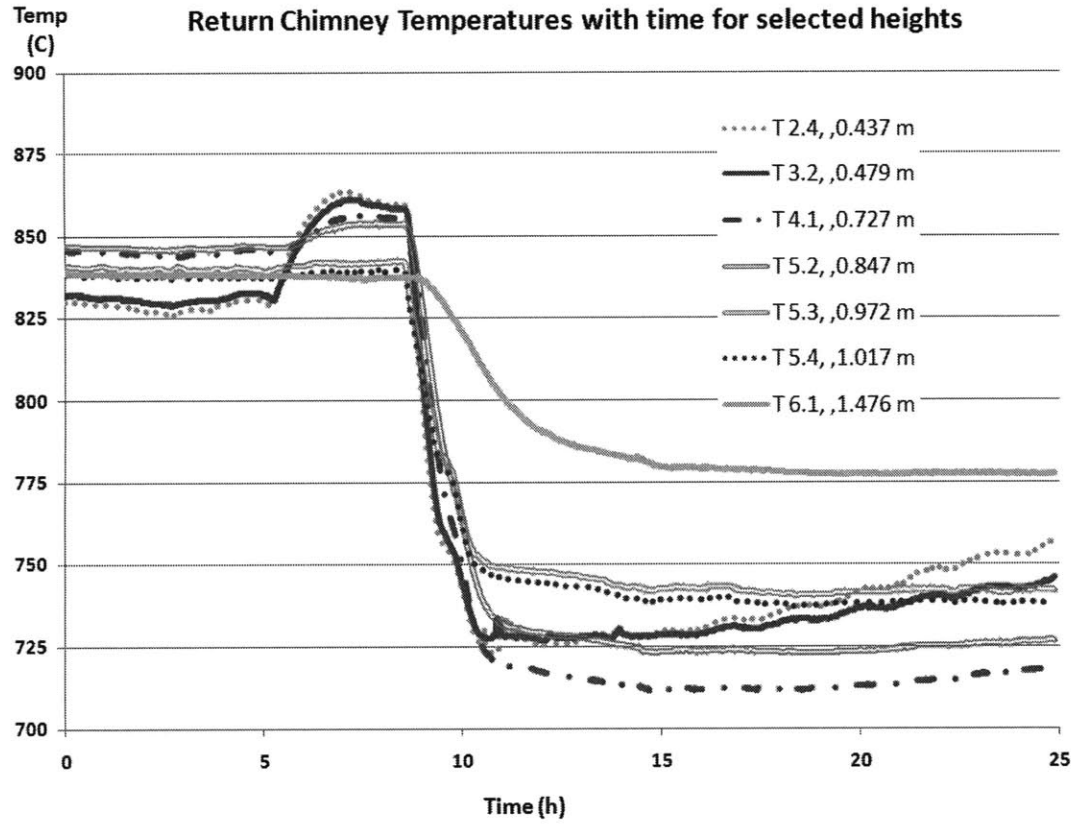


FIGURE 4-9: RETURN CHIMNEY TEMPERATURES AT SEVERAL HEIGHTS OVER DURATION OF EXPERIMENT

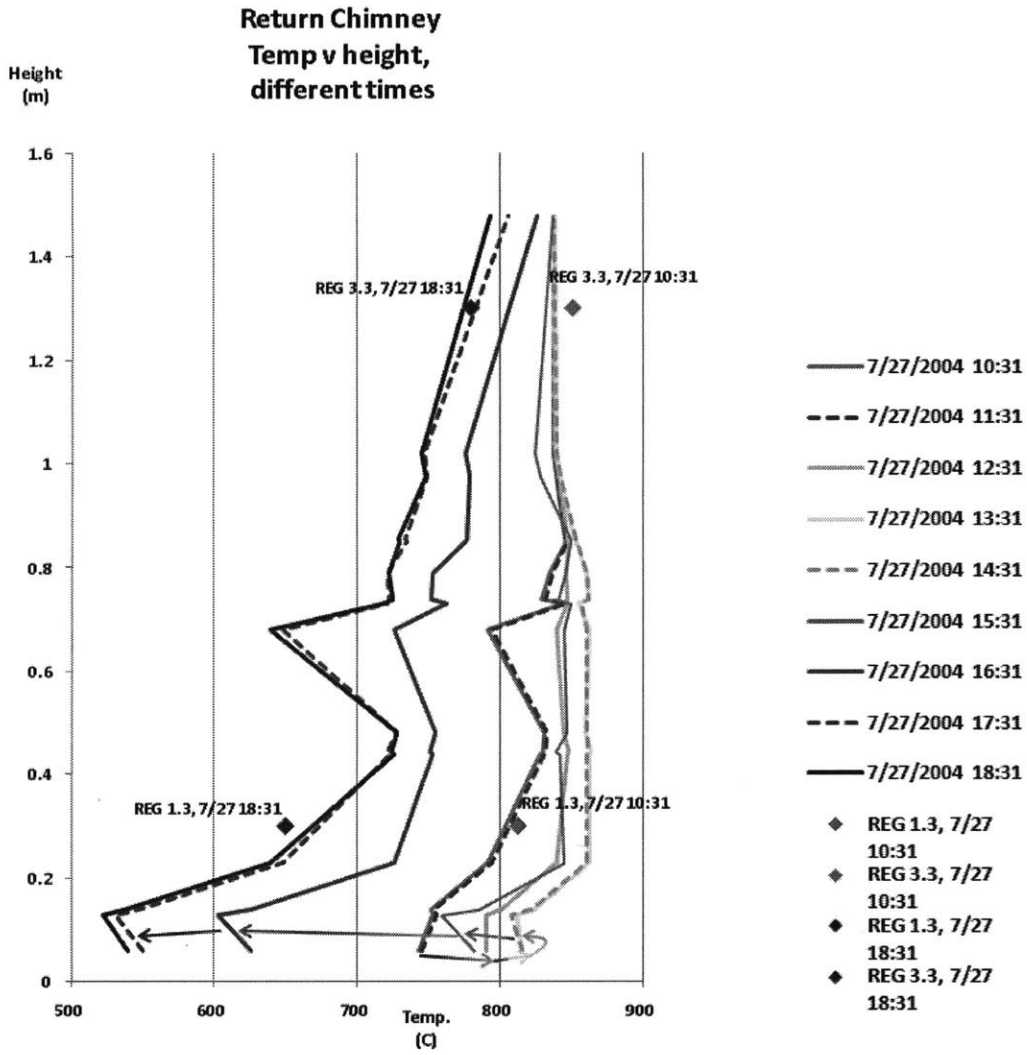


FIGURE 4-10: RETURN CHIMNEY TEMPERATURE (CELSIUS) VS. HEIGHT FOR SELECTED TIMES

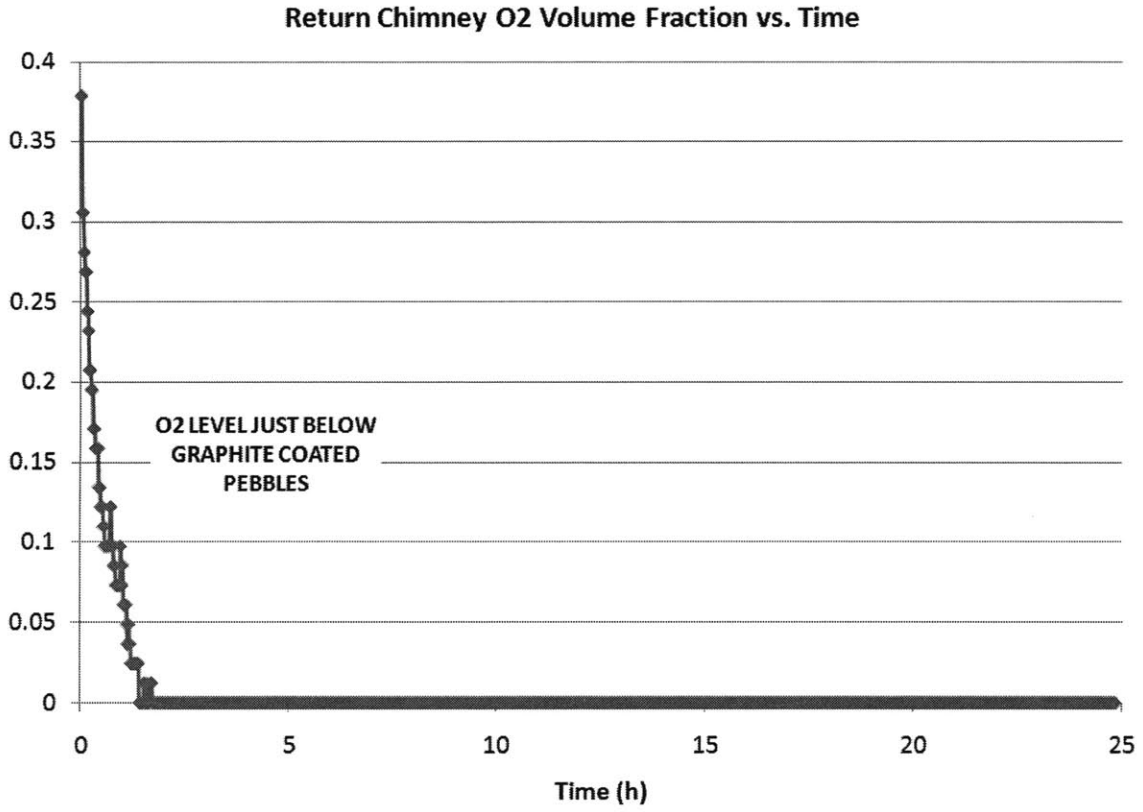


FIGURE 4-11: RETURN CHIMNEY O2 VOLUME FRACTION VS. TIME

Figure 4-11 shows that by two hours into the return chimney experiment, there is no appreciable oxygen reaching the topmost pebble bed, at a height of approximately 1.2 meters. This shows that at the very low flow rates for the first few hours, as shown in Figure 4-7, and at these temperatures, the oxidation rates may be low enough that oxygen can travel through a large-scale graphite core without being reacted. However, it may be primarily due to experimental error, considering there is a significant amount of oxygen at such a height in the reactor at time zero, and the level drops rapidly in the first hour at a low flow rate.

## 4.3. SUMMARY ON DATA AND INFORMATION CLARITY

The most significant hindrance to the project has been a lack of consistent and complete data from NACOK. Critical portions of data, reports and operator's logs only were also only available in abbreviated German.

One point of misunderstanding that was finally clarified was that the mass flow rates for both tests seem to have been held constant as opposed to allowed to naturally circulate. The only data we received from the 2 tests regarding mass flow was excel data for total volumetric flow (m^3) in the return chimney test, apparently taken less frequently than once a minute, and stated as taken at STP. By taking the change in total volumetric flow in certain time intervals, the volumetric flow per unit time was calculated. Using the density of air at STP (g/m^3), the approximate mass flow per unit time was found.

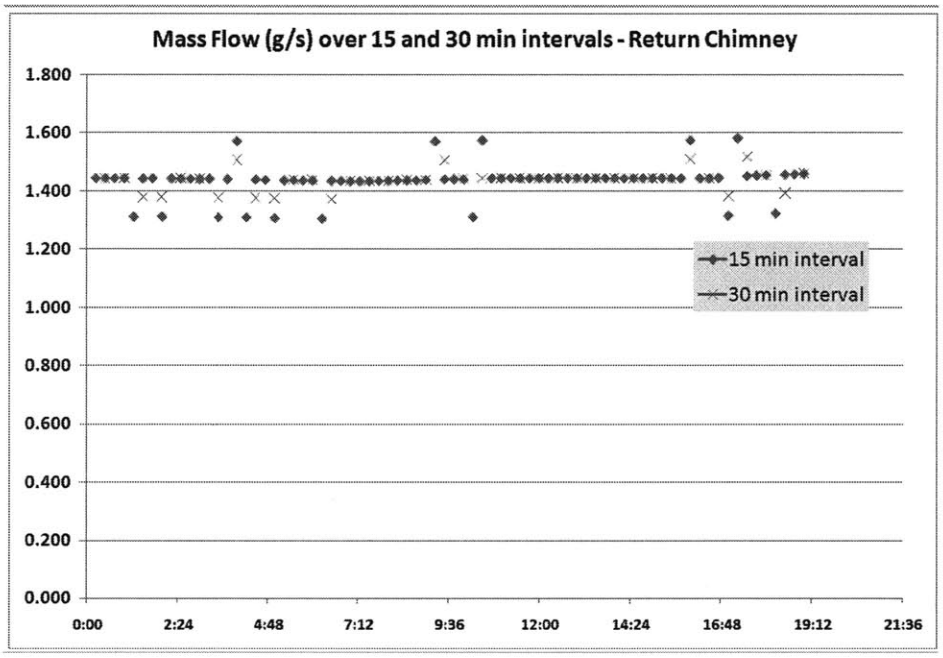


FIGURE 4-12: RETURN CHIMNEY MASS FLOW RATE VS. TIME

For the open chimney experiment, we did not receive any data on mass flow rate. However, an operator's log was provided, which was a document containing hand-written notes from the German operator along with screen captures at a few time points over the course of the experiment. The operator's log provided several points where the "Control" Mass Flow was written down or taken in screen captures:

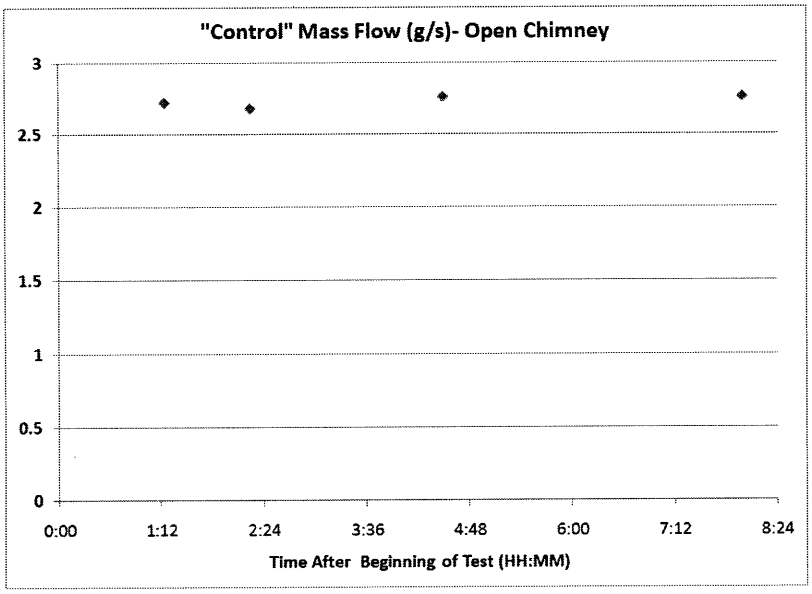


FIGURE 4-13: OPEN CHIMNEY MASS FLOW RATE VS. TIME

It is also stated in the Operator Log "Konstante… 3.31 g/s" and a single screen capture shows that there is a Control Rate of 2.65-2.68 g/s with a "Regleabweichung" or "Deviation from Control" of about 0.9 g/s. Velocity in a section of the test stand with constant cross-sectional area is calculated by dividing the volumetric flow rate (m^3/time) by the cross-sectional area (m^2) to gain velocity (m/time). Because the mass flow rate is constant, the velocity in any one section is constant at all times:

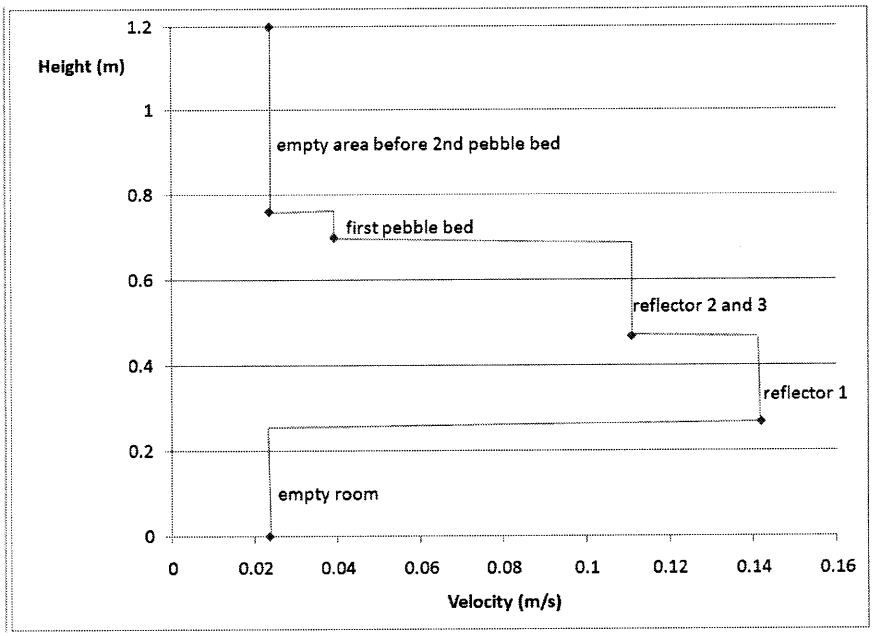


FIGURE 4-14: AIR FLOW VELOCITY IN DIFFERENT CROSS-SECTIONS

Figure 4-14 illustrates the differing velocities found in the experiment given a constant mass flow rate, pressure, and density. The vertical lines do not denote exact locations of the velocities, but rather indicate the relative steps in velocities based on geometries, while the locations of the points do indicate the velocity of air based on geometry at that exact location.

The importance of velocity in the oxidation of graphite is that it supplies more oxygen for oxidation. The Kuhlman reports from NACOK (2) include an equation for oxidation similar to that used by Takeda, with a compensation for velocity. This equation is given in Equation 9-7 and discussed in Section 9.1. However, the contribution of this compensation is quite small. Moreover, the variance from the slow bulk rate of approximately 0.02 m/s to a maximum bulk rate in reflector 1 of 0.14 m/s are both still very low velocities, as should be characteristic of natural convection accidents. These bulk rates are not as important as the surface characteristics and small turbulences at relatively rough surfaces, and the increasing force of viscosity as temperatures heat up post-LOCA.

# 5. FLUENT AND THE MIT CFD MODELS

FLUENT is an advanced computational fluid dynamics (CFD) software, capable of modeling an array of fluid flow, heat transfer, chemical reactions, diffusion, turbulence, combustion, and other phenomenon. The software can be used to create 2- or 3-dimensional models, explicitly modeled geometry or porous media, and steady state or transient computations. FLUENT version 6.0 was used both in the prior MIT models and the current work. The array of customizable computational selections and inputs are numerous, however, the most important options are explained here. The grid or mesh is the first step to developing a model. The preprocessing software GAMBIT is provided with FLUENT for building the mesh. In GAMBIT, the mesh can be created automatically or fine tuned manually. The primary element options are triangular or quadrilateral (3). Triangular meshes generally result in better interpolation across an element, while quadrilateral or tetrahedral can reduce the number of elements required and result in similar or better accuracy if used such that the quadrilateral elements align to the direction of flow, in cases of low turbulence. A key step in generating the mesh is creating zones which will be used in FLUENT to define solid, fluid, and porous areas of the model, along with areas with different material and boundary conditions.

The primary options in FLUENT include the Model Settings, Material Settings, Operating Conditions, Boundary Conditions, and Solver Controls.

## 5.1. MODEL SETTINGS

The Solver options under the Models setting establishes the critical settings for the way the model case file is calculated. It includes the options of Pressure or Density Based and whether the Superficial or Physical Velocity is used in the Porous Zones. The pressure based solver is generally recommended for low-velocity, incompressible flows, while the density based solver was developed for high-velocity, compressible flows. Moreover, the pressure based solver is the only choice allowing for the physical velocity formulation for the porous zones. The superficial velocity assumes flow as unobstructed, or the same as outside the porous zone, and does not incorporate the increase in flow velocity due to the smaller volume or pore size.

Therefore, it is important that the pressure-based solver and the physical velocity options were selected by the previous MIT CFD models and the current work.

The viscosity model can be an important factor in modeling flow; however, previous studies by Brudieu (18) showed that different viscosity settings made little impact in the outcome of a case run. The options available through the viscosity model include: inviscid, laminar, k-epsilon, k-omega, and others. The air flow has a low Reynolds number and could be considered in the laminar flow regime, and this setting was used for the past and present model work at MIT.

The species model is a complex set of options including basics on species and their properties, from thermal to mechanical and transport. The FLUENT database includes libraries of common species properties which can be uploaded. In addition, one is able to select for different methods to input these properties, such as allowing for temperature dependence as opposed to constant properties. Sub-menus allow for selections regarding the chemical reactions between the species and all of the rates options and inputs necessary to define the reactions and calculations.

The Operating Conditions menu offers inputs for operating pressure and gravity. It also includes an operating temperature for the Boussinesq calculations. The Boundary Conditions menu is more detailed, with sub-menus with important setting options. Boundary conditions must be set for each zone and wall, inlet and outlet. For fluid zones, the submenus include settings for motion terms, porous media, reactions, and source terms. For solid zones and walls, the submenus include momentum, thermal, radiation, and species, among others. The settings for the inlets and outlets are varied and depend on the outside pressure, pressure drops, defined or free mass flows, etc.

Solver Controls include options for controlling convergence and affecting the numerical methods used by the FLUENT solvers. These options include the pressure-velocity coupling method, and the discretization options, but perhaps the most important setting is that of the under-relaxation factors for the energy, momentum, and species, etc. In the complicated and

difficult convergence of low-velocity, buoyancy dominated flows, decreasing the under-relaxation factors is a necessary compromise of stiffness and speed for slow convergence. Setting solution limits also helps guide the solution by reducing the range of variables considered in calculations, for instance, temperature and pressure upper and lower limits. Last, the initialization of a case can critically determine convergence or divergence of a solution, by setting the zones (including "all zones") to begin computation and by setting reasonable initial values such as temperature, velocities, and species concentrations for those zones.

## 5.2. THE MIT FLUENT MODELS

FLUENT models of the NACOK experiments were made by M. Brudieu (18) using the Fluent modeling techniques of Zhai (7). Brudieu used 3D models which were first made "blind" (results unknown) in order to assess the ability of the modeling approximations and once some data was received, were modified to more accurately benchmark the tests. Brudieu's final model utilized explicit geometrical modeling only for the lowest reflector, then used separate porous media zones for the next two higher reflectors, and the two pebble zones. Brudieu's Fluent modeling showed good results for both the blind and updated models for temperature distributions but some non-physical temperature drops were found which were further examined in this thesis.

The characteristics of the Brudieu models, especially the final "modified" model of the open chimney are described below. Figure 5-1 shows the mesh of the final open chimney model, and Table 5-1 gives a few important chemical reaction inputs and pressures for all the FLUENT models.

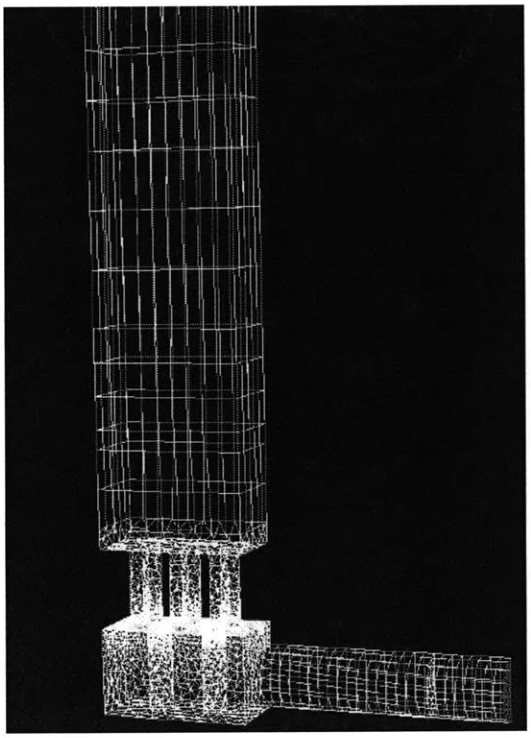

FIGURE 5-1: MODIFIED FLUENT OPEN CHIMNEY MODEL MESH, LOWER SECTIONS

TABLE 5-1: KEY FLUENT CHEMICAL INPUTS AND PRESSURES FOR BRUDIEU MODELS

| Variable/Model | Blind model for open chimney | Modified model for open chimney | Blind model for return duct | Modified model for return duct |
|---|---|---|---|---|
| k Graphite Corrosion | $3.6 * 10^{12}$ | $10^{11}$ | $5 * 10^{10}$ | $10^{12}$ |
| $E_A$ Graphite corrosion | $2.09 * 10^{*}$ | $2.09 * 10^{*}$ | $2.09 * 10^{*}$ | $2.09 * 10^{*}$ |
| x/y Stoichiometry | 0.86 | 1.86 | 1.5 | 1.5 |
| k Boudouard reaction | N.A. | N.A. | 1000 | 200 |
| $E_A$ Boudouard reaction | N.A. | N.A. | $2.6 * 10^{8}$ | $2.6 * 10^{8}$ |
| Pressure outlet pressure gauge | -27.4 Pa | -27.4 Pa | 0 Pa | 0 Pa |
| k CO oxidation | $2.8 * 10^{12}$ | $2.8 * 10^{12}$ | $2.8 * 10^{12}$ | $2.8 * 10^{12}$ |
| $E_A$ CO oxidation | $1.7 * 10^{8}$ | $1.7 * 10^{8}$ | $1.7 * 10^{8}$ | $1.7 * 10^{8}$ |

# 6. Analysis and Assessment of Previous FLUENT work and New FLUENT Work

## 6.1. Assessment of Discrepancies

Past theses at MIT were focused on understanding and modeling air ingress events (7)(19)(18). The most recent thesis that was aimed at benchmarking NACOK tests did well relative to predicting peak temperature and amount of graphite consumed. Brudieu (18) was able to model the open chimney experiment in FLUENT using steady state, porous media, and constant mass flow assumptions, all of which being reasonably applicable to the experiment. The work was able to reasonably approximate burnoff and conservatively over-predict maximum temperatures. However, Brudieu's work was not able to model the axial temperature distribution as well. The remaining problem was to explain the non-physical drop in temperature from reflector 1 to reflector 2 as shown on Figure 5-1.

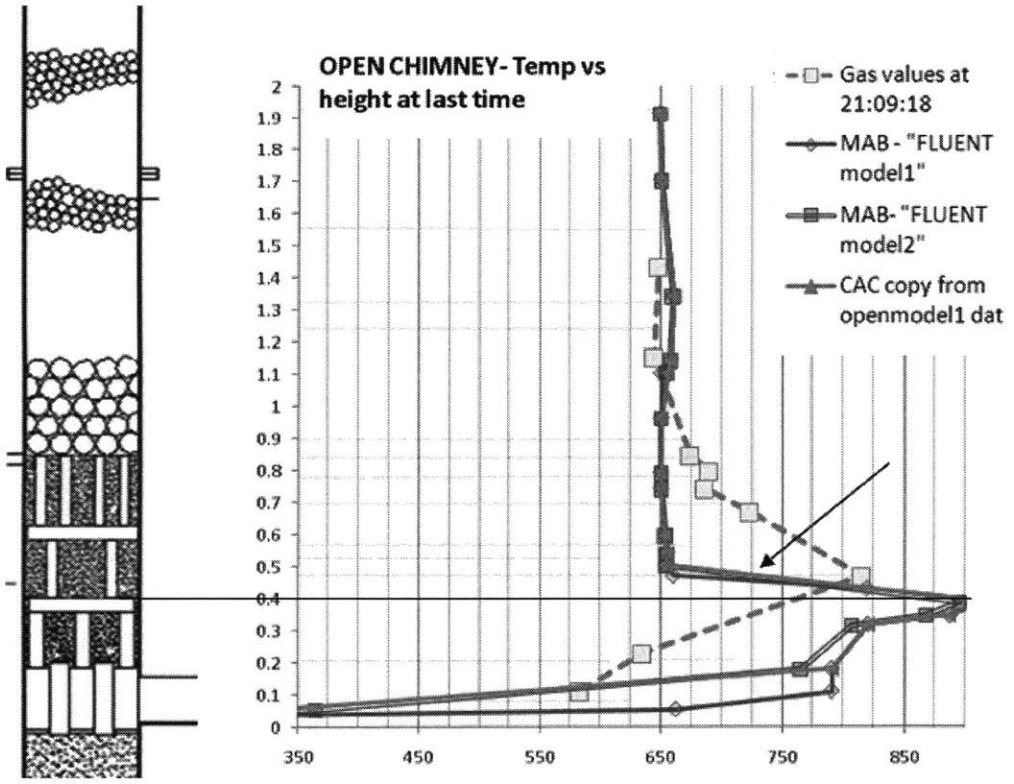


FIGURE 6-1: OPEN CHIMNEY- PREVIOUS FLUENT RESULTS COMPARED WITH DATA

The 3 points at the drop were just above reflector 1 in the empty space between reflector 1 and reflector 2, and at the bottom of reflector 2, respectively. Because of the wall constraints in FLUENT which set the wall to 650 degrees C, the slow moving air quickly cools in the empty space. In reflector 2, we do not see significant heat transfer from reflector 1 for two reasons: 1) no radiative heat transfer being modeled, and 2) no contact between reflectors is modeled and no conduction within the outermost, steel walls is modeled in FLUENT.

The primary reason for the dramatic drop is FLUENT's method for calculating temperatures in a porous media. FLUENT assumes thermal equilibrium between the solid and fluid in a porous media (3). Even though some heat should be generated in reflector 2 through chemical reaction, and through the 2 methods above as well as heat transfer from the heated air, it is muted out of the output because porous media takes a mass-weighted average of temperatures. Therefore, even if the air and the outer faces of the graphite heat up, this is overwhelmed by the bulk of the reflector porous media volume, which is much denser and is also

tied to the wall constraint of 650 degrees C. Figure 6-2 gives the energy equation used in FLUENT calculations for porous media.

### *6.19.2 Treatment of the Energy Equation in Porous Media*

FLUENT solves the standard energy transport equation (Equation 8.3-1) in porous media regions with modifications to the conduction flux and the transient terms only. In the porous medium, the conduction flux uses an effective conductivity and the transient term includes the thermal inertia of the solid region on the medium:

$$\frac{\partial}{\partial t}(\phi\rho_f h_f + (1-\phi)\rho_s h_s) + \frac{\partial}{\partial x_i}(\rho_f u_i h_f) = \frac{\partial}{\partial x_i}\left(k_{\text{eff}}\frac{\partial T}{\partial x_i}\right) -$$

$$\phi\frac{\partial}{\partial x_i}\sum_{j'} h_{j'}\, J_{j'} + \phi\frac{Dp}{Dt} + \phi\tau_{ik}\frac{\partial u_i}{\partial x_k} + \phi S_f^h + (1-\phi)S_s^h \qquad (6.19\text{-}8)$$

where

| | | |
|---|---|---|
| $h_f$ | = | fluid enthalpy ($\int c_{p,f}dT$) |
| $h_s$ | = | solid medium enthalpy ($\int c_{p,s}dT$) |
| $\phi$ | = | porosity of the medium |
| $k_{\text{eff}}$ | = | effective thermal conductivity of the medium |
| $S_f^h$ | = | fluid enthalpy source term |
| $S_s^h$ | = | solid enthalpy source term |

FIGURE 6-2: FLUENT CALCULATION OF ENERGY IN POROUS MEDIA (3)

Thus it is not clear that FLUENT can be used to model the details of an air ingress event using a porous media assumption. It may be appropriate to predict peak temperatures and overall graphite corrosion within a reasonable margin.

## 6.2. NEW 2D AND TRANSIENT MODELS

In response to these difficulties, a meticulously meshed 2-D FLUENT time dependent model (as compared to Brudieu's steady state 3-D model with porous media sections) was developed which allowed for a transient analysis to be run ten times longer than that run by the previous student, with double as opposed to single precision.

### *6.2.1. THE MODEL SETUP*

The meshing is shown in Figure 6-3 and Figure 6-4, and the overall geometry matches that of Brudieu's model, and the NACOK experiment. Table 6-1 compares the sizes of the meshes for the final adapted 3-D model by Brudieu with those of the 2-D model.

TABLE 6-1: FLUENT MESH SIZES

| FLUENT Model | Cells | Faces | Nodes |
|---|---|---|---|
| Brudieu adapted 3-D | 48,787 | 103,929 | 12,331 |
| 2-D | 17,570 | 37,258 | 19,607 |

Similar setup conditions for the 2D model were chosen as for the previous model, as shown in Table 5-1. However, the 2D model allowed for more detailed computational selections, such as allowing for double precision and $2^{nd}$ order schemes.

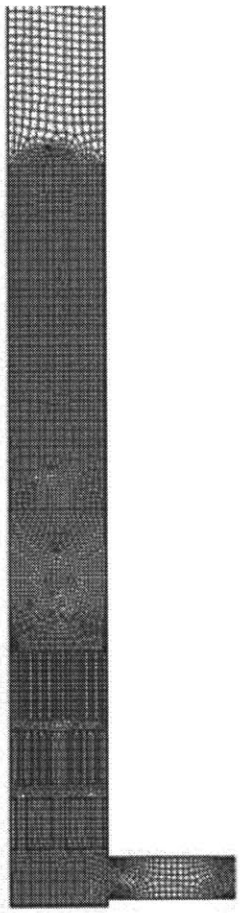

FIGURE 6-3: ZOOMED OUT VIEW OF 2-D FLUENT MESH

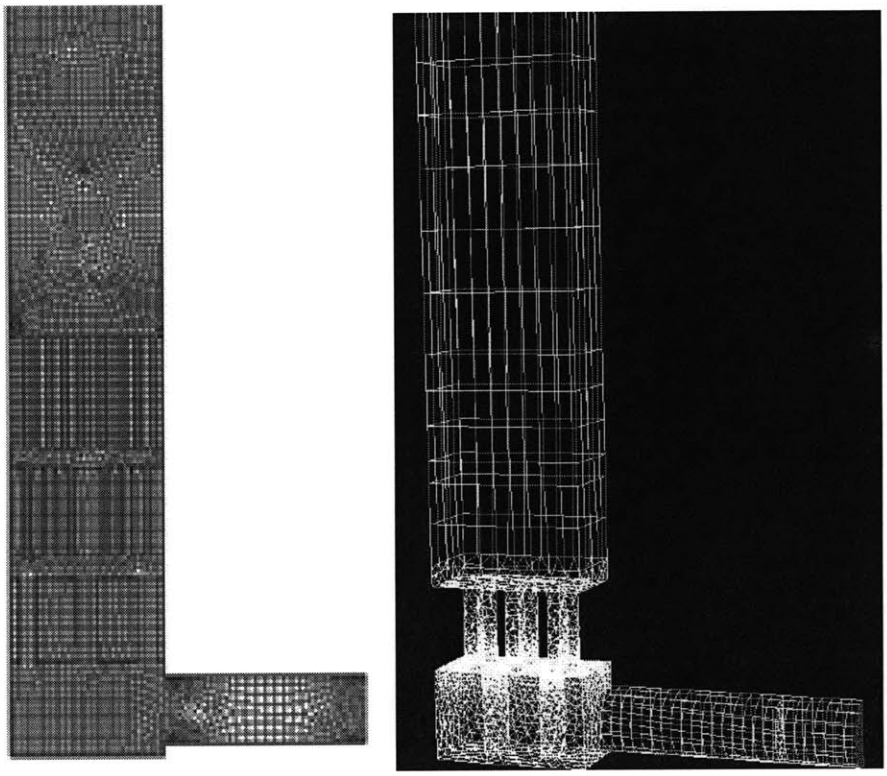

FIGURE 6-4: FLUENT 2-D MESH COMPARED TO 3-D MODEL

### *6.2.2. 2-D TRANSIENT RESULTS*

The results of this simplified transient analysis for an open chimney show that the arrival of a true steady state is not as quick as was shown previously using porous media assumptions. This is due to several factors. First, although after about 1-2 minutes a maximum velocity reaches steady state, this does not realistically represent the distribution of velocity in the channel.

Figure 6-5 below shows the FLUENT model maximum velocity agrees with Brudieu's calculations (18), which was assumed to be the point that a steady state natural convection velocity was achieved. However, as shown in Figure 6-6, it can be seen this is the same time that oxygen is just reaching the first of the reflectors which will begin the major source of reactions and release of heat. This will then cause a significant change in temperature and then the velocity of air ingress, which will continue to increase proportionally to the reactions' heat input

to buoyancy creating natural convection until the amounts of oxygen consumed by reaction versus coming in by this mass flow stabilize over time, creating a truer steady state. Diffusion alone, as assumed in previous analyses, is not sufficient to determine steady state points and conditions. Also, in Figure 6-8 it can be seen that the velocity magnitude and especially direction are not uniform and further time points have shown they are not at a steady state.

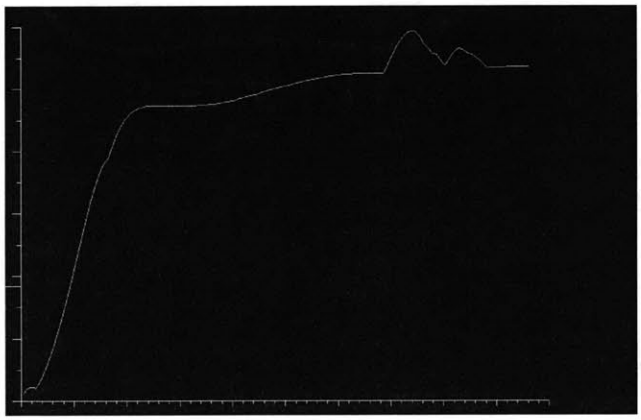

FIGURE 6-5: MAXIMUM FLOW VELOCITY AT INLET (ARBITRARY SCALES)

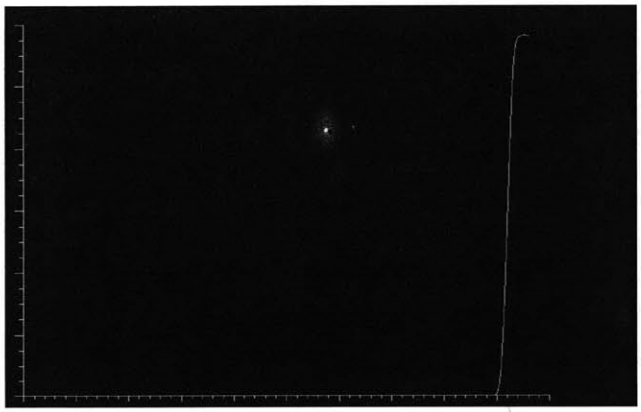

FIGURE 6-6: PERCENT MOLE FRACTION OF O2 AT THE FIRST REFLECTOR (ARBITRARY MOLE FRACTION SCALE, TIME SCALE EQUIVALENT TO PREV. FIGURE AT APPROX. 4 MINUTES), SHOWING THAT OXYGEN DOES NOT REACH THE FIRST REFLECTOR TILL SIGNIFICANTLY LATER THAN PRESUPPOSED ONSET OF NATURAL CONVECTION

Another reason for the difference in steady state estimates from previous work is that the heating of graphite to steady state temperatures takes longer than assumed by an effective conductivity and thermal inertia of a porous media. This also matches with NACOK data, as

described below. Also shown on Figure 6-7 is an illustration of the significant temperature variation (in Kelvin) within a channel even after 4 minutes.

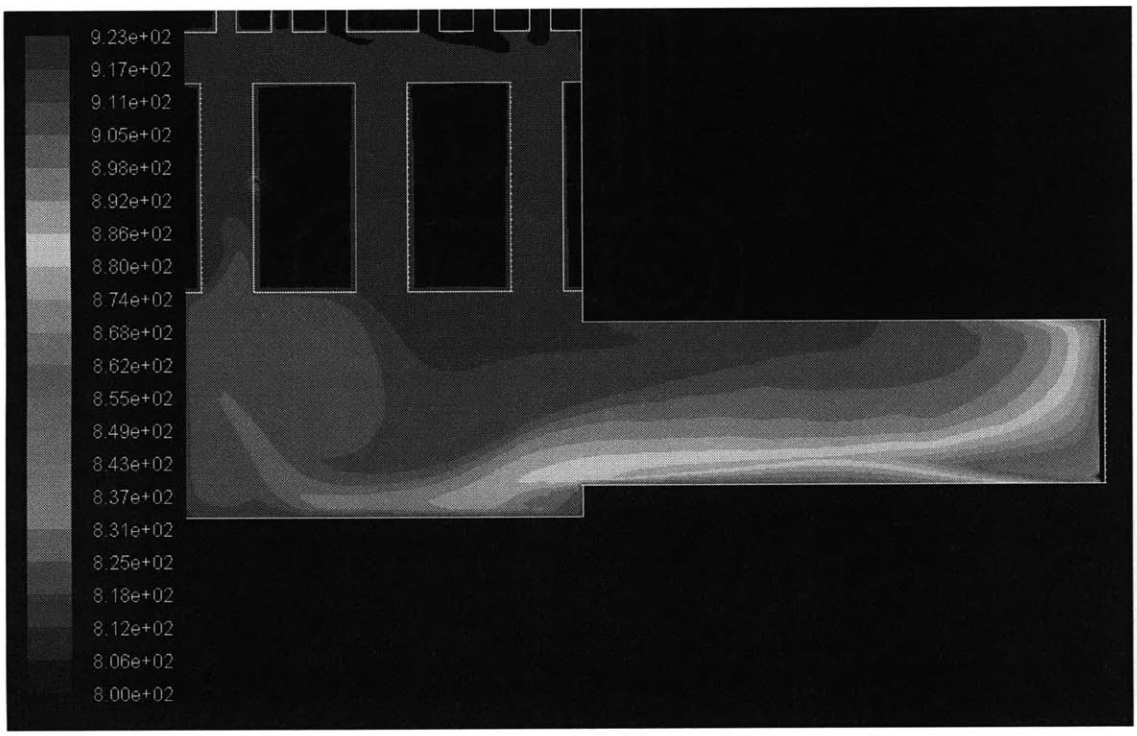


FIGURE 6-7: TEMPERATURE DISTRIBUTION (K) OF FLUID AT 4 MINUTES

The transient model has also allowed for insight into fluid flow and velocity in the ingress experiment. For one, the point that fluid velocities may vary extremely within certain points of the channel- from 0 to 10 m/s and that the vectors are in different directions. The results of our model also aligned with the observations by Chang Oh (8) at INL regarding stratified flow as shown by the vectors in Figure 6-8.

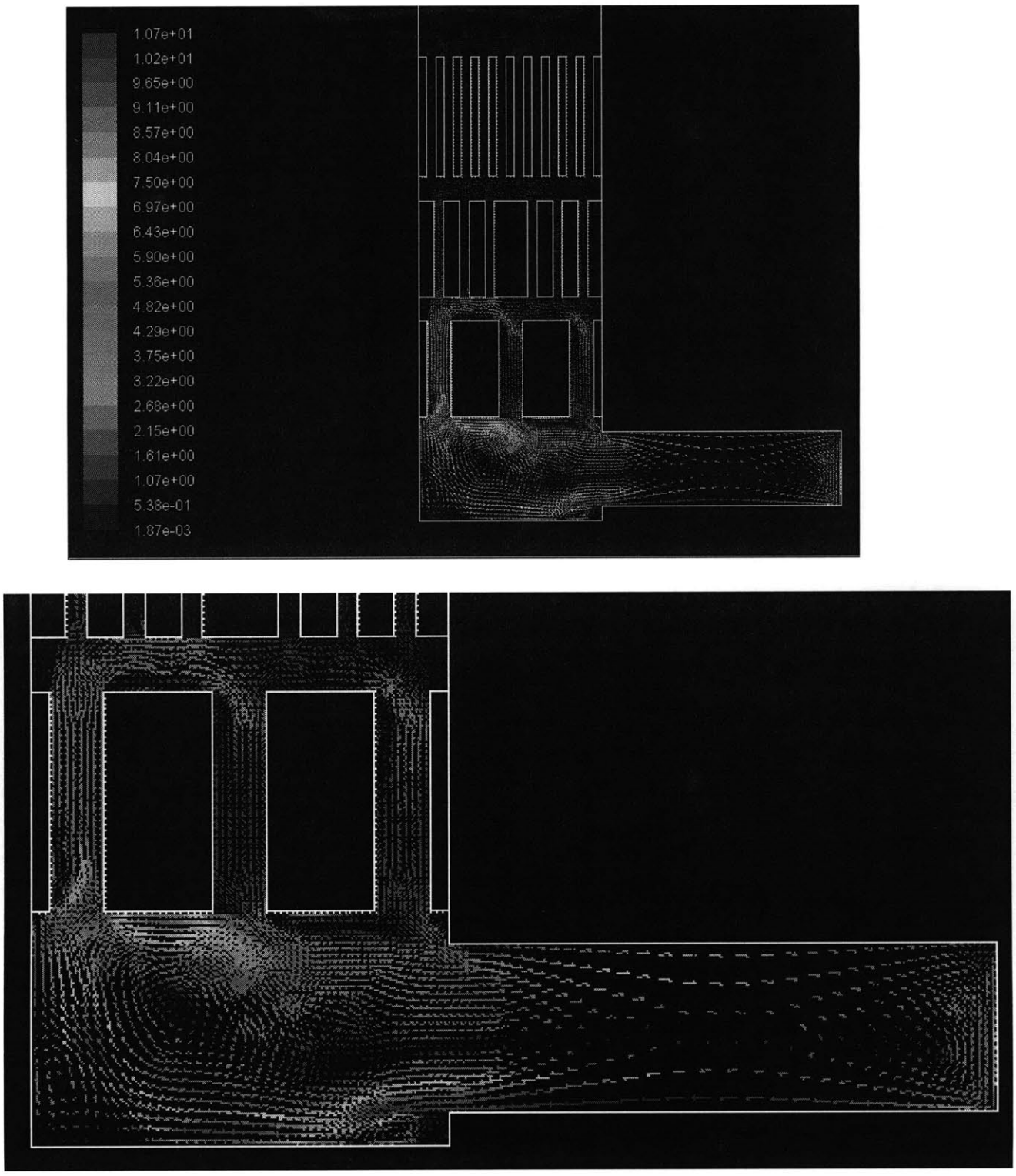


FIGURE 6-8: VECTORS OF VELOCITY MAGNITUDE (M/S) AT 4 MINUTES, ILLUSTRATING STRATIFIED FLOW AT INLET

The transient model has shown more clearly at which points in time and what orders of magnitude species concentrations reach different levels in the experiment assembly, especially, what points in time oxygen reaches the reflectors and if/when it reaches the graphite coated pebble bed.

### *6.2.3. 2-D Steady State Results*

Although a transient study is necessary to effectively model natural convection cases, because the NACOK experiments were found to have constant mass flow rates, the same boundary conditions could be used to find a steady state solution in the 2-D model. With appropriate initialization, the solution converges between 500 and 1,000 iterations. This is a significant time improvement to the 3-D model. In addition, by avoiding the porous media assumption and explicitly modeling the geometry, the temperature results seem to better match the NACOK data as shown in Figure 6-9. The line for the 2-D results follows the average values for a section, but the maximum and minimum temperature/height points in a section are also shown for comparison. It can be seen that the maximum temperatures found correlate well to the NACOK data and that the locations of the maximums also correlate well to the closest time point to a steady state for the NACOK data, which was at 8 hours.

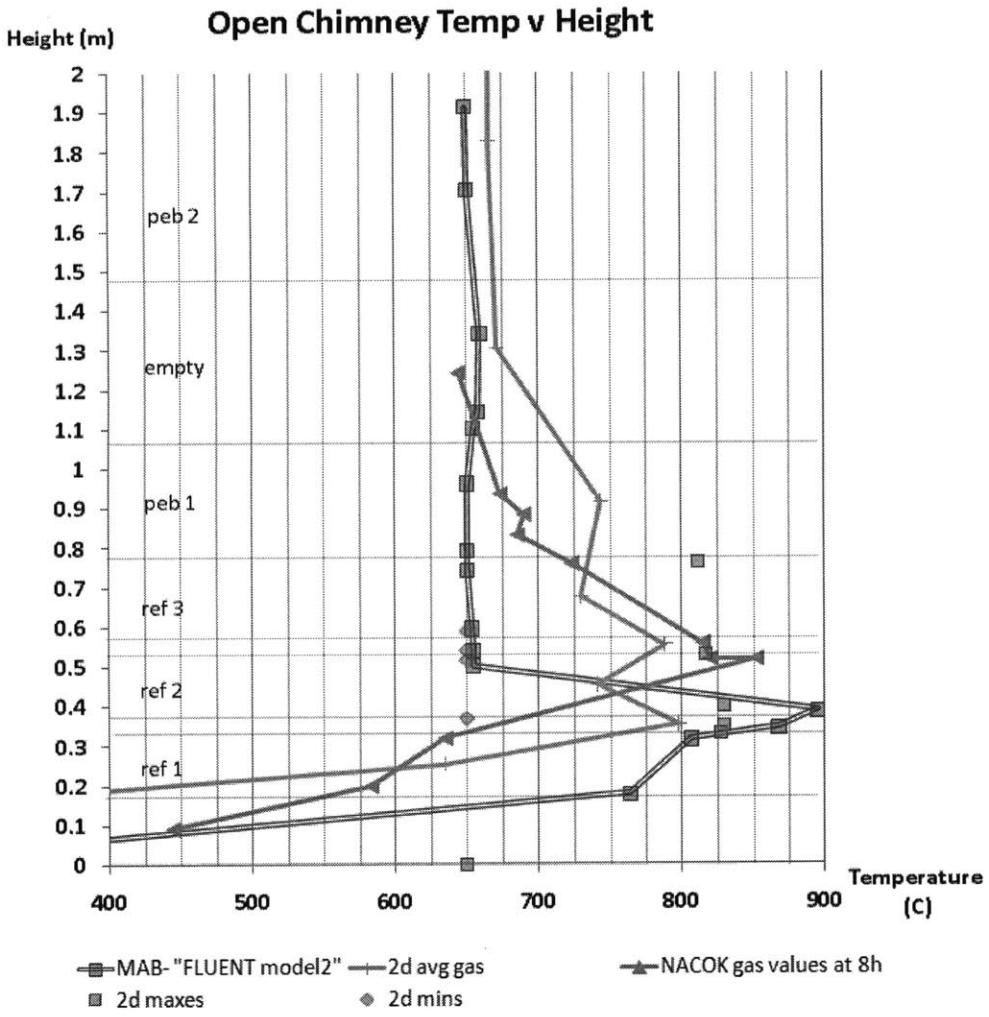


FIGURE 6-9: FLUENT 2-D STEADY STATE COMPARED WITH PREVIOUS 3-D STEADY STATE AND NACOK DATA

The species data was on the correct order of magnitude generally. However, it showed some error in the porous region used for the pebble bed. The oxygen data is presented in Figure 6-10.

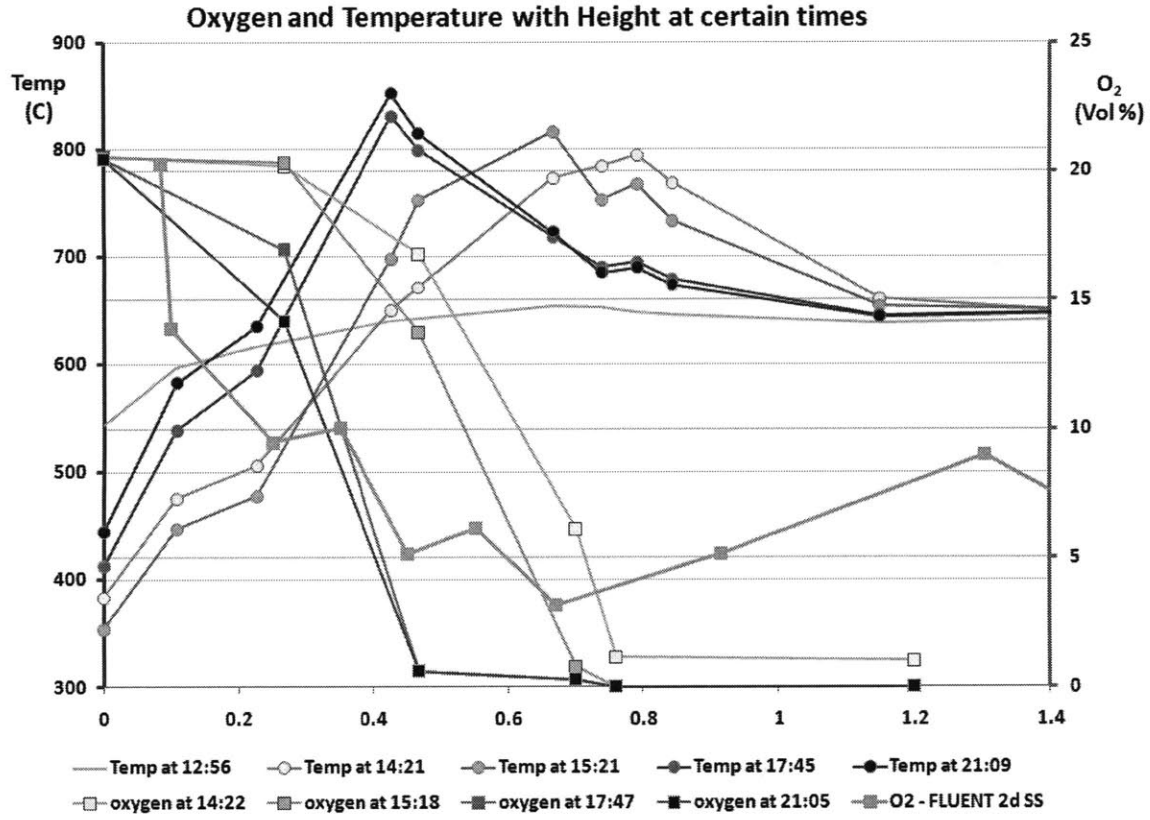


FIGURE 6-10: OPEN CHIMNEY OXYGEN DATA COMPARED WITH 2-D FLUENT SS RESULTS

## 6.3. FUNDAMENTAL MODELING LIMITATIONS

Brudieu was able to model the open chimney experiment in FLUENT using steady state, porous media, and constant mass flow assumptions, among others, in order to have any reasonable processing times which gave reasonable results compared to the key items of interest in the NACOK experiment – namely peak temperature and amount of graphite consumed during the experiment. The reason that truly transient and 3-D modeling of natural convection processes are not modeled is because it is simply time and processing power limited in order to gain any convergence for such a complicated scenario. For instance, the FLUENT manual has an accepted equation for determining the approximate timestep necessary for natural convection phenomena, and for our experiment it is on the order of .001 s. Taking into account the minimum recommended iterations per time step at around 10 iterations, 10,000 iterations are required to model one second of experiment time. Estimates for modeling the full experiment time of 8 hours is on the order of 3 years of computer time (not using supercomputers).

The use of a steady state assumption allows for the simplification in the 3-D model which may not be the best assumption in understanding the development of an air ingress event. The other major assumption used in air ingress analysis is that of a porous media representing the pebble bed or graphite reflectors. The porous media assumptions built into FLUENT make the label "3-D" misleading as the porous media section becomes a node in the analysis. Geometrical details are lost in this formulation as compared to the 2D.

In summary, the 2 D work highlighted a few key points: emphasizing the possible implications of layered flow over diffusion, more accurately determining how much time might be necessary for oxygen to reach the first reflector which determines onset of convection, and by showing the flow patterns in the lower reflector explained the physical observation of significantly higher corrosion on the far side of the first reflector. The overall validity of the possible simplification of 3-D to 2-D for these experiments was generally verified, which significantly reduces computational time. The ability to reduce dimension without losing accuracy is important to the goal of producing a nodal code capturing the effects of natural convection and chemical reactions.

# 7. DATA SET AND ANALYSIS

One of the goals of this thesis was to use the specific and detailed data coming from the FLUENT analysis of the NACOK tests to develop correlations which can be used in faster running codes such as MELCOR or RELAP. The process of data mining was explored to see if correlations could be found between important and relevant parameters. If there was sufficient data coming from the experiments, this data could also be data mined for relationships.

## 7.1. CONCEPT FOR DATA MINING

Data mining can be a powerful technique for analyzing large sets of data with interrelated variables for underlying correlations, which may be used to build simplified equations with predictive value. The technique is most valuable when sufficient data is taken from a number of experiments that have both variations and controls in the variables considered so that extrapolation is well founded.

The potential for data mining as having valuable predictive value for air ingress accident scenarios has been largely unrealized due to the combination of a lack of sufficient number of experiments with comparable setups, or on the other hand, by the time-consuming nature of building and running simulations on reasonable time scales with a variety of initial conditions, still reaching convergence, with enough repetition to have the large data set required.

While these are challenges, data mining should not be discounted by the air ingress community due to advances in computational power. Data mining may have the ability to predict the maximum temperature reached within a margin without necessarily needing to perform endless complicated iterations using codes such as FLUENT. Logically, the air ingress accident could be viewed as a steady state problem assuming that little overall cooling of the mass of graphite and other materials occurs in the span of time required for onset of natural convection and if the heat produced by the reactions is on the same order as the amount of heat removed by the air.

## 7.2. Data Mining Software and Results from Open Chimney Data

Commercially available software for data mining includes SPSS, SAS, and ADVIZOR. SAS is a dominant software in the industry. As an initial set of relationships, the data from the open chimney experiment was analyzed in SAS. The data was first pre-processed in order to create as uniform of a data set as possible. As discussed in section 4.1, this was a very non-uniform data set and the pre-processing step was time-intensive.

The data set was arranged in spreadsheets by species: oxygen, carbon monoxide, carbon dioxide and helium. In each sheet, the columns represented the reading of the species at a certain time, while the rows gave the height or gas measurement sensor number. These sheets were converted into comma-separated value files (.csv), read into SAS and a Pearson correlation assessment was performed. SAS then produced output files which were manually analyzed in MS Excel.

The Pearson product-moment correlation coefficient is one of the most commonly used correlation statistical methods and is a measurement of the linear correlation of two variables in both strength and direction (20). The Pearson coefficient ranges from -1 to +1, and when

measured in a sample, it is given the symbol "r". See Table 7-1 for ranges of values for r and what the values may be regarded to indicate, information gained from (21).

TABLE 7-1: PEARSON R-VALUE RANGES AND CORRELATION INDICATIONS

| R value (+/-) | Correlation |
|---|---|
| 0.0-0.2 | No or negligible correlation |
| 0.2-0.4 | Low degree of correlation |
| 0.4-0.6 | Moderate degree of correlation |
| 0.6-0.8 | Marked degree of correlation |
| 0.8-1.0 | High correlation |

The "coefficient of determination," or $R^2$, is used more frequently than R, because it is a more stringent qualifier of correlation.

The following variables were compared at as many time and sensor points as possible: oxygen with temperature (T), oxygen and carbon monoxide, oxygen and carbon dioxide, and carbon monoxide and carbon dioxide. Because mass flow rate was constant through the open chimney test, mass flow rate was not compared with any of the variables. The variable combinations with more than 2 observations of sensor points compared at within 5 minute intervals of each other, with an r value higher than 0.6 are shown in Table 7-2.

TABLE 7-2: R-VALUES FROM OPEN CHIMNEY EXPERIMENTAL DATA

| Variables | Time point (h:mm after test started) | Number of Sensor Observations | R value | Approx. R2 value |
|---|---|---|---|---|
| CO and O2 | 7:59 | 5 | -0.65480 | 0.42876 |
| O2 and CO2 | 1:04 | 6 | -0.99976 | 0.99952 |
| | 1:12 | 7 | -0.99976 | 0.99952 |
| | 1:56 | 5 | -0.99998 | 0.99996 |
| | 4:35 | 5 | -0.99995 | 0.99990 |
| | 7:59 | 5 | -0.99978 | 0.99956 |

| | | | | |
|---|---|---|---|---|
| CO and CO2 | 7:59 | 8 | 0.95078 | 0.90398 |
| O2 and T | 1:24 | 7 | -0.75306 | 0.56710 |
| | 4:34 | 5 | -0.69619 | 0.48468 |
| | 7:59 | 5 | -0.71701 | 0.51410 |

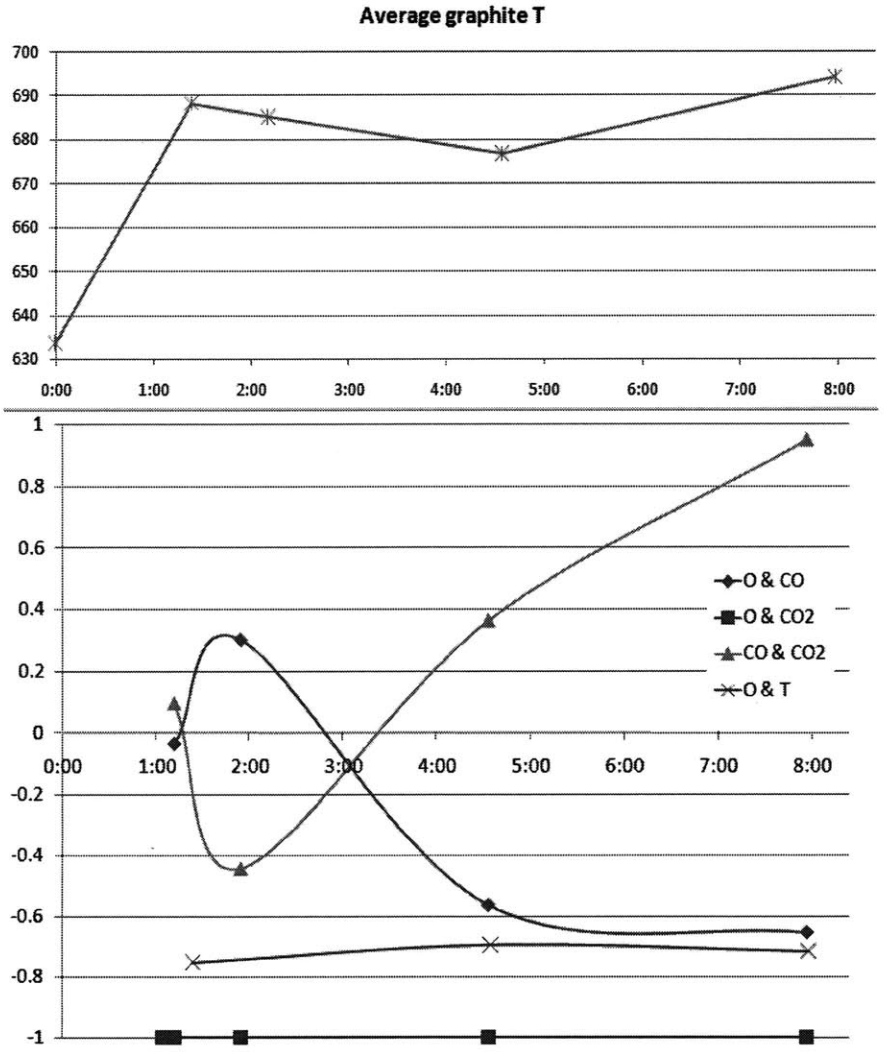


FIGURE 7-1: R-VALUES WITH TIME FOR OPEN CHIMNEY

Table 7-2 shows that there are not as significant correlations between oxygen and carbon monoxide or temperature as between carbon dioxide and oxygen or carbon monoxide. More r

values are shown in Figure 7-1. Interestingly, Figure 7-1 shows that the correlations between CO/CO2 and O2/CO increase, decrease, then after the first hour, increase significantly with the opposite sign. Comparing this to the average graphite temperature depicted in the top chart of Figure 7-1, we see these coincide roughly with the increases in temperature and the approximate reach of steady state around one hour after the beginning of the experiment.

Overall, the results of the data mining for correlations support the basic theory for reactions. The levels of oxygen should be inversely proportional to carbon monoxide and carbon dioxide as it is reacted. Further, due to the ratio given in Equation 9-7, Section 9.1, at these temperatures, the amount of carbon dioxide produced from oxygen will be significantly more than the amount of carbon monoxide and thus will be more closely correlated to oxygen. The relationship between carbon monoxide and carbon dioxide is largely dictated by this same reaction, and becomes stronger with increasing time at a relative steady state temperature.

## 7.3. Data Set from NACOK and Difficulties for Data Mining

However, data mining can show simple relationships even within a limited data set. Simple relationship studies were performed for the open chimney experiment. Within a section of the experiment, such as a reflector, however, there might be only one temperature and species reading. Considering the strong dependence of temperature and reactions on the geometry and material in a section, as well as the necessity of constant bulk velocity in an area with constant cross section and relatively constant density, it is difficult or perhaps inappropriate to find correlations between the key variables such as temperature and species with the height in the experiment or the velocity in a section. Despite this, simple relationships could be confirmed using the data mining software.

While data mining "involves fitting models to, or determining patterns from, observed data" (22) it must be said that in the case of the air ingress situation that while the phenomena are complex, this research and other research such as that of Chang Oh (23) show that the scientific understanding of the phenomena are sufficient to be able to reasonably model the accident. In this sense, this analysis is more interested in fitting models to the observed data in order to

complement the development of predictive correlations, as opposed to discovering unknown patterns.

# 8. COMPARING NACOK OUTCOMES TO OTHER GRAPHITE CORROSION EXPERIMENTS

## 8.1. GRAPHITE USED IN NACOK AND APPLICABILITY TO OTHER NUCLEAR GRADE GRAPHITES

The graphites used for the NACOK open chimney test were ASR-1RS for the reflectors and A3-3 for the pebbles (2). Chemical correlations for the FLUENT model followed the Arrhenius form for chemical reactions:

$$k = A \cdot e^{-\frac{E}{R \cdot T}}, \quad (8\text{-}1)$$

where k is the reaction rate and A is the rate constant, which have consistent units depending on the order of the reaction, E is the activation energy, R is the gas constant, and T is the temperature in Kelvin. The order of the graphite corrosion reaction varies in the literature and from experiment to experiment, but generally falls between 0.5 and 1, and the first order is what is used by Brudieu, The first order was used in this analysis for simplicity and consistency of units.

The results from the NACOK experiments depend on the precise type of graphite used, which may or may not be similar to the type of graphite used in industrial application. Even the same form of graphite can present significantly different chemical/combustion characteristics (24)(25).(24)(25).

As far as pure experimental results regarding different nuclear grade behaviors, the definitive papers compiling nuclear graphite corrosion rates are done by Moormann. In a 1998 paper Moormann concisely, in the Arrhenius form, and with the same order of reaction listed the reaction rate constants and properties for different graphites (26). The following table of properties for common nuclear graphites is given, along with the assumed reaction rate functions:

TABLE 8-1: RATE COEFFICIENTS FOR C/O2 REACTION

| | A3-3 | A3-27 | V483T | ASR-1RS | ASR-1RG | ATR-2E | AO5 |
|---|---|---|---|---|---|---|---|
| $k_0$ | 35.85 | 1.051 | 18.25 | 17.95 | 36.71 | 57.11 | $6.72 \cdot 10^6$ |
| $k_2$ | 0.037 | | - | | | | |
| $E_0$ | 15370. | 11196. | 15840. | | | | 26253. |
| m | - | - | 1. | | | | 0.671 |

$$r = k_0 \cdot \exp(-E_0 / T) \cdot f(p_i) \cdot f(B) \cdot \sqrt{D/D_0} \quad [mol_C \cdot m^{-2} \cdot s^{-1}]$$

8-2

Where

$$f(p_i) = p_i^m \text{ or } f(p_i) = 1/(1 + k_2 \cdot \sqrt{p_i})$$

8-3

which compensates for dependence on partial pressures of the oxidizing gas. In all LOCA situations assuming full decompression and pressure equalization with atmospheric air at standard temperature and pressure, this formula should not vary. The f(B) function accounts for burnoff and the D/Do portion accounts for differing diffusions. For the AO5 graphite at STP partial pressure of oxygen, and as the suggested approximation for other graphites, the burnoff function takes the following form:

$$f(B) = \exp(69.93/(B + 29.2))$$

8-4

Noting that the adjustments for partial pressure, burnoff and diffusion do not explicitly depend on temperature, and assuming that these adjustments are small compared to the base Arrhenius function, some basic comparisons of the difference in graphite corrosion properties with temperature can be shown in the following two graphs:

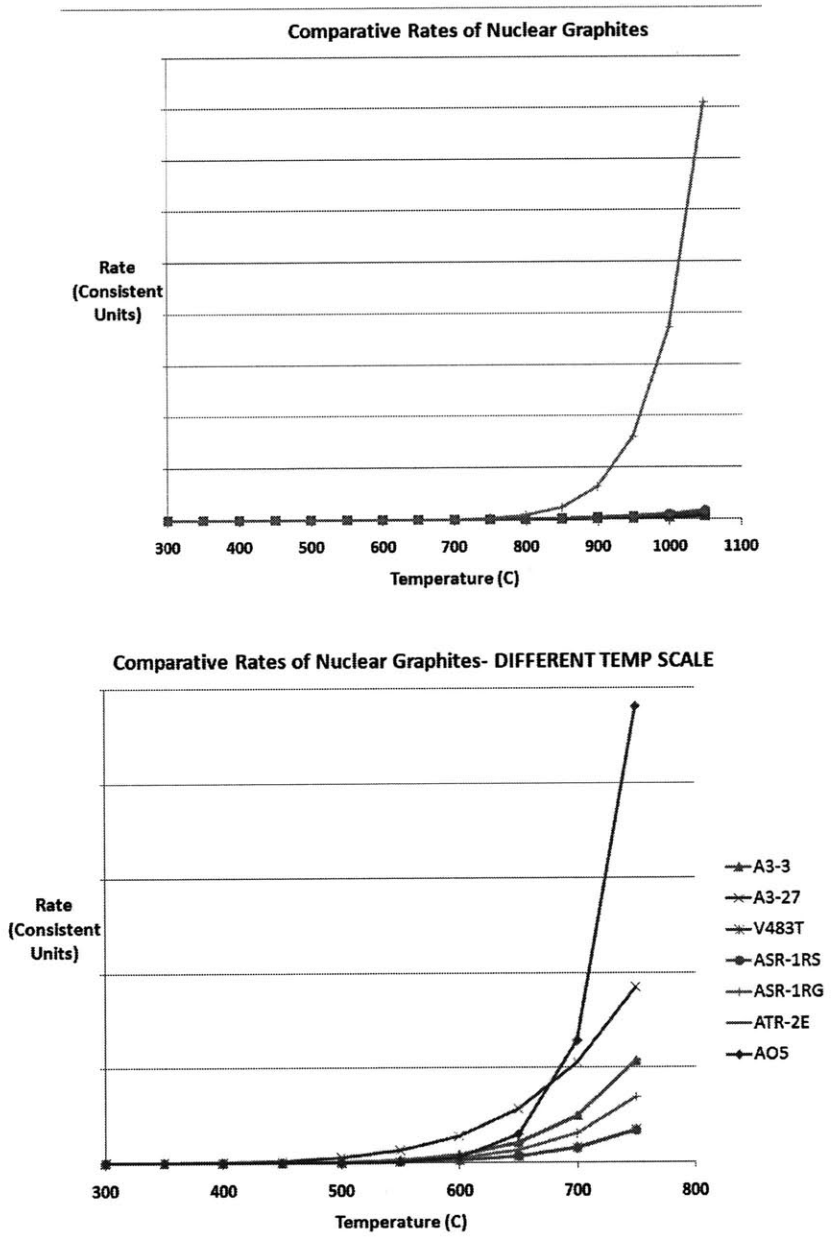


FIGURE 8-1: CARBON OXIDATION REACTION RATES FOR DIFFERENT GRAPHITES TO 800C

These figures show what follows from the AO5 graphite having a rate constant that is orders of magnitude higher than the other graphites as shown in Table 8-1. This means it is far more temperature sensitive, especially above about 750C or 1000K.

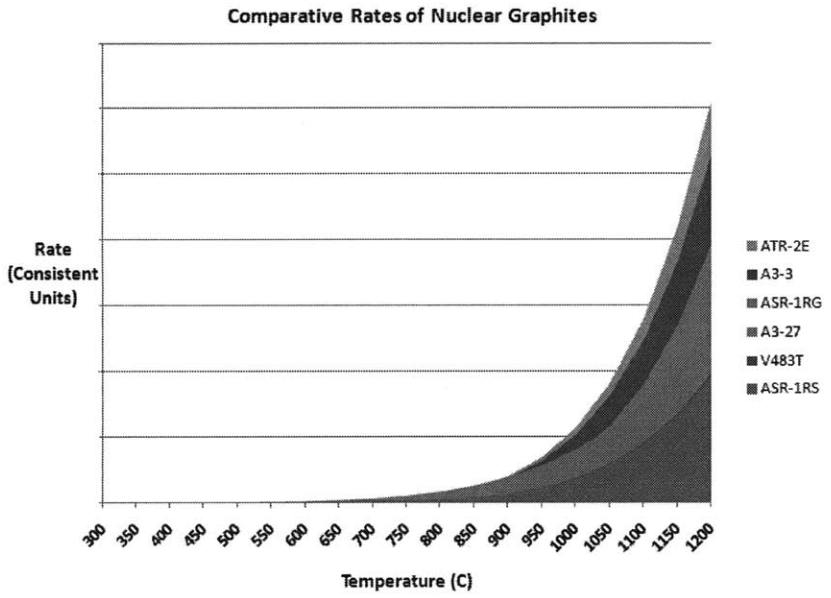


FIGURE 8-2: CARBON OXIDATION REACTION RATES FOR DIFFERENT GRAPHITES TO 1200C

Taking the AO5 graphite out, and comparing the remaining graphite types, we see that using the A3-3 rate is both relatively very close to the other rates and generally conservative for all graphite types, except for the A3-27 below 900C and for the ATR-2E above 900C. However, the ATR-2E has the closest rate behavior to A3-3 and the discrepancy at high temperatures is relatively low, so the use of A3-3 is still reasonably approximate.

## 8.2. Differences between NACOK and Other Graphite Corrosion Experimental Results

There is discussion in the HTGR community regarding wide differences between such experimental results surrounding the capacity for nuclear graphite to burn in a potential air ingress accident. For instance, the oft-referred to Hanford experiment (1) of applying an oxyacetylene torch to graphite, which showed no appreciable oxidation or "burning," while the two NACOK experiments have pointed to large temperature increases due to graphite reactions with air, along with significant and possible structurally compromising graphite burn-off amounts.

Resolving these differences was recently made a priority by this community in the spring of 2009 (1). Reasons for potential discrepancies between these experiments are several. For

instance, the presence of significant amounts of dust, which can ignite, can cause changes air properties for heat capacity significantly. The amount of contained and heated space affects cooling, the air velocity around the graphite, and containment of other gases such as CO which also react with the graphite. All these factors affect whether there will be significant corrosion or burning.

## 8.3. The Burning Question

The question of whether the graphite would "burn" and how, is complicated. Using the theories and conclusions by Syd Ball (18), however, the ignition temperature is found to be necessary in order to sustain a flame. Likewise, Moormann et al discussed the necessary conditions for burning and illustrated these included at least a self-sustaining reaction above an ignition temperature (17).

In the case of these experiments, both of these can be addressed readily. Regarding ignition temperature, although there is much variation on prediction of this value, it can be assumed to be on an order of magnitude far higher than considered in at least our experiments, for instance, 2000K, while the maximum temperature reached in either NACOK test is under 900C or 1173K. This conclusion is solidified by Ball's conclusion that oxygen, even in the worst case scenarios, is generally consumed long before reaching the pebbles. In the NACOK tests, what was observed was significant corrosion of the graphite at test temperatures but no reported burning. This corrosion becomes a structural problem requiring mitigation action either to lower the temperature of the graphite or halt the air ingress.

# 9. NODAL CODE AND IMPLEMENTATION IN MELCOR

Given the time consuming FLUENT analysis and needed simplifications which contribute to non-physical results of certain parameters and the difficulty in data mining given the complexity of the multi-variable phenomenon, a simpler fundamental model will be developed for use in a nodal code such as MELCOR. MATLAB was used to develop a nodal code to be used as a subroutine in the MELCOR code to analyze the effects of air entering the graphite and fuel zone in a pebble bed reactor.

Access to the source code for MELCOR could have been useful in order to better formulate the code to work in tandem seamlessly. However, having a stand-alone application is both useful and potentially necessary. Because the chemical reactions, flow, and temperature are all dependent and must be calculated iteratively, it is necessary this code form its own iterations and using time steps which may require significantly more iterations and smaller time steps than possible or useful within MELCOR. The inputs were, however, designed to be as similar as possible to what MELCOR requires for its runs especially within heat structures, and the heat contributions due to chemical reactions could then be input at appropriate points into MELCOR.

## 9.1. THE 1-D MATLAB CODE

A one dimensional nodal code was developed to model transient simple buoyant flow in a chimney, or in LOCA terms, for a double-guillotine break in a graphite-moderated gas reactor, which constitutes a worst case, if unreasonable, scenario. However, with proper user definitions, it could likely be used to calculate reaction heat source terms for an existing more complicated code. It includes basic geometry definitions for each section, and vertical nodes for each time step within a section calculated dependent on the velocity for the section and overall buoyancy.

The code calculates and keeps track of the values for oxygen, carbon monoxide, carbon dioxide, heat generated by each reaction, heat transferred to and from the air, heat transfer between graphite sections or within the graphite, the temperature of graphite and the gas temperature, and errors calculated for both gas and graphite temperatures at each location for a time step. The code is then able to output these values both as averages for a section and in detail with height for all sections. The code has customizable time steps and overall run times,

along with relaxation factors for heat transfer mechanisms, and initialization values for inlet air temperature and graphite temperature and inlet air species concentrations.

The code is essentially composed of two nearly identical pieces: the initial flow through the vertical nodes until the time is long enough that the initial flow has reached the outlet, and then the continuation of the transient through to the total amount of time desired. For each node at a point in time, heat transfer terms are calculated along with chemical reactions, which then determine changes in species concentrations and heat sources or losses. All of these terms are dependent on temperature terms for the air and the graphite. A simplified illustration of the flow of the code is given below, where the indices n, i, and j signify time step, section, and slice, respectively.

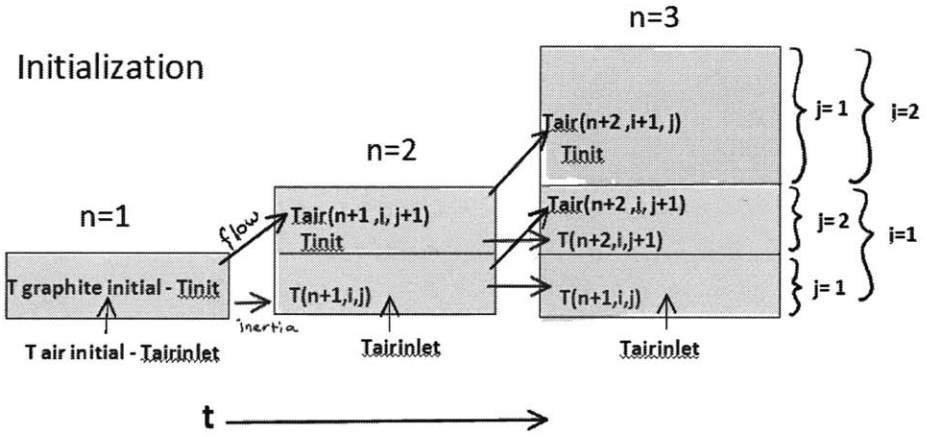


FIGURE 9-1: SCHEMATIC FOR TEMPERATURE ($T_{AIR}$, $T_{GRAPHITE}$) IN CODE BETWEEN NODES (I) AND SLICES WITHIN NODES (J) WITH TIME (N)

It can be seen that with the progression of each time step, the new calculation for the air temperature is then used for the next slice because of the air flow, while the new calculation for graphite is used in the same slice because of the inertia of the heat in the graphite. Not shown are the calculations for heat generation and loss terms including the reactions, conduction, convection, and radiation. Details of these calculations are described in detail below.

First, initial conditions for the overall setup are defined, which include:

$T_{in}$ = air temperature at inlet [Kelvin (K)]. This is the ambient temperature at the break.

$T_{out}$ = estimated air temperature at outlet of the reactor [K]. This should be the previous outlet temperature of the structure. This is necessary to get a rough estimate for air velocity due to buoyancy.

$A_{in}$ = cross sectional area at inlet [$m^2$]

$z_{tot}$ = height of buoyancy section [m], which is usually the height of the reactor vessel between breaks

$p_{O2i}$ = inlet oxygen partial pressure [Pa/Pa]

$p_{CO2i}$ = inlet carbon dioxide partial pressure [Pa/Pa]

$p_{COi}$ = inlet carbon monoxide partial pressure [Pa/Pa]

$CXA$ = cross-sectional area of the outermost geometry, for instance, for an empty section or the section containing pebbles. [$m^2$] This assumes a constant outer geometry for the 1-D channel.

Then, structure of the individual nodes is defined by the following parameters:

$z_i$ = height of the i-th node or section [m]

$A_{surfpz}$ = effective graphite surface area for node [$m^2$]

$por(i)$ = porosity of the node [dimensionless]

$CL_{air}$ = critical length for heat transfer through solid media [m]

Using these parameters, the initial rough estimation for mass flow rate through the 1-D vertical channel due to buoyancy can be calculated.

$$\dot{m} = \rho_{air} \cdot A_{in} \cdot \frac{\sqrt{2 \cdot g \cdot z_{tot} \cdot \Delta T \cdot T_{in}}}{T_{in} + \Delta T} [kg/s]$$

9-1

$$\rho_{air} = \frac{101325}{R_{dry} \cdot T_{avg}} [\text{kg/m}^3]$$

9-2

$$\Delta T = T_{out} - T_{in}$$

9-3

where

$\dot{m}$ = mass flow rate [kg/s]

$\rho_{air}$ = air density [kg/m$^3$], assuming dry air, approximately ideal gas, and atmospheric pressure.

$g$ = gravitational acceleration constant=9.81 [m/s$^2$]

$z_{tot}$ = height of buoyancy section [m]

$\Delta T$ = change in air temperature in buoyancy section height [consistent units, e.g., K]

$T_{avg}$ = average air temperature

Using this overall mass flow rate, the velocity of air can be calculated for each node section, using:

$$v = \frac{\dot{m}}{por(i) \cdot A_{xs}} [\text{m/s}]$$

9-4

where

$v$ = velocity [kg/s]

$\dot{m}$ = mass flow rate [kg/s]

$A_{xs}$ = cross-sectional area [$m^2$]

$por(i)$ = porosity of the ith section [dimensionless]

The velocity then determines the number of nodes (index j) of each section calculated per time step by using the ratio:

$$ii(i) = \frac{z_i}{ts \cdot v}$$

9-5

where

$ts$ = time step size [s]

which then also determines a volume and surface area for each slice.

The reaction rates for each slice are then calculated in order of reaction magnitude, starting with the first slice with a given incoming air composition. The reaction rate for the oxidation of carbon to produce carbon dioxide and carbon monoxide is by far the most significant reaction, on the order 10^6 times greater than the oxidation of carbon monoxide and another 10^6 times greater still than the Boudouard reaction of carbon dioxide with carbon in the ranges of temperatures seen in the experiment (about 600C to 1300C). This was discussed in Section 2.5 and shown in Figure 2-3 and Figure 2-4. Although in reality the reactions are occurring simultaneously, they are calculated successively in the code per each slice. The amount of error introduced by this method is limited by calculating the most significant reactions first, followed by successively smaller magnitude reactions, which have been shown to be almost negligible compared with the graphite oxidation reactions.

As conventionally used in many studies (16) (18) (19), the Arrhenius form of the reaction rate is taken. This also allows for easier translation for different types of graphite, and customization of activation energies and coefficients by the user. The reaction rate equations used to model NACOK are as follows.

The reaction of oxygen in the air with carbon was taken from the NACOK report released by the Julich institute (20) which found the reaction rate takes the Arrhenius form and added a modification based on velocity:

$$RO2 = \left( \frac{1}{(7.2 \cdot 10^9) \cdot e^{-\frac{16140}{T}} \cdot pO2i(n,i,j))} + \frac{1}{(770) \cdot v^{0.65} \cdot T^{0.34} \cdot pO2i(n,i,j)} \right)^{-1}$$

9-6

[mg-C / cm$^2$-h]

Which assumes a reaction constant of $7.2 \cdot 10^9$ mg/cm$^2$-h, and an activation energy of 16140/R. This equation was also useful because it placed the form of the equation into units of mass per surface area per time.

The reaction rate RO2 is then multiplied by the time step and surface area, and converted from mg to get moles of oxygen reacted in the slice for the time step. This is then subtracted from the partial pressure of oxygen, pO2i(n,i,j), where n represents the time step, i represents the node or section, and j represents the time step slice of the section.

The ratio of RO2 reacted which results in carbon monoxide or carbon dioxide is calculated by many sources for many types of graphite. One definitive calculation of this ratio for nuclear grade graphites was done by Takeda (13), and the ratio, "A", is given as follows:

$$A = \frac{CO}{CO_2} = (7943) \cdot e^{-\frac{78300}{R \cdot T}}$$

9-7

which then means that the ratio of CO produced to total product is given by A/(A+1) and the ratio of CO2 produced to total product is given by 1/(1+A).

Since the equations for oxygen reacting with carbon are stoichiometrically represented by

$$0.5O_2 + C \rightarrow CO$$

9-8

$$O_2 + C \rightarrow CO_2$$

9-9

Using this, the increase in CO and CO2 for each mole of C reacted in slice (n,i,j) are then calculated by

$$dmolCO = RO2mol \cdot \frac{A}{A+1}$$

9-10

and

$$dmolCO_2 = RO2mol \cdot \frac{1}{A+1}.$$

9-11

And the consumption of oxygen is given by

$$dmolO_2 = RO2mol \cdot \frac{1}{A+1} + 0.5 \cdot RO2mol \cdot \frac{A}{A+1} = RO2mol \cdot \frac{0.5 \cdot A + 1}{A+1}$$

9-12

Next, if the amount of carbon monoxide for the slice, pCOi(n,i,j) is greater than zero, the reaction for carbon monoxide with oxygen is calculated, using another equation by Takeda (13).

This is not a surface reaction, like oxygen with the carbon on the graphite surface, but instead is volumetric.

$$RCOnO2 = (1.3 \cdot 10^8) \cdot e^{-\frac{126000}{R \cdot T}} \cdot pCOi(n,i,j) \cdot (pO2i(n,i,j))^{0.5} \cdot (pCOi(n,i,j))^{0.5}$$

9-13

[mol/m$^3$-s]

The change in the quantity of CO, CO2, and O2 is then calculated in similar fashion per slice, per time step.

Last, the endothermic reaction between carbon dioxide and the graphite producing carbon monoxide, or the Bouduoard reaction is evaluated. In this case, carbon dioxide is the limiting agent, but it is assumed that carbon dioxide is not in such limited quantities to affect the reaction. So, if the partial pressure of carbon dioxide is greater than zero, the following rate equation is calculated:

$$RCO2nC = (2220) \cdot e^{-\frac{306350}{R \cdot T}}$$

9-14

[mol C / m$^2$-s]

Finally, the change in CO and CO2 are similarly calculated.

These three reaction rates provide the cumulative heat generated due to the exothermic reactions or lost due to the endothermic reactions. The heat of reaction for each equation is given below.

TABLE 9-1: HEAT OF REACTION FOR CHEMICAL REACTIONS

| | Reaction | $\Delta H$ (J/mol) |
|---|---|---|

| | | |
|---|---|---|
| Graphite Oxidation | $0.5O_2 + C \rightarrow CO$ | 111,000 |
| | $O_2 + C \rightarrow CO_2$ | 394,000 |
| O2 and CO | $0.5O_2 + CO \rightarrow CO_2$ | 283,000 |
| Boudouard | $CO_2 + C \rightarrow 2CO$ | -172,000 |

Conduction, convection and radiative heat transfer terms are then calculated for each slice in similar units of Joules. Other than the carbon monoxide oxidation reaction, the reaction heat terms are considered as being effectively added directly to the graphite surface, because the conductivity of graphite is so much higher than that of air, and the reaction is occurring at the graphite/air interface. Heat gains and losses are calculated for conduction of the slice versus the slices above and below, for convection and radiation to and from the air, and, if there is no graphite and just a wall, to and from the wall to the air. The wall temperature is held at a constant temperature in the current formulation of the code.

The equation used to calculate the convection to and from the air to the graphite (or the wall) in a timestep slice was taken from Todreas and Kazimi (27) and is as follows:

$$Qfromwall_{\text{OR}}\, Qtoair1 = Asurfts(n,i) \cdot \frac{k}{CL} \cdot (24/11) \cdot (T - Tair(n,i,j)) \cdot ts$$

9-15

[J]

Where

$Asurfts(n,i)$ = the surface area per time step, or a ratio of the number of nodes in a section to the total surface area per section, or zone, Asurfpz. It has a time index because of incorporation of burnoff effects on surface area with time.

$k =$ the conductivity of air

$CL = \frac{4 \cdot A_{xs}}{P_w}$, or the critical length, where $P_w$ is the wetted perimeter.

A second equation as a very rough approximation for heat transfer to and from air, due to radiative heat transfer, is given as:

$$Qtoair3 = arad \cdot Asurfts(n,i) \cdot B \cdot \varepsilon \cdot (Tavg^4 - Tair(n,i,j)^4) \cdot ts$$

9-16

[J]

Where

$arad =$ relaxation constant for radiative heat transfer because the calculations are very volatile.

$B =$ Boltzmann constant

$\varepsilon =$ emissivity, which can be modified accounting for the humidity of the air, in this case held as a constant at 0.35 for dry air and 0.45 for steam.

$B = 5.67 \cdot 10^{-8}$ [W/m$^2$-K$^4$]

$Qtoair2$ is the heat to the air due to the carbon monoxide oxidation heat production:

$$Qtoair2 = QCOnO2$$

9-17

[J]

Last, the conduction equations for heat transfer between slices in the same section are:

$$Qcondin = \frac{k_{graphite} \cdot (1 - por(i)) \cdot (T(n,i,j-1) - T(n,i,j)) \cdot ts}{zi(i)/ii(i)}$$

9-18

$$Qcondout = \frac{k_{graphite} \cdot (1 - por(i)) \cdot (T(n-1,i,j+1) - T(n,i,j)) \cdot ts}{zi(i)/ii(i)}$$

9-19

Here, "in" and "out" are used to signify heat transfer of the previous or following slice, respectively, and is not meant to indicate whether the heat is lost or gained to the previous or following slice. Both Qcondin and Qcondout can be positive or negative indicating heat lost or gained by the current slice.

For heat transfer between a slice and the previous section:

$$Qcondin = \frac{k_{graphite} \cdot (1 - por(i)) \cdot (T(n,i-1,ii(i-1)) - T(n,i,j)) \cdot ts}{0.5 \cdot (zi(i)/ii(i)) + 0.5 \cdot (zi(i-1)/ii(i-1))}$$

9-20

And for heat transfer between a slice and the following section:

$$Qcondout = \frac{k_{graphite} \cdot (1 - por(i)) \cdot (T(n-1,i+1,1) - T(n,i,j)) \cdot ts}{0.5 \cdot (zi(i)/ii(i)) + 0.5 \cdot (zi(i+1)/ii(i+1))}$$

9-21

For the conduction between different sections, it is assumed that the contact between the graphite blocks is approximated by the porosity ratio.

Finally, it is possible to calculate a total graphite heat loss and gain per slice:

$$Qtot3(n,i,j) = -Qtoair(n,i,j) + QOtoCO(n,i,j) + QOtoCO2(n,i,j) + QCO2nC(n,i,j) + Qcondin + Qcondout$$

9-22

[J]

And similarly for air:

$$Qtotair(n,i,j) = Qtoair(n,i,j) + Qfromwall(n,i,j)$$

9-23

[J]

Using these heat transfer equations, new temperatures for air and graphite can be calculated. The temperature of the graphite for the next time step is calculated:

$$T(n+1,i,j) = T(n,i,j) + \frac{1}{Cp\_C \cdot m\_C} \cdot Qtot3(n,i,j)$$

9-24

And for air:

$$Tair(n+1,i,j+1) = Tair(n,i,j) + \frac{1}{Cp\_air \cdot \rho_{air} \cdot Volts(i)} \cdot Qtotair(n,i,j)$$

9-25

Where

$Cp\_C$ = specific heat of graphite

$Cp\_air$ = specific heat of air, in this case, similar to the emissivity, is modified to account for the humidity of air, and is held as a constant.

Last, the species concentrations must be updated. This is done by taking a ratio of the moles of the species reacted in each reaction and the ideal gas equation to find a change in partial pressure of the species.

For example,

$$delO2 = \frac{dO2 + dO2\_1}{P_{atm} \cdot Volts(i) \Big/ 8.314 \cdot T}$$

9-26

$dO2$ = change in $O_2$ from graphite oxidation

$dO2\_1$ = change in $O_2$ from carbon monoxide oxidation

Then, pO2i(n+1,i,j+1) is updated:

$$pO2i(n+1, i, j+1) = pO2i(n, i, j) + delO2$$

9-27

And this is done similarly for each of the other species tracked: CO and CO2.

## 9.2. A POTENTIAL REFINEMENT FOR CALCULATION OF VELOCITY IN CASE OF HIGH VISCOSITY

The equations Zhai used to calculate velocity vs. viscosity are:

$$\Delta P_1 = (\rho_{cold} - \rho_{hot}) \cdot g \cdot h$$

9-28

This is the basic buoyancy force equation, where:

$\rho_{hot}$ = hot density of the air

$\rho_{cold}$ = cold density of the incoming air

$g$ = gravitational acceleration

$h$ = height

And the pressure drop in pebble bed correlation given by the Germans:

$$\Delta P_2 = \Psi \cdot (\frac{H}{d}) \cdot (\frac{1-\varphi}{\varphi^3}) \cdot \rho_{hot} \cdot \frac{v^2}{2}$$

9-29

Where

$H$ = height

$d$ = diameter of the pebbles

$\varphi$ = porosity

$v$ = velocity of the air

and $\Psi$ is a function of porosity and of the Reynold's number, Re, given by:

$$\text{Re} = \frac{d_{pebble} \cdot v \cdot \rho_{hot}}{\mu}$$

9-30

Where

$\mu$ = viscosity

All the geometry factors- height, diameters, porosity- are constant with temperature, and the cold density stays at atmospheric or some other relatively fixed temperature, so these two equations reduce to being functions of the following variables:

Delta P1 = f ( $\rho_{hot}$ )

Delta P2 = f ( $\Psi$ ( $v$ , $\rho_{hot}$ , $\mu$ ), $\rho_{hot}$ , and $v$ )

All of which are variables dependent on temperature.

As can be seen by the below plots of Viscosity and Density, at the reasonable hot temperatures of between 400 C and 1200 C (and up), density of air reaches a limit and is nearly constant with increasing temperature. However, viscosity only continues to increase.

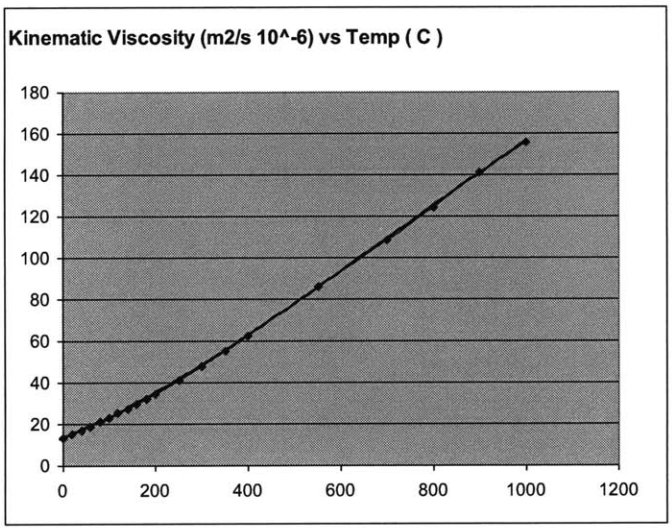


FIGURE 9-2: AIR PROPERTY OF KINEMATIC VISCOSITY VS. TEMPERATURE

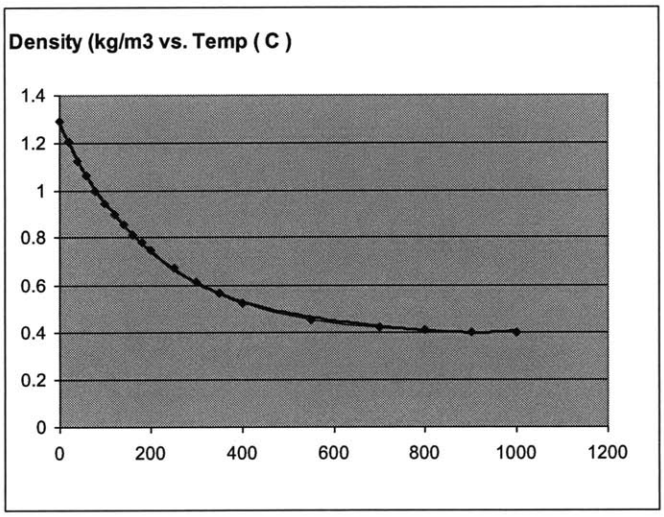


FIGURE 9-3: AIR PROPERTY OF DENSITY VS. TEMPERATURE

Zhai's formulation was iterative and does not allow for direct calculation of velocity. So, in order to develop a formulation which allows for direct calculation of velocity, which will be useful to the code, the equations are simplified so that velocity can be solved for. A simplifying assumption is to assume the hot density as a constant value. It is reasonable to assume the hot density as the constant value of 0.4, since it is reasonably constant from about 650C to 1000 C, which are the temperature values for most of the air ingress experiments. Moreover, this is a conservative assumption, only overpredicting velocity, and the overprediction only decreasing with increasing temperature as seen in Figure 9-4. Although these equations were derived assuming the hot density as a constant, it can also be calculated as a function of temperature, and these calculations are also shown in Figure 9-4.

The functions are:

$$\Delta P_1 = \Delta P_2$$

Which leads to an equation of the form

$$C_1 \cdot (v^{1.9}) \cdot (\mu^{0.1}) + C_2 \cdot (v) \cdot (\mu) = C_3$$

9-31

Where $C_1$, $C_2$, and $C_3$ are the respective constants regarding geometry, porosity, etc.

This formulation also does not allow direct isolation of velocity from viscosity. So, v^1.9 is approximated as v^2, which makes this equation a quadratic equation, and the solution given by the quadratic solution. Because we are defining v as positive, only the positive root is taken.

$$C_1 = a = \frac{(1-\varphi)^{1.1} \cdot 6 \cdot \rho_{hot}}{d^{1.1} \cdot \varphi^3 \cdot g \cdot \rho_{cold}}$$

9-32

$$C_2 = b = \frac{(1-\varphi)^2 \cdot 320}{d \cdot \varphi^3 \cdot g \cdot \rho_{cold}}$$

9-33

$$C_3 = c = \frac{\rho_{hot}}{\rho_{cold}}$$

9-34

The final equation is given:

$$v = \frac{-\left[\frac{(1-\phi)^2 \cdot 320}{d}\right] \cdot \mu(T) + 2 \cdot \phi^2 \cdot g \sqrt{\left[\frac{(1-\phi)^4 \cdot 160^2}{d^2 \cdot \phi^4 \cdot g^2}\right] \cdot \mu(T)^2 - \left[\frac{(1-\phi)^{1.1} \cdot 6 \cdot \rho_h{}^2}{d^{1.1} \cdot \phi \cdot g}\right] \cdot \mu(T)^{0.1}}}{\left[\frac{(1-\phi)^{1.1} \cdot 12 \cdot \rho_h}{d^{1.1}}\right] \cdot \mu(T)^{0.1}}$$

9-35

Using this formulation gives a good approximation to the velocities calculated by Zhai, with a reasonable overprediction, as shown in Figure 9-4. Two ways of calculating were then tried: one using different hot densities in the equation, the "variable ph" line shown in Figure 9-4, and using only the hot density at the limit, shown by the line labeled as "ph at limit". The dotted line is the average of the two, and seems to be an excellent approximation, down to about 200 degrees Celsius, which could then be linearly approximated to 0 at 0 delta T. This is a potentially valuable refinement for the 1-D code in order to calculate velocities, which are vitally important to chemical reaction behavior.

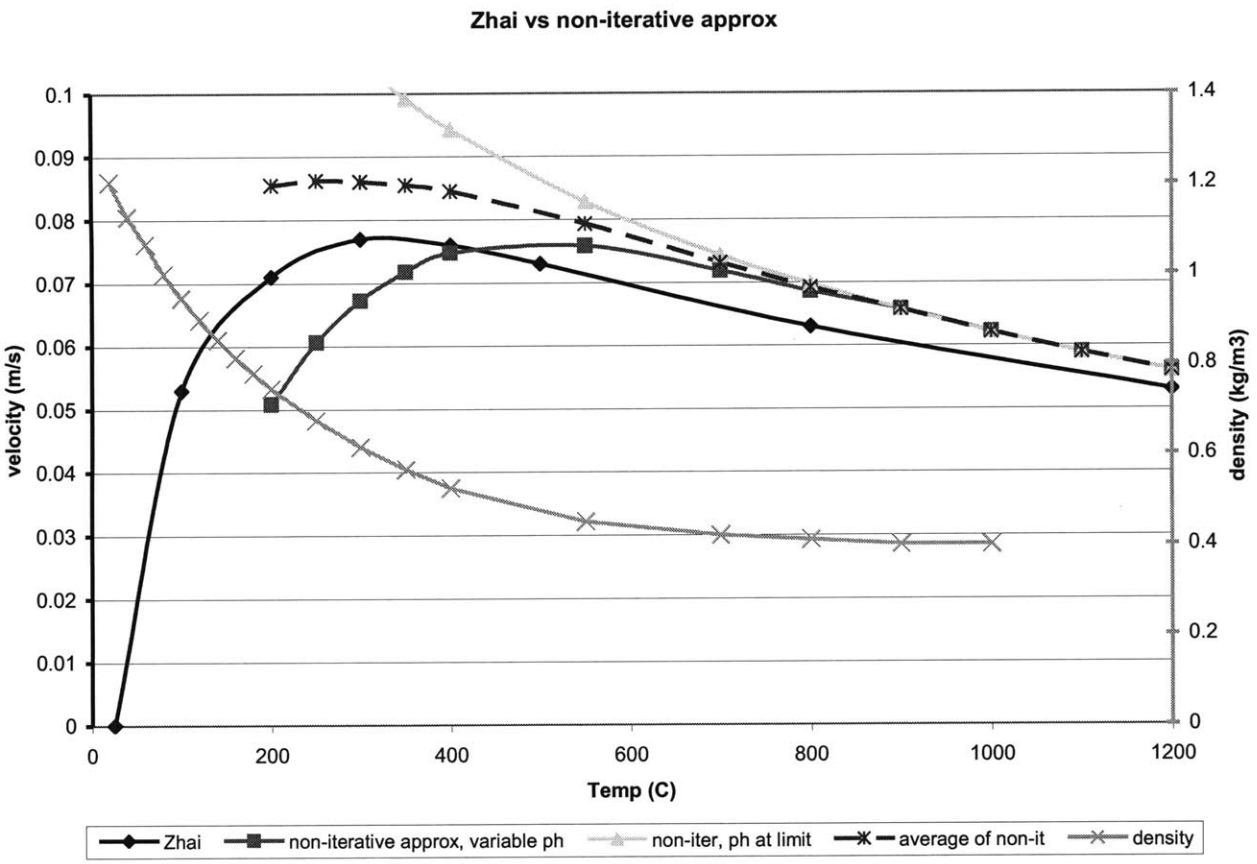


FIGURE 9-4: NON-ITERATIVE CALCULATION OF AIRFLOW VELOCITY

## 9.3. SENSITIVITY ISSUES AND CODE/CORRELATION INSTABILITIES

### *9.3.1. PHYSICAL SOURCES OF INSTABILITY*

In Figure 8-1 and Figure 8-2, the reaction rates for the graphite oxidation reaction for different graphites were shown, which illustrated the strong dependence of reaction rates on temperature. Clearly, the temperature of the experiment at initialization, and the local temperatures through the experiment influence the reaction rate, which then affects all the other parameters, importantly, burnoff and the ratio of carbon monoxide and carbon dioxide, as well as heat production, which then affects temperature in a circular effect. The effect of burnoff is significant and further increases reaction rates by increasing surface area. As shown by Brudieu's work on sensitivity, and copied in Figure 9-5, the burnoff is affected dramatically by

temperature, and further, that the temperature of the experiment is highly sensitive to the Arrhenius constant used.

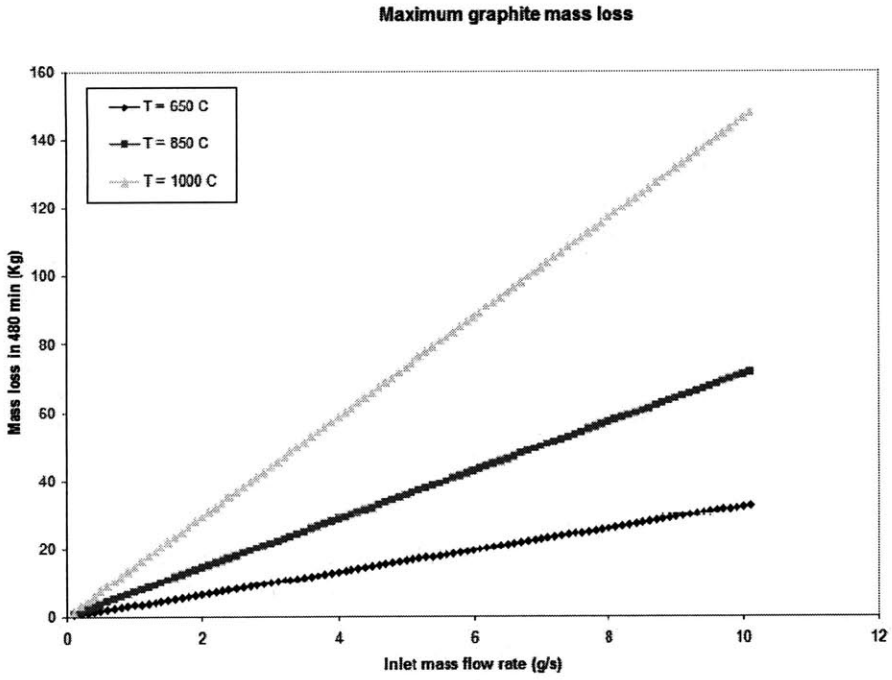


FIGURE 9-5: TOTAL BURNOFF IN 8 HOURS AT DIFFERENT INITIAL TEMPERATURES VS. MASS FLOW RATE (18)

All of these nonlinearities contribute to fundamental instabilities in creating a code, not to mention other physical properties affected by temperature and burnoff, such as airflow velocity, heat capacity, density, and viscosity.

### *9.3.2. NUMERICAL METHOD OR CODING SOURCES OF INSTABILITY*

The other side of coding instabilities is inherent in the solution method of the code. The formulation of the solutions and iterations also directly impact computation time. Methods for reducing instability include adding relaxation factors and error corrections at each step. These have both been implemented in the current code. However, use of the relaxation factors should be used cautiously unless considering the code as solving for steady state. Because there are not

iterations for each time step, using relaxation factors effectively changes the heat produced per time step artificially.

Understanding these limitations to predictive value and accuracy are imperative to use of this code. Moreover, these issues explain why such a code should be considered a work in progress; never having a definitive, final single result which is not able to be further refined.

### *9.3.3. Comparison to NACOK Data*

Figure 9-6 compares code output to NACOK data from the open chimney. As can be seen, the code is not necessarily conservative, but does provide output of a similar magnitude to experimental data. Differences between the NACOK setup and the MATLAB model include assumptions on the conduction within the graphite and through the graphite blocks into the wall.

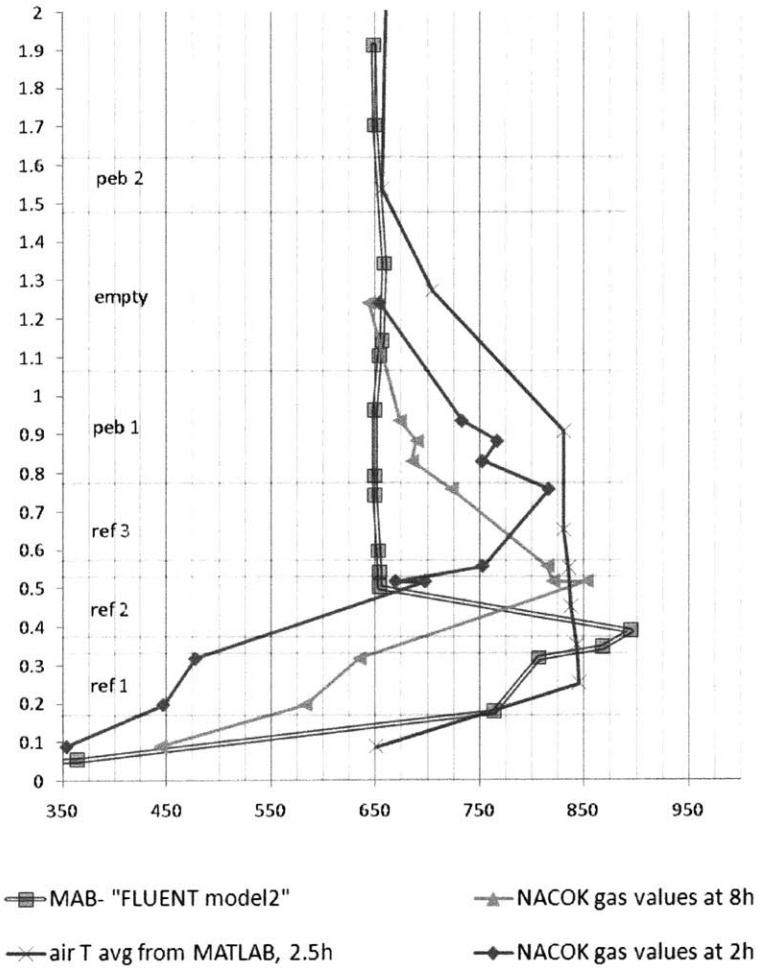


FIGURE 9-6: CODE OUTPUT COMPARED TO NACOK OPEN CHIMNEY AND PREVIOUS FLUENT MODEL, GAS TEMPERATURE (C) V. HEIGHT (M.)

### *9.3.4. THE MELCOR MODEL OF THE NACOK EXPERIMENT*

A simple, pure flow with temperature model was created in MELCOR (28), with structure as shown in Figure 9-7. The numbers are flow paths through each control volume.

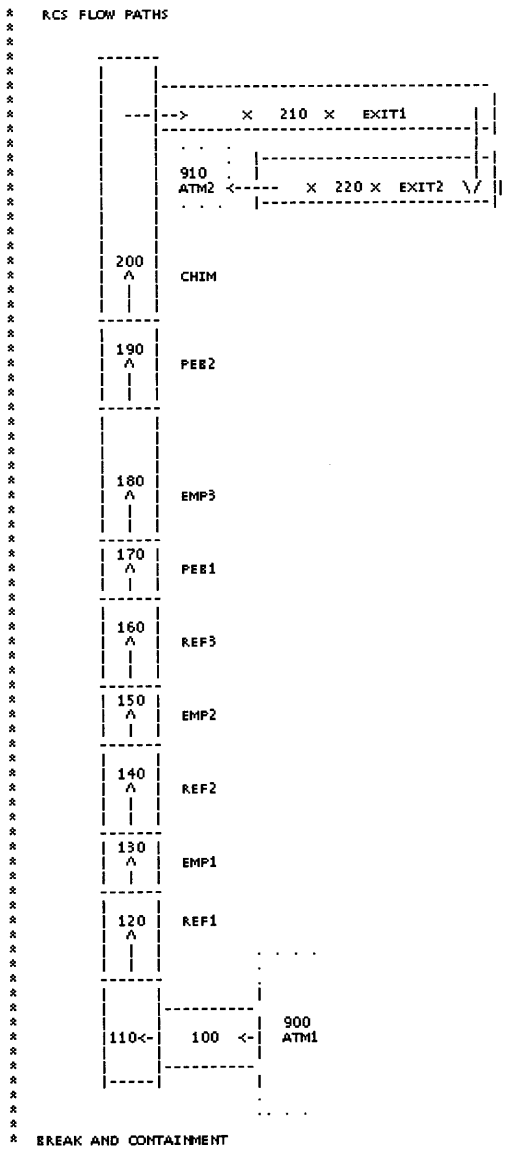


FIGURE 9-7: MELCOR SIMPLE MODEL

This model was run and showed a quick depressurization and equalization with the environment. Ultimately, the exercise of building a simplistic MELCOR model helped to inform the structure of the code, without providing useful data because it is not structured to include chemical reactions.

# 10. CONCLUSION

The previous MIT work was reviewed and the inquiry into the reasons for the portions of non-physical results obtained through past FLUENT models showed that FLUENT is unable to accurately calculate temperature in a steady state analysis using porous media, because of the assumptions inherent in the calculation method for temperatures in a porous media. The 2-D FLUENT model was described, and shown to have some beneficial results. Further development could potentially use 2-D FLUENT models as reasonable approximations to the 3-D with faster runtimes.

The data provided by the NACOK experiments was reviewed and assessed with respect to data mining for correlations for potential use in a code or correlations characterizing the effects of graphite oxidation on the HTGR air ingress accident. Simple correlations between the data were found. The difficulties for data mining in this project are presented, along with some reflections on the potential for data mining in general, to inform analyses of the graphite oxidation process in air ingress accidents.

Finally, the 1-D MATLAB code was described, which is at a point that can produce some reasonable results although the outputs are highly subject to instabilities. The code overcomes the described limitations found in FLUENT, and the limitations of the data set, which is surprising given its relative simplicity. The sample results of the code showed remarkable similarities to the NACOK data considering the simplistic formulas used. Given the potential usefulness of this code, future work to address the source of instabilities should be pursued. The exercise of building a simplistic MELCOR model helped to inform the structure of the code, however, it would be advantageous for any future work on similar subroutines to be given access to the source code for MELCOR.

# REFERENCES


1. **Facilitated by Bryan Parker and William West.** *Technology Integration Review for NGNP Air Ingress.* Salt Lake City, Utah : s.n., 2009.

2. **Kuhlmann, M. B.** *Experiments to Investigate Flow Transfer and Graphite Corrosion in Case of Air Ingress Accidents in a High Temperature Reactor.* s.l. : Report of the Julich Research Center, NRC Translation 3686, 2002. ISSN 0944-2952.

3. Fluent 6.3 User's Guide. s.l. : copyright 2006 by Fluent Inc., Sept 2006.

4. **Matzi, R. A.** Pebble Bed Modular Reactor (PBMR) Project Update. s.l. : Westinghouse Electric Company, Presentation on June 16, 2004.

5. **Venter, Pieter J.** Integrated Design Approach of the Pebble Bed Modular Reactor Using Models. *Nuclear Engineering and Design.* 2007, Vol. 237.

6. **Ion, S., et al.** Pebble Bed Modular Reactor- The First Generation IV Reactor to be Constructed. *Nuclear Energy.* 2004, Vol. 43, 1, Feb.

7. **Baker, D.E.** Graphite as a Neutron Moderator and Reflector Material. *Nuclear Engineering and Design.* 1970, Vols. 14: 413-444.

8. **Oh, Chang H., et al.** *Experimental Validation of Stratified Flow Phenomena, Graphite Oxidation, and Mitigation Strategies of Air Ingress Accidents.* s.l. : Produced by Idaho National Labs for the U.S. Department of Energy, Dec 2008. INL/EXT-08-14840.

9. *Accident Simulation and Consequence Analysis in Support of MHTGR Safety Evaluations.* **Ball, S. J. et al.** s.l. : Water Reactor Safety Meeting, Oct. 27-30, 1991. CONF-9110210.

10. **Cussler, E. L.** *Diffusion: Mass Transfer in Fluid Systems, 2nd ed.* Cambridge, UK : Cambridge University Press, 1997.

11. **Turner, J. S.** *Buoyancy Effects in Fluids.* Cambridge, UK : Cambridge University Press, 1980.

12. *Analysis of Geometrical Effects on Graphite Oxidation through Measurement of Internal Surface Area.* **Kim, Eung Soo, et al.** s.l. : Journal of Nuclear Materials, 2006, Vols. 348: 174-180.

13. **Takeda, Tetsuaki and Hishida, Makato.** Studies on Molecular Diffusion and Natural Convection in a Multicomponent Gas System. *Int. J. Heat Mass Transfer.* 1996, Vol. 39, 3: 527-536.

14. **Kotz., John C. et al.** *Chemistry and Chemical Reactivity, 7th ed.* s.l. : Thomson Brooks/Cole, Feb 2008.

15. **Hayhurst, A.N. et al.** Does Solid Carbon Burn in Oxygen to Give the Gaseous Intermediate CO or Produce CO2 Directly? Some Experiments in a Hot Bed of Sand Fluidized by Air. *Chemical Engineering Science.* 1997, Vol. 53, 3.

16. *Oxidation Behaviour of Carbon-Based Materials Used for High-Temperature Gas-Cooled Reactors and Fusion Reactors.* **Moormann, R.** Florence (Italy) : Proceedings of the 9th CIMTEC, 1998.

17. **Moormann, R. et al.** *Corrosion Behaviour of Carbon-Based Materials for High-Temperature Gas-cooled Reactors and Fusion Reactors in Oxidizing Gases.* s.l. : the European Union NET/ITER technology contracts, 5th EU framework program, 2000.

18. **Kuhlmann, M. B.** Experiments to Investigate Flow Transfer and Graphite Corrosion in Case of Air Ingress Accidents in a High-Temperature Reactor. 1999.

19. **Kadak, Andrew C. and Zhai, Tieliang.** Air Ingress Benchmarking with Computational Fluid Dynamics Analysis. *Nuclear Engineering and Design.* 2006, 236: 587-602.

20. **Zhai, Tieliang.** *LOCA and Air Ingress Accident Analysis of a Pebble Bed Reactor.* s.l. : copyright Massachussetts Institute of Technology, Thesis submitted Aug 2003.

21. **Brudieu, Marie-Anne.** *Blind Benchmark Predictions of the NACOK Air Ingress Tests Using the CFD Code FLUENT.* s.l. : copyright 2007 Massachusetts Institute of Technology, Feb 2007.

22. **Parks, Benjamin T.** *Using the FLUENT Computational Fluid Dynamics Code to Model the NACOK Corrosion Test.* s.l. : Massachusetts Institute of Technology, Thesis Submitted Aug 2004.

23. *Base SAS 9.2 Procedures Guide: Statistical Procedures, Second Edition.* September 2009.

24. **Franzblau, A.** *A Primer of Statistics for Non-Staticians.* s.l. : Harcourt, Brace & World, 1958.

25. **Fayyad, Usama, et al.** From Data Mining to Knowledge Discovery in Databases. *AI Magazine, American Association for Artificial Intelligence.* Fall, 1996.

26. **Oh, Chang, et al.** *Development of Safety Analysis Codes and Experimental Validation for a Very High Temperature Gas-Cooled Reactor.* s.l. : Idaho National Lab (INL), Mar 2006. INL/EXT-06-01362.

27. **Petti, DA, et al.** Key Differences in Fabrication, Irradiation, and High Temperature Accident Testing of US and German TRISO-Coated Particle Fuel, and Their Implications on Fuel Performance. *Nuclear Engineering and Design.* 2003, Vols. 222: 281-297.

28. **Todreas, N. and Kazimi.** *Nuclear Systems, Volume 1: Thermal Hydraulic Fundamentals, 2nd edition.* s.l. : Hemisphere Publishing Corp., 1990.

29. **Sandia National Labs for the U.S. Nuclear Regulatory Commission.** MELCOR Computer Code Manuals: Primer and User's Guide, Version 2.0. Sept 2008. Vols. Vol. 1, Rev.4. NUREG/CR-6119.

# APPENDIX A: THE MELCOR INPUT DECK

```
************************************************************************
*  SIMPLIFIED NACOK DOUBLE GUILLOTINE OPEN CHIMNEY EXPERIMENT MOCKUP   *
*   JAN 2009  -    CAROLINE COCHRAN -  UNDER PROF. KADAK                *
*                                                                      *
************************************************************************
*
*   RCS VOLUMES
*
*         -------
*         |     |-----------------------------------
*         |     |                                  |
*         |     |        X    210   X not used yet                 |
*         |     |----------------------------------|
*         |     |
*         |     |          |-------------------------|
*         |     |          |                         |
*         |     |          |   X     220   X           |
*         |     |          |-------------------------|
*         |     |
*         | 200 |  CHIM
*         |     |
*         |     |
*         |     |
*         -------
*         |     |
*         | 190 |
*         |     |  PEB2
*         |     |
*         |     |
*         -------
*         |     |
*         |     |
*         |     |
*         |     |
*         | 180 |
*         |     |  EMP3
*         |     |
*         |     |
*         -------
*         | 170 |
*         |     |  PEB1
*         |     |
*         -------
*         |     |
*         | 160 |
*         |     |  REF3
*         |     |
*         |     |
```

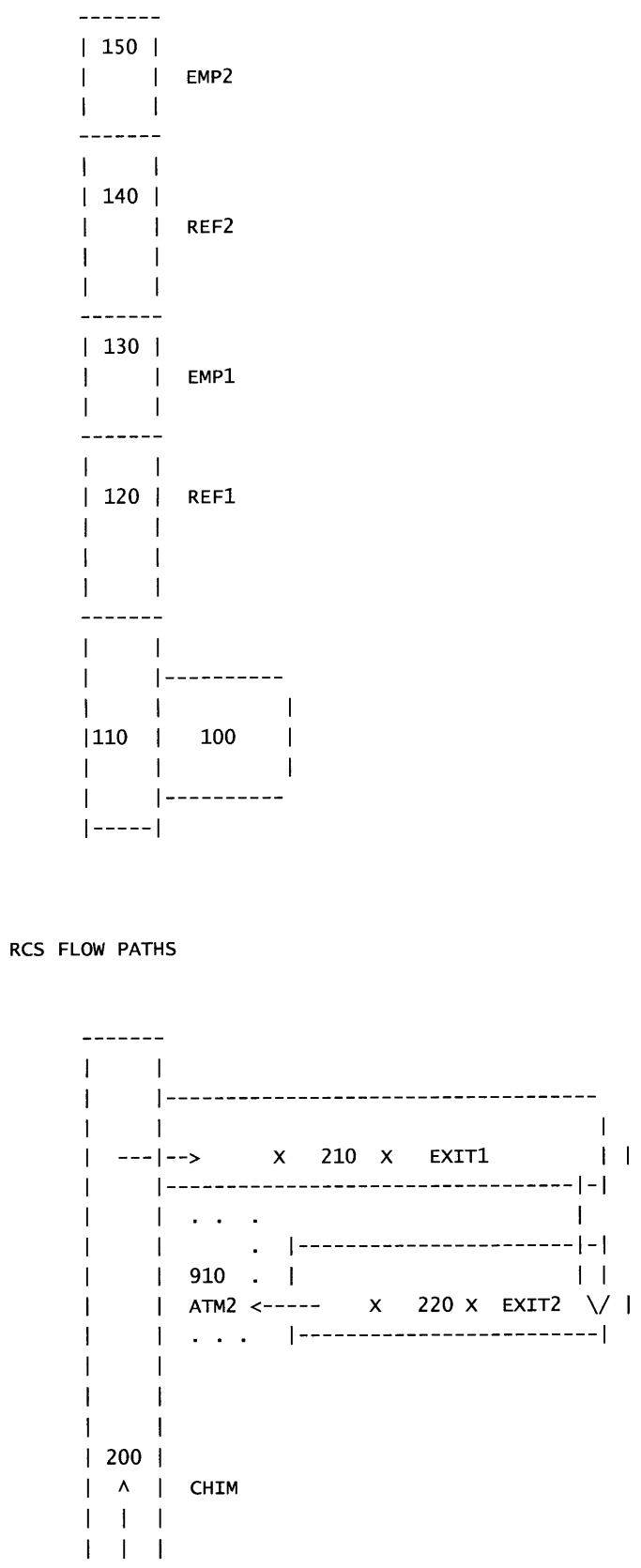
150
EMP2
140
REF2
130
EMP1
120
REF1
110
100
RCS FLOW PATHS
210
EXIT1
910
ATM2
220
EXIT2
200
CHIM

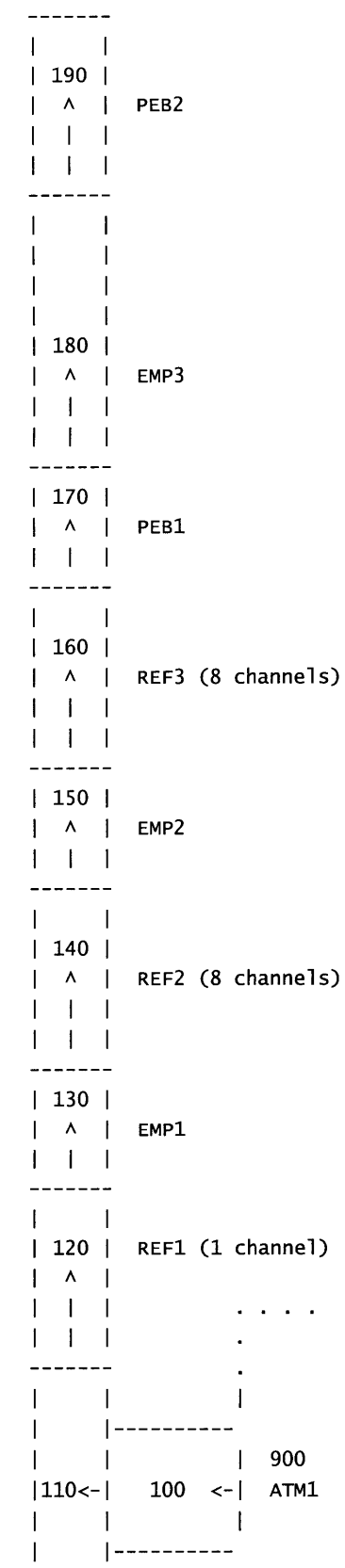
190
PEB2
180
EMP3
170
PEB1
160
REF3 (8 channels)
150
EMP2
140
REF2 (8 channels)
130
EMP1
120
REF1 (1 channel)
110
100
900
ATM1

```
*         |-----|          |
*                          .
*                          .. . .
*
*  BREAK AND CONTAINMENT
*
*
*eor* melgen
**********************
**********************
***                ***
***  MELGEN INPUT  ***
***                ***
**********************
**********************
*
TITLE     'Simple Nacok Mod Blowdown'
*
OUTPUTFILE   MODBLOWDOWN_G_OUT.txt
DIAGFILE     MODBLOWDOWN_G_DIA.txt
RESTARTFILE  MODBLOWDOWN.RST
*
*************
* NCG INPUT *
*************
*
NCG001     N2    4
NCG002     O2    5
*NCG003     CO2   6
*NCG004     CO    7
*
****************
* VOLUME INPUT *
****************
*
*         Name               Thermo flag Always use 2 (NEQ)
*         |                  |   Flow direction (unused)
*         |                  |   |   "Type" for RN accounting
*         vvvvvvvvvvv        v   v   v
*
CV10000   'Inlet'            2   2  20
CV100A1   PVOL 1.0E5                                              * 1 bar
CV100A3   TATM 923.   RHUM 0.2                                    * Atmosphere at 298 K, 20%
relative humidity
CV100A4   MLFR.4 1.0  MLFR.5 0.0  *MLFR.6 0.00056  MLFR.7 0.00001      * 80% N2, 20% O2
CV100B0    0.0    0.0                                             * 50000 m^3 between 0 and 50
m
CV100B1    0.17    .018
*
*
CV11000   'Open'           2   2  20
CV110A1   PVOL 1.0E5                  * 1 bar
```

```
CV110A3   TATM 923.    RHUM 0.2          * Atmosphere at 298 K, 20% relative humidity
CV110A4   MLFR.4 1.0  MLFR.5 0.0  *MLFR.6 0.00056  MLFR.7 0.00001       * 80% N2, 20% O2
CV110B0    0.0    0.0                                                  * 50000 m^3 between 0 and 50
m
CV110B1    0.17    .00255
*
*
CV12000   'Ref1'             2   2  20
CV120A1   PVOL 1.0E5                  * 1 bar
CV120A3   TATM 923.    RHUM 0.2       * Atmosphere at 298 K, 20% relative humidity
CV120A4   MLFR.4 1.0  MLFR.5 0.0      * 100% N2, 0% O2
CV120B0    0.17    0.0                                                  * 50000 m^3 between 0 and 50
m
CV120B1    0.33    0.0024
*
*
CV12000   'R1ch1of1'             2   2  20
CV120A1   PVOL 1.0E5                  * 1 bar
CV120A3   TATM 923.    RHUM 0.2       * Atmosphere at 298 K, 20% relative humidity
CV120A4   MLFR.4 1.0  MLFR.5 0.0      * 100% N2, 0% O2
CV120B0    0.17    0.0                                                  * 50000 m^3 between 0 and 50
m
CV120B1    0.33    0.000032
*
*
CV13000   'Emp1'             2   2  20
CV130A1   PVOL 1.0E5                  * 1 bar
CV130A3   TATM 923.    RHUM 0.2       * Atmosphere at 298 K, 20% relative humidity
CV130A4   MLFR.4 1.0  MLFR.5 0.0      * 100% N2, 0% O2
CV130B0    0.33    0.0                                                  * 50000 m^3 between 0 and 50
m
CV130B1    0.37    0.0006
*
*
CV14000   'Ref2'             2   2  20
CV140A1   PVOL 1.0E5                  * 1 bar
CV140A3   TATM 923.    RHUM 0.2       * Atmosphere at 298 K, 20% relative humidity
CV140A4   MLFR.4 1.0  MLFR.5 0.0      * 100% N2, 0% O2
CV140B0    0.37    0.0                                                  * 50000 m^3 between 0 and 50
m
CV140B1    0.53    .0024
*
*
CV14100   'R2ch1of8'             2   2  20
CV141A1   PVOL 1.0E5                  * 1 bar
CV141A3   TATM 923.    RHUM 0.2       * Atmosphere at 298 K, 20% relative humidity
CV141A4   MLFR.4 1.0  MLFR.5 0.0      * 100% N2, 0% O2
CV141B0    0.37    0.0                                                  * 50000 m^3 between 0 and 50
m
CV141B1    0.53    .000201
*
*
```

```
CV14200   'R2ch2of8'              2   2  20
CV142A1   PVOL 1.0E5                    * 1 bar
CV142A3   TATM 923.   RHUM 0.2          * Atmosphere at 298 K, 20% relative humidity
CV142A4   MLFR.4 1.0  MLFR.5 0.0        * 100% N2, 0% O2
CV142B0    0.37    0.0                                    * 50000 m^3 between 0 and 50
m
CV142B1    0.53    .000201
*
*
CV14300   'R2ch3of8'              2   2  20
CV143A1   PVOL 1.0E5                    * 1 bar
CV143A3   TATM 923.   RHUM 0.2          * Atmosphere at 298 K, 20% relative humidity
CV143A4   MLFR.4 1.0  MLFR.5 0.0        * 100% N2, 0% O2
CV143B0    0.37    0.0                                    * 50000 m^3 between 0 and 50
m
CV143B1    0.53    .000201
*
*
CV14400   'R2ch4of8'              2   2  20
CV144A1   PVOL 1.0E5                    * 1 bar
CV144A3   TATM 923.   RHUM 0.2          * Atmosphere at 298 K, 20% relative humidity
CV144A4   MLFR.4 1.0  MLFR.5 0.0        * 100% N2, 0% O2
CV144B0    0.37    0.0                                    * 50000 m^3 between 0 and 50
m
CV144B1    0.53    .000201
*
*
CV14500   'R2ch5of8'              2   2  20
CV145A1   PVOL 1.0E5                    * 1 bar
CV145A3   TATM 923.   RHUM 0.2          * Atmosphere at 298 K, 20% relative humidity
CV145A4   MLFR.4 1.0  MLFR.5 0.0        * 100% N2, 0% O2
CV145B0    0.37    0.0                                    * 50000 m^3 between 0 and 50
m
CV145B1    0.53    .000201
*
*
CV14600   'R2ch6of8'              2   2  20
CV146A1   PVOL 1.0E5                    * 1 bar
CV146A3   TATM 923.   RHUM 0.2          * Atmosphere at 298 K, 20% relative humidity
CV146A4   MLFR.4 1.0  MLFR.5 0.0        * 100% N2, 0% O2
CV146B0    0.37    0.0                                    * 50000 m^3 between 0 and 50
m
CV146B1    0.53    .000201
*
*
CV14700   'R2ch7of8'              2   2  20
CV147A1   PVOL 1.0E5                    * 1 bar
CV147A3   TATM 923.   RHUM 0.2          * Atmosphere at 298 K, 20% relative humidity
CV147A4   MLFR.4 1.0  MLFR.5 0.0        * 100% N2, 0% O2
CV147B0    0.37    0.0                                    * 50000 m^3 between 0 and 50
m
CV147B1    0.53    .000201
```

```
*
*
CV14800   'R2ch8of8'             2   2  20
CV148A1   PVOL 1.0E5                  * 1 bar
CV148A3   TATM 923.   RHUM 0.2        * Atmosphere at 298 K, 20% relative humidity
CV148A4   MLFR.4 1.0  MLFR.5 0.0      * 100% N2, 0% O2
CV148B0    0.37    0.0                                      * 50000 m^3 between 0 and 50
m
CV148B1    0.53    .000201
*
*
CV15000   'Emp2'             2   2  20
CV150A1   PVOL 1.0E5                  * 1 bar
CV150A3   TATM 923.   RHUM 0.2        * Atmosphere at 298 K, 20% relative humidity
CV150A4   MLFR.4 1.0  MLFR.5 0.0      * 100% N2, 0% O2
CV150B0    0.53    0.0                                      * 50000 m^3 between 0 and 50
m
CV150B1    0.57    0.0006
*
*
CV16000   'Ref3'             2   2  20
CV160A1   PVOL 1.0E5                  * 1 bar
CV160A3   TATM 923.   RHUM 0.2        * Atmosphere at 298 K, 20% relative humidity
CV160A4   MLFR.4 1.0  MLFR.5 0.0      * 100% N2, 0% O2
CV160B0    0.57    0.0                                      * 50000 m^3 between 0 and 50
m
CV160B1    0.73    .0024
*
*
CV16100   'R3ch1of8'             2   2  20
CV161A1   PVOL 1.0E5                  * 1 bar
CV161A3   TATM 923.   RHUM 0.2        * Atmosphere at 298 K, 20% relative humidity
CV161A4   MLFR.4 1.0  MLFR.5 0.0      * 100% N2, 0% O2
CV161B0    0.57    0.0                                      * 50000 m^3 between 0 and 50
m
CV161B1    0.73    .000201
*
*
CV16200   'R3ch2of8'             2   2  20
CV162A1   PVOL 1.0E5                  * 1 bar
CV162A3   TATM 923.   RHUM 0.2        * Atmosphere at 298 K, 20% relative humidity
CV162A4   MLFR.4 1.0  MLFR.5 0.0      * 100% N2, 0% O2
CV162B0    0.57    0.0                                      * 50000 m^3 between 0 and 50
m
CV162B1    0.73    .000201
*
*
CV16300   'R3ch3of8'             2   2  20
CV163A1   PVOL 1.0E5                  * 1 bar
CV163A3   TATM 923.   RHUM 0.2        * Atmosphere at 298 K, 20% relative humidity
CV163A4   MLFR.4 1.0  MLFR.5 0.0      * 100% N2, 0% O2
```

```
CV163B0    0.57    0.0                                          * 50000 m^3 between 0 and 50
m
CV163B1    0.73    .000201
*
*
CV16400   'R3ch4of8'            2   2  20
CV164A1   PVOL 1.0E5                 * 1 bar
CV164A3   TATM 923.   RHUM 0.2       * Atmosphere at 298 K, 20% relative humidity
CV164A4   MLFR.4 1.0  MLFR.5 0.0     * 100% N2, 0% O2
CV164B0    0.57    0.0                                          * 50000 m^3 between 0 and 50
m
CV164B1    0.73    .000201
*
*
CV16500   'R3ch5of8'            2   2  20
CV165A1   PVOL 1.0E5                 * 1 bar
CV165A3   TATM 923.   RHUM 0.2       * Atmosphere at 298 K, 20% relative humidity
CV165A4   MLFR.4 1.0  MLFR.5 0.0     * 100% N2, 0% O2
CV165B0    0.57    0.0                                          * 50000 m^3 between 0 and 50
m
CV165B1    0.73    .000201
*
*
CV16600   'R3ch6of8'            2   2  20
CV166A1   PVOL 1.0E5                 * 1 bar
CV166A3   TATM 923.   RHUM 0.2       * Atmosphere at 298 K, 20% relative humidity
CV166A4   MLFR.4 1.0  MLFR.5 0.0     * 100% N2, 0% O2
CV166B0    0.57    0.0                                          * 50000 m^3 between 0 and 50
m
CV166B1    0.73    .000201
*
*
CV16700   'R3ch7of8'            2   2  20
CV167A1   PVOL 1.0E5                 * 1 bar
CV167A3   TATM 923.   RHUM 0.2       * Atmosphere at 298 K, 20% relative humidity
CV167A4   MLFR.4 1.0  MLFR.5 0.0     * 100% N2, 0% O2
CV167B0    0.57    0.0                                          * 50000 m^3 between 0 and 50
m
CV167B1    0.73    .000201
*
*
CV16800   'R3ch8of8'            2   2  20
CV168A1   PVOL 1.0E5                 * 1 bar
CV168A3   TATM 923.   RHUM 0.2       * Atmosphere at 298 K, 20% relative humidity
CV168A4   MLFR.4 1.0  MLFR.5 0.0     * 100% N2, 0% O2
CV168B0    0.57    0.0                                          * 50000 m^3 between 0 and 50
m
CV168B1    0.73    .000201
*
*
CV17000   'Peb1'            2   2  20
CV170A1   PVOL 1.0E5                 * 1 bar
```

```
CV170A3   TATM 923.    RHUM 0.2          * Atmosphere at 298 K, 20% relative humidity
CV170A4   MLFR.4 1.0  MLFR.5 0.0        * 100% N2, 0% O2
CV170B0    0.73     0.0                                    * 50000 m^3 between 0 and 50
m
CV170B1    1.08     0.00525
*
*
CV18000   'Emp3'              2   2  20
CV180A1   PVOL 1.0E5                    * 1 bar
CV180A3   TATM 923.    RHUM 0.2          * Atmosphere at 298 K, 20% relative humidity
CV180A4   MLFR.4 1.0  MLFR.5 0.0        * 100% N2, 0% O2
CV180B0    1.08     0.0                                    * 50000 m^3 between 0 and 50
m
CV180B1    1.46     0.0057
*
*
CV19000   'Peb2'              2   2  20
CV190A1   PVOL 1.0E5                    * 1 bar
CV190A3   TATM 923.    RHUM 0.2          * Atmosphere at 298 K, 20% relative humidity
CV190A4   MLFR.4 1.0  MLFR.5 0.0        * 100% N2, 0% O2
CV190B0    1.46     0.0                                    * 50000 m^3 between 0 and 50
m
CV190B1    1.61     0.00225
*
CV20000   'Chim'              2   2  20
CV200A1   PVOL 1.0E5                    * 1 bar
CV200A3   TATM 923.    RHUM 0.2          * Atmosphere at 298 K, 20% relative humidity
CV200A4   MLFR.4 1.0  MLFR.5 0.0        * 100% N2, 0% O2
CV200B0    1.61     0.0                                    * 50000 m^3 between 0 and 50
m
CV200B1    5.61     0.06
*
*
CV20000   'ATM1'              2   2  20
CV200A1   PVOL 1.0E5                    * 1 bar
CV200A3   TATM 298.    RHUM 0.2          * Atmosphere at 298 K, 20% relative humidity
CV200A4   MLFR.4 1.0  MLFR.5 0.0        * 80% N2, 20% O2
CV200B0    0.00     0.0                * 50000 m^3 between 0 and 7.50 m
CV200B1    7.50     5.0E4
*
*
CV20000   'ATM2'              2   2  20
CV200A1   PVOL 1.0E5                    * 1 bar
CV200A3   TATM 298.    RHUM 0.2          * Atmosphere at 298 K, 20% relative humidity
CV200A4   MLFR.4 0.8  MLFR.5 0.2        * 80% N2, 20% O2
CV200B0    0.00     0.0                * 50000 m^3 between 0 and 7.50 m
CV200B1    7.50     5.0E4
*
*******************
* FLOW PATH INPUT *
*******************
*
```

```
*                    VOLUMES      JUNCT.ELEV
*                    FM    TO     FM     TO
FL10000   'open in'   100   110    0.1    0.1   * Connect DC to LP at 2 m
FL10001   0.09    1.0     1.0                   * Nominal A, Inertial L, Fract open (est)
FL100S0   0.01     1.0     0.06                   * Segment: A, Segment L, HydDiam
*
FL11000   'ref1 in'    110   121    0.1    0.3   * Connect LP to core at 3 m
FL11001   0.09     0.2     1.0                    * Nominal A, Inertial L, Fract open
FL11003   1.3    1.3                            * Forward and Reverse Form loss
FL110S0   0.09     0.2     0.01                   * Segment: A, Segment L, HydDiam
*                                                 * (half of core, with bundle HD)
*
FL11100   'emp1 in1'  121   130    0.3    0.41   * Connect LP to bypass at 3 m
FL11101   0.09     0.2     1.0                    * Nominal A, Inertial L, Fract open
FL11103   1.3   1.3                          * Forward and Reverse Form loss
FL111S0   0.09     0.2     0.01                    * Segment: A, Segment L, HydDiam
*                                                  * (half of bypass with appropriate HD)
*
FL12100   'ref2 in1'   130   141    0.41    0.52   * Connect core to UP at 7 m
FL12101   0.09     0.2     1.0                    * Nominal A, Inertial L, Fract open
FL12103   1.3    1.3                            * Forward and Reverse Form loss
FL121S0   0.09     0.2     0.01                   * Segment: other half of core
*
*
FL12200   'ref2 in2'   130   142    0.41    0.52   * Connect core to UP at 7 m
FL12201   0.09     0.2     1.0                    * Nominal A, Inertial L, Fract open
FL12203   1.3    1.3                            * Forward and Reverse Form loss
FL122S0   0.09     0.2     0.01                   * Segment: other half of core
*
*
FL12300   'ref2 in3'   130   143    0.41    0.52   * Connect core to UP at 7 m
FL12301   0.09     0.2     1.0                    * Nominal A, Inertial L, Fract open
FL12303   1.3    1.3                            * Forward and Reverse Form loss
FL123S0   0.09     0.2     0.01                   * Segment: other half of core
*
*
FL12400   'ref2 in4'   130   144    0.41    0.52   * Connect core to UP at 7 m
FL12401   0.09     0.2     1.0                    * Nominal A, Inertial L, Fract open
FL12403   1.3    1.3                            * Forward and Reverse Form loss
FL124S0   0.09     0.2     0.01                   * Segment: other half of core
*
*
FL12500   'ref2 in5'   130   145    0.41    0.52   * Connect core to UP at 7 m
FL12501   0.09     0.2     1.0                    * Nominal A, Inertial L, Fract open
FL12503   1.3    1.3                            * Forward and Reverse Form loss
FL125S0   0.09     0.2     0.01                   * Segment: other half of core
*
*
FL12600   'ref2 in6'   130   146    0.41    0.52   * Connect core to UP at 7 m
FL12601   0.09     0.2     1.0                    * Nominal A, Inertial L, Fract open
FL12603   1.3    1.3                            * Forward and Reverse Form loss
FL126S0   0.09     0.2     0.01                   * Segment: other half of core
```

```
*
*
FL12700   'ref2 in7'   130   147    0.41    0.52   * Connect core to UP at 7 m
FL12701   0.09     0.2     1.0              * Nominal A, Inertial L, Fract open
FL12703   1.3    1.3                     * Forward and Reverse Form loss
FL127S0   0.09     0.2     0.01             * Segment: other half of core
*
*
FL12800   'ref2 in8'   130   148    0.41    0.52   * Connect core to UP at 7 m
FL12801   0.09     0.2     1.0              * Nominal A, Inertial L, Fract open
FL12803   1.3    1.3                     * Forward and Reverse Form loss
FL128S0   0.09     0.2     0.01             * Segment: other half of core
*
FL13100   'emp2 in1' 141   150    0.52    0.63   * Connect bypass to UP at 7 m
FL13101   0.09     0.2     1.0              * Nominal A, Inertial L, Fract open
FL13103   1.3   1.3                     * Forward and Reverse Form loss
FL131S0   0.09     0.2     0.01              * Segment: other half of bypass
*
*
FL13200   'emp2 in2' 142   150    0.52    0.63   * Connect bypass to UP at 7 m
FL13201   0.09     0.2     1.0              * Nominal A, Inertial L, Fract open
FL13203   1.3   1.3                     * Forward and Reverse Form loss
FL132S0   0.09     0.2     0.01              * Segment: other half of bypass
*
*
FL13300   'emp2 in3' 143   150    0.52    0.63   * Connect bypass to UP at 7 m
FL13301   0.09     0.2     1.0              * Nominal A, Inertial L, Fract open
FL13303   1.3   1.3                     * Forward and Reverse Form loss
FL133S0   0.09     0.2     0.01              * Segment: other half of bypass
*
*
FL13400   'emp2 in4' 144   150    0.52    0.63   * Connect bypass to UP at 7 m
FL13401   0.09     0.2     1.0              * Nominal A, Inertial L, Fract open
FL13403   1.3   1.3                     * Forward and Reverse Form loss
FL134S0   0.09     0.2     0.01              * Segment: other half of bypass
*
*
FL13500   'emp2 in5' 145   150    0.52    0.63   * Connect bypass to UP at 7 m
FL13501   0.09     0.2     1.0              * Nominal A, Inertial L, Fract open
FL13503   1.3   1.3                     * Forward and Reverse Form loss
FL135S0   0.09     0.2     0.01              * Segment: other half of bypass
*
*
FL13600   'emp2 in6' 146   150    0.52    0.63   * Connect bypass to UP at 7 m
FL13601   0.09     0.2     1.0              * Nominal A, Inertial L, Fract open
FL13603   1.3   1.3                     * Forward and Reverse Form loss
FL136S0   0.09     0.2     0.01              * Segment: other half of bypass
*
*
FL13700   'emp2 in7' 147   150    0.52    0.63   * Connect bypass to UP at 7 m
FL13701   0.09     0.2     1.0              * Nominal A, Inertial L, Fract open
FL13703   1.3   1.3                     * Forward and Reverse Form loss
```

```
FL137S0   0.09     0.2     0.01              * Segment: other half of bypass
*
*
FL13800   'emp2 in8' 148   150    0.52    0.63   * Connect bypass to UP at 7 m
FL13801   0.09     0.2     1.0                * Nominal A, Inertial L, Fract open
FL13803   1.3   1.3                     * Forward and Reverse Form loss
FL138S0   0.09     0.2     0.01              * Segment: other half of bypass
*
*                      VOLUMES       JUNCT.ELEV
*                      FM    TO      FM     TO
FL14100   'ref3 in1' 150   161    0.63    0.74   * Connect UP to Hot side at 8.5 m
FL14101   0.09     0.2     1.0                * Nominal A, Inertial L, Fract open
*FL14103   8.25    8.75                       * Top and bottom of connections
FL141S0   0.09     0.2     0.01               * Segment: hot leg pipe and plenum
*FL141S1   2.0     5.0     0.02              * Segment: half of up tubes
*
FL14200   'ref3 in2' 150   162    0.63    0.74   * Connect UP to Hot side at 8.5 m
FL14201   0.09     0.2     1.0                * Nominal A, Inertial L, Fract open
*FL14203   8.25    8.75                       * Top and bottom of connections
FL142S0   0.09     0.2     0.01               * Segment: hot leg pipe and plenum
*FL142S1   2.0     5.0     0.02              * Segment: half of up tubes
*
FL14300   'ref3 in3' 150   163    0.63    0.74   * Connect UP to Hot side at 8.5 m
FL14301   0.09     0.2     1.0                * Nominal A, Inertial L, Fract open
*FL14303   8.25    8.75                       * Top and bottom of connections
FL143S0   0.09     0.2     0.01               * Segment: hot leg pipe and plenum
*FL143S1   2.0     5.0     0.02              * Segment: half of up tubes
*
FL14400   'ref3 in4' 150   164    0.63    0.74   * Connect UP to Hot side at 8.5 m
FL14401   0.09     0.2     1.0                * Nominal A, Inertial L, Fract open
*FL14403   8.25    8.75                       * Top and bottom of connections
FL144S0   0.09     0.2     0.01               * Segment: hot leg pipe and plenum
*FL144S1   2.0     5.0     0.02              * Segment: half of up tubes
*
FL14500   'ref3 in5' 150   165    0.63    0.74   * Connect UP to Hot side at 8.5 m
FL14501   0.09     0.2     1.0                * Nominal A, Inertial L, Fract open
*FL14503   8.25    8.75                       * Top and bottom of connections
FL145S0   0.09     0.2     0.01               * Segment: hot leg pipe and plenum
*FL145S1   2.0     5.0     0.02              * Segment: half of up tubes
*
FL14600   'ref3 in6' 150   166    0.63    0.74   * Connect UP to Hot side at 8.5 m
FL14601   0.09     0.2     1.0                * Nominal A, Inertial L, Fract open
*FL14603   8.25    8.75                       * Top and bottom of connections
FL146S0   0.09     0.2     0.01               * Segment: hot leg pipe and plenum
*FL146S1   2.0     5.0     0.02              * Segment: half of up tubes
*
FL14700   'ref3 in7' 150   167    0.63    0.74   * Connect UP to Hot side at 8.5 m
FL14701   0.09     0.2     1.0                * Nominal A, Inertial L, Fract open
*FL14703   8.25    8.75                       * Top and bottom of connections
FL147S0   0.09     0.2     0.01               * Segment: hot leg pipe and plenum
*FL147S1   2.0     5.0     0.02              * Segment: half of up tubes
*
```

```
FL14800   'ref3 in8' 150   168    0.63    0.74   * Connect UP to Hot side at 8.5 m
FL14801   0.09     0.2     1.0              * Nominal A, Inertial L, Fract open
*FL14803   8.25    8.75                     * Top and bottom of connections
FL148S0   0.09     0.2     0.01             * Segment: hot leg pipe and plenum
*FL148S1   2.0     5.0     0.02             * Segment: half of up tubes
*
*
FL15100   'peb1 in1'   161   170   0.74   0.94   * Connect hot side to cold side at 20 m
FL15101   0.09     0.2    1.0              * Nominal A, Inertial L, Fract open
FL1510F   19.0    21.0                     * Top and bottom of connections
FL1510T   19.0    21.0                     *   corresponding to 2.0 m bundle diam
FL151S0   2.0     10.0    0.02            * Segment: Half of Up and down tubes
*
*
FL15200   'peb1 in2'   162   170   0.74   0.94   * Connect hot side to cold side at 20 m
FL15201   0.09     0.2    1.0              * Nominal A, Inertial L, Fract open
FL1520F   19.0    21.0                     * Top and bottom of connections
FL1520T   19.0    21.0                     *   corresponding to 2.0 m bundle diam
FL152S0   2.0     10.0    0.02            * Segment: Half of Up and down tubes
*
*
FL15300   'peb1 in3'   163   170   0.74   0.94   * Connect hot side to cold side at 20 m
FL15301   0.09     0.2    1.0              * Nominal A, Inertial L, Fract open
FL1530F   19.0    21.0                     * Top and bottom of connections
FL1530T   19.0    21.0                     *   corresponding to 2.0 m bundle diam
FL153S0   2.0     10.0    0.02            * Segment: Half of Up and down tubes
*
*
FL15400   'peb1 in4'   164   170   0.74   0.94   * Connect hot side to cold side at 20 m
FL15401   0.09     0.2    1.0              * Nominal A, Inertial L, Fract open
FL1540F   19.0    21.0                     * Top and bottom of connections
FL1540T   19.0    21.0                     *   corresponding to 2.0 m bundle diam
FL154S0   2.0     10.0    0.02            * Segment: Half of Up and down tubes
*
*
FL15500   'peb1 in5'   165   170   0.74   0.94   * Connect hot side to cold side at 20 m
FL15501   0.09     0.2    1.0              * Nominal A, Inertial L, Fract open
FL1550F   19.0    21.0                     * Top and bottom of connections
FL1550T   19.0    21.0                     *   corresponding to 2.0 m bundle diam
FL155S0   2.0     10.0    0.02            * Segment: Half of Up and down tubes
*
*
FL15600   'peb1 in6'   166   170   0.74   0.94   * Connect hot side to cold side at 20 m
FL15601   0.09     0.2    1.0              * Nominal A, Inertial L, Fract open
FL1560F   19.0    21.0                     * Top and bottom of connections
FL1560T   19.0    21.0                     *   corresponding to 2.0 m bundle diam
FL156S0   2.0     10.0    0.02            * Segment: Half of Up and down tubes
*
*
FL15700   'peb1 in7'   167   170   0.74   0.94   * Connect hot side to cold side at 20 m
FL15701   0.09     0.2    1.0              * Nominal A, Inertial L, Fract open
FL1570F   19.0    21.0                     * Top and bottom of connections
```

```
FL157OT   19.0    21.0                    *   corresponding to 2.0 m bundle diam
FL157S0   2.0     10.0    0.02            * Segment: Half of Up and down tubes
*
*
FL15800   'peb1 in8'   168   170   0.74   0.94   * Connect hot side to cold side at 20 m
FL15801   0.09     0.2    1.0              * Nominal A, Inertial L, Fract open
FL1580F   19.0    21.0                    * Top and bottom of connections
FL1580T   19.0    21.0                    *   corresponding to 2.0 m bundle diam
FL158S0   2.0     10.0    0.02            * Segment: Half of Up and down tubes
*
FL16000   'emp3 in' 170   180    0.94    1.2   * Connect cold side to DC at 8.5 m
FL16001   0.09     0.2     1.0              * Nominal A, Inertial L, Fract open
FL160S0   0.09     0.2     0.02             * Segment: Half of down tubes
*FL160S1   1.2     4.0     0.7              * Segment: Plenum and cold leg pipes
*
FL17000   'peb2 in' 180   190   1.2    1.92   * Connect PRZR at 12 m to hot side at 8.5 m
FL17001   0.09    0.2    1.0              * Nominal A, Inertial L, Fract open
FL170S0   0.09    0.2    0.02             * Segment: A, Segment L, HydDiam
*                                             corresponding to 20 m line
*
FL18000   'chim in' 190   200   1.92    4.25
FL18001   0.09     1.0    1.0              *
FL180S0   0.09     1.0    0.25             * Segment: A, Segment L, HydDiam
*
FL00100   'From ATM1' 900   100  0.1    0.1   * Connect inlet to atm at 0.1 m
FL00101   0.09     1.0    0.0              * Nominal A, Inertial L, Fract open
FL001S0   0.09     1.0    0.3              * Segment: A, Segment L, HydDiam
*
*
FL00200   'To ATM2' 200   910  4.25    7.5   * Connect chim to atm at 7.5 m
FL00201   0.09     1.0    0.0              * Nominal A, Inertial L, Fract open
FL002S0   0.09     3.25    0.3             * Segment: A, Segment L, HydDiam
*
*
**********************
* HEAT STRUCTURE INPUT*
**********************
*
*
*            STEEL WALL BETWEEN TUBE AND SHELL
*
HS10001000    4                  2            0
HS10001001    TUBE-WALL
HS10001002    1.1              0.0
HS10001100    -1                 1         0.04
HS10001101    0.0433             2
HS10001102    0.0467             3
HS10001103    0.05               4
HS10001200    -1
HS10001201    STAINLESS-STEEL    3
HS10001300    0
HS10001400    1                  200          INT          0.5       0.5
```

```
HS10001500    1.256              5.0          5.0
HS10001600    1                  100          EXT          0.5       0.5
HS10001700    1.571              5.0          5.0
*
.
*<<<<<<<<<<<<<< Variations >>>>>>>>>>>>>
*
*?ALLOWREPLACE
*
**********************
*** 'STEADY STATE' ***
**********************
*      XX not used XX
* ---------------------------
* Add approximate static heads
* ---------------------------
*
* Pressurizer defines pressure of 16MPa at elevation of 22 m
*   Density in pressurizer is 584 kg/m^3
*   Pressure at prssurizer outlet (12 m) is 16.057 MPa
* Water density in rest of system is 690-770 kg/m^3
*   Approximate static head is 6.8-7.6 kPa/m
*   Use 7.0 kpa/m in initialization
*
*eor* skip
*CV100A1   PVOL 16.071E6              * 16.057 MPa + 2 m head
*CV110A1   PVOL 16.120E6              * 16.057 MPa + 9 m head
*CV120A1   PVOL 16.092E6              * 16.057 MPa + 5 m head
*CV130A1   PVOL 16.092E6              * 16.057 MPa + 5 m head
*CV140A1   PVOL 16.064E6              * 16.057 MPa + 1 m head
*CV210A1   PVOL 15.994E6              * 16.057 MPa - 9 m head
*CV220A1   PVOL 15.994E6              * 16.057 MPa - 9 m head
*eor* melgen
*
* ------------------------
* Use initilization option
* ------------------------
*
*eor* skip
CV30001   0    -3          * Pressurizer time-independent for initialization
TSTART -100.               * Start at -100 s
CVHTENDINI    0.0          * End initialization at 0 s
*eor* melgen
*
*
*****************
*** TRANSIENT ***
*****************
*
* ---------------------------------
* Open the break and vary parameters
* ---------------------------------
```

```
*
*          AREA    LENGTH   FOPEN
FL00101   0.09      1.0     1.0              * Fract open chg from 0 to 1
FL00201   0.09      1.0     1.0              * Fract open chg from 0 to 1
*
*          XL2PF
FL00101    1.0                    * Change momentum exchange length to 1.0 m

*          XL2PF
FL00201    1.0                    * Change momentum exchange length to 1.0 m
*
*          K_fwd  K_rev  C_f   C_r
FL00103    2.5    2.5    0.4   0.4 * Change K to 2.5, discharge coeff to 0.4
FL00203    2.5    2.5    0.4   0.4 * Change K to 2.5, discharge coeff to 0.4
*
* ------------------------------------
* Turn on flashing model for break flow
* Use default drop size
* ------------------------------------
*
*          Activation
*?FL001FF    1                      *  Default diam is C4500(3)=65.E-6 m
*
*
*****************
*** RN TRACER ***
*****************
*
* ---------------------------------------
* Add Barium as RN "tracer" in initial RCS
* ---------------------------------------
*
*?r*i*f   rn.txt
*
*<<<<<<<<<<<<<< Variations >>>>>>>>>>>>>
.
*eor* melcor
**********************
**********************
***                ***
***  MELCOR INPUT  ***
***                ***
**********************
**********************
*
TITLE     'Simple Blowdown'
*
RESTARTFILE  BLOWDOWN.RST
OUTPUTFILE   BLOWDOWN_OUT.txt
DIAGFILE     BLOWDOWN_DIA.txt
EXTDIAGFILE  BLOWDOWN_EXTDiag.txt
MESSAGEFILE  BLOWDOWN_MES.txt
```

```
PLOTFILE      BLOWDOWN.PTF
*
CPULIM        500.
CPULEFT       100.
RESTART       0
DTTIME        0.0003
*
EXACTTIME1    0.0
*
TEND          100.
*                TIME      DTMAX     DTMIN     DTEDIT    DTPLOT    DTREST
TIME0           -100.0      0.02      0.0001    25.0      1.0       100.
*
NOFLUSH           * Don't flush output files
*
*<<<<<<<<<<<<<< Variations >>>>>>>>>>>>>
*
* ------------------------------------------
* Try changes in timestep, edit frequency, etc.
* ------------------------------------------
*
*                TIME      DTMAX     DTMIN     DTEDIT    DTPLOT    DTREST
*?TIME0          -100.0      0.001     0.0001    25.0      1.0       100.
*
*<<<<<<<<<<<<<< Variations >>>>>>>>>>>>>
```

# APPENDIX B: THE 1-D MATLAB CODE

```
%%%%%%%%%%%%%%%%%%%%%%%%%%%%%%%%%%%%%%%%%%%%%%%%%%%%%%%%%%%%%%%%%%%%%%%%%%%%%%%
%
%   1-D nodal chemical reaction and heat transfer code for
%   graphite-moderated reactors
%
%   Caroline Cochran
%   for Prof. Kadak, MIT Dept of Nuclear Engineering
%   draft Oct 2009
%
%%%%%%%%%%%%%%%%%%%%%%%%%%%%%%%%%%%%%%%%%%%%%%%%%%%%%%%%%%%%%%%%%%%%%%%%%%%%%%%

%Example initial calculation following before iteration

%calculate velocity from Buoyancy:
Rdry=287.05; %J/kg*K
T=650;
Ain = (.025^2)*pi;
ztot=4;
g=9.81;
```

# APPENDIX B: THE 1-D MATLAB CODE

```
%%%%%%%%%%%%%%%%%%%%%%%%%%%%%%%%%%%%%%%%%%%%%%%%%%%%%%%%%%%%%%%%%%%%%%%%%%%%
%
%   1-D nodal chemical reaction and heat transfer code for
%   graphite-moderated reactors
%
%   Caroline Cochran
%   for Prof. Kadak, MIT Dept of Nuclear Engineering
%   draft Oct 2009
%
%%%%%%%%%%%%%%%%%%%%%%%%%%%%%%%%%%%%%%%%%%%%%%%%%%%%%%%%%%%%%%%%%%%%%%%%%%%%

%Example initial calculation following before iteration

%calculate velocity from Buoyancy:
Rdry=287.05; %J/kg*K
T=650;
Ain = (.025^2)*pi;
ztot=4;
g=9.81;
Tout=1123; % 850C
Tin=300;
delT=Tout-Tin;
Tavg=923;
rho_dry = 101325/(Rdry*Tavg); %kg/m3
mdot = rho_dry*Ain*((2*g*ztot*(delT)*Tin)^.5)/(Tin+delT);
mdot %kg/s
Axs=.04; %this is cross section for refs 2 and 3
v=mdot/Axs;
v
%vin=(2*(delT/Tin)*g*ztot)^.5;
%Aout=.09;
%vout=vin*Ain/Aout;
%vout
%v=vout;


%Reaction Rate of O2 from NACOK modified with velocities
T=650+273;
pO2=.23;
ReactO2=(((7.2*10^10)*(exp(-16140/(2*T)))*pO2)^(-1)+(770*(v^.65)*(T^.34)*pO2)^(-1))^(-1);
%in mg/cm^2-h

%this is per hour, per timestep calc, where ts is in s:
```

```
%(restriction, 1/ts should be whole number)
ts=0.5;
ReactO2ts=ReactO2*ts/3600;

%apply to volume (here, geometry of refs 2 and 3)

%first, give volume parameters:
Asurf=pi*.016*.2*96; %m^2 diameter 16mm
zi=.2; %m
Vol=.3*.3*.2;
por=(pi*(.008^2)*.2*96)/Vol;

%ratio assumptions
K1=7943;
R=8.314;
E1=78300;
%Ratio, A, = K1 * EXP(-E1/R*T) and unitless.

% will add if statement to account for not-instant heat transfer through
% graphite.  ....if


% create arrays to save values of T and Qtot over timesteps for evaluation:
k=10; %number of sections
h=2.5; %number of hours #v9 8->1
ts=0.5; %#chged ts to 0.5 #v9 0.5->.25, unstable for conduction terms
zi=[0.17,0.16,0.04,0.16,0.04,0.16,.350,.380,.150,4]; %#v11p2 more specific heights
%0,  .17, .33, .37, .53, .57, .73,1.08,1.46,1.61,5.61
%  ent   r1  s1   r2   s2    r3  p1   s3   p2   s4
%     1    2    3    4    5    6   7    8    9   10
Reffts=zeros(1,k+1);
ii=zeros(1,k);
ie=zeros(1,k);
CXA=.3*.3; %cross-sectional area for geometry
Vol=zeros(1,k+1); %can be input or calc

%#p6 added ability of source term per m
SQ=0;

% for reflectors, surf area = height times pi*D times no. channels
% for porous media eg pebbles area is input.
Asurfpz=[pi*.05*4, pi*.040*12, 0, pi*.016*96, 0, pi*.016*96, 53.58*.3*.3, 0, 53.58*.3*.3, 0];
%div by zi
%          entry       ref1          ref2         ref3          peb1
Asurfts=zeros(h*3600/ts,k+1); %v11p4 add time dim to Asurf for burnoff
Volts=zeros(1,k+1);
```

```
por=[.89,.2145,1,.2145,1,.2145,.13,1,.13,1];
%v16 CLair=[.025,.02,.02,.008,.01,.008,.01,.1,.008,1];
%#v15 CLair=[.8,.8,.8,.8,.8,.8,.8,.8,.8,.8]
Tmax=650+273;
maxii=20;
it=10;

T2=zeros(h*3600/ts, k+1, maxii);
Tair=zeros(h*3600/ts, k+1, maxii);
%TairRCO=zeros(h*3600/ts, k+1, maxii);
QCOnO2=zeros(h*3600/ts, k+1, maxii);
QOtoCO=zeros(h*3600/ts, k+1, maxii);
QOtoCO2=zeros(h*3600/ts, k+1, maxii);
QCO2nC=zeros(h*3600/ts, k+1, maxii);
Qtoair=zeros(h*3600/ts, k+1, maxii);
Qfromwall=zeros(h*3600/ts, k+1, maxii);
%Qtot2=zeros(h*3600/ts, k+1, maxii); p7
Qtot3=zeros(h*3600/ts, k+1, maxii);
Qcondinout=zeros(h*3600/ts, k+1, maxii); %into 2 variables
Qcondout1=zeros(h*3600/ts, k+1, maxii);
pO2i=zeros(h*3600/ts, k+1, maxii);
pCOi=zeros(h*3600/ts, k+1, maxii);
pCO2i=zeros(h*3600/ts, k+1, maxii);
errorg=zeros(h*3600/ts, k+1, maxii);
errora=zeros(h*3600/ts, k+1, maxii);

%v3:mean values
T2m=zeros(h*3600/ts, k+1);
Tairm=zeros(h*3600/ts, k+1);
%TairRCOm=zeros(h*3600/ts, k+1);
QCOnO2m=zeros(h*3600/ts, k+1);
QOtoCOm=zeros(h*3600/ts, k+1);
QOtoCO2m=zeros(h*3600/ts, k+1);
QCO2nCm=zeros(h*3600/ts, k+1);
Qtoairm=zeros(h*3600/ts, k+1);
Qfromwallm=zeros(h*3600/ts, k+1);
%Qtot2m=zeros(h*3600/ts, k+1);
Qtot3m=zeros(h*3600/ts, k+1);
Qcondinoutm=zeros(h*3600/ts, k+1);
Qcondoutm=zeros(h*3600/ts, k+1);
pO2im=zeros(h*3600/ts, k+1);
pCOim=zeros(h*3600/ts, k+1);
pCO2im=zeros(h*3600/ts, k+1);
errorgm=zeros(h*3600/ts, k+1);
erroram=zeros(h*3600/ts, k+1);
Qmaxcount=0;
```

```
heightj=zeros(1,sum(ii));
Tairmax=650+273;
Tmaxn=650+273;
a=1; %$relaxation factor #v3: changed from .3 to .2 v4:chged back to .3 v6:.3->.5 v7->.7 v8:->1
arad=0;%v22 .00001; %$radiation Q more unstable with 4th power v3:chgd fr .001 to .01 v5: .01->.3
v6:->.5 v7->.7 v8:->1 v11p3->.01
arada=0;%v22 .035; %v19
ainc=1.000001; %increase in surface area ratio with burnoff
nch=[4,12,0,96,0,96,0,0,0,0]; %0 indicates no channels or porous media eg pebbles
pebr=[0,0,0,0,0,0,.02,0,.008,0];
CLair=zeros(1,k);
minii=1; %v17 %#v22 chg to 1

c2=0;
for i=1:k; %(each i is a section)
    %#v10set: added velocity per section
    v=mdot/(por(i)*CXA);
    Reffts(i)=((zi(i)/(ts*v))^-1);
    ii(1,i)=round(zi(i)/(ts*v)); %number timesteps for air to travel through section
    if ii(1,i)==0
        ii(1,i)=1;
    end;
    if ii(1,i)>maxii
        ii(1,i)=maxii;
    end;

    %v17 min ii
    if ii(1,i)<minii
        ii(1,i)=minii;
    end;
    ie(i)=(1/(Reffts(i)))-ii(1,i); %extra

    for j=1:ii(i)
        if i>1
            heightj(1,c2+j)=heightj(1,sum(ii(1:i-1)))+j*((zi(i))/(ii(i)));
        else
            heightj(1,c2+j)=j*((zi(i))/(ii(i)));
        end;
    end;
        c2=c2+ii(i);
    %v17 new CLair
    if por(i)<1
        if nch(i)>0
        CLair(i)=4*zi(i)/(ii(i)*nch(i));
        else
```

```
        CLair(i)=2*(pi()*(pebr(i)))/(CXA*(1-por(i))/(pi()*(pebr(i)^2))); %made up CLair for
pebbles
        end;
    end;
end;

T2Ch=zeros(h*3600/ts,sum(ii));
TairCh=zeros(h*3600/ts,sum(ii));
pO2ih=zeros(h*3600/ts,sum(ii));
pCOih=zeros(h*3600/ts,sum(ii));
pCO2ih=zeros(h*3600/ts,sum(ii));

%assume all O2 reacts with C to form either CO or CO2, with ratio
T2(1:sum(ii),:,:)=650+273; %set initial T value for first section
Tair(:,1,1)=300; %set initial T value for first section
pO2i(:,1,1)=.23*.55; % inlet partial pressure same for first section for all ts
% #multiply by 0.55 for moist air
pCOi(:,1,:)=.00001*.55; % inlet partial pressure same for first section for all ts
pCO2i(:,1,:)=.005*.55; % inlet partial pressure same for first section for all ts
kondgra=168; % W/m-K
n=1; %initialize
i=1;

%BUILD UP- TRANSIENT
%for n=1:(h*(3600/ts)) %calculate for h hours
for n=1:sum(ii)
    c=n;
    %Tmax for timestep reset
    Tmaxn=650;
    for i=1:k; %(each i is a section)
        %#v3: added velocity per section
        v=mdot/(por(i)*CXA);
        nn=c2;

        %v11p4 adding some sort of burnoff increase in surface area
        Asurfts(n,i)=Reffts(i)*Asurfpz(i)/zi(i);
%         if n>1
% %             if n>nn% && n>1
%                 if (sum(QOtoCO(n-1,i,1:j))+sum(QOtoCO2(n-1,i,1:j)))>0
%                  Asurfts(n,i)=ainc*Asurfts(n-1,i);
%                 end;
% %             end;
%         end;

        Vol(i)=CXA*zi(i);
        Reffts(i)=((zi(i)/(ts*v))^-1);
```

```
        Volts(i)=(Reffts(i))*Vol(i); %v6 took out *por(i) which led to bad graphite calcs...
assume both vol and surf A have same cross sections with height.

         if i>1
         previi=ii(1,i-1);
         end;
         if i>2
         prev2ii=ii(1,i-2);
         end;
         curii=ii(1,i);

        for j=1:ii(1,i)
            c2=n-(c-1);
            %for s=1:it
               if pCOi(n,i,j)<0
                   pCOi(n,i,j)=0; %p4 to1 dbstop out...
%                    delCO
%                    dbstop
               end;
               if T2(n,i,j)>4000
                   Tnew
                   dbstop
               end;

               if T2(n,i,j)<300
                   T2(n,i,j)=300;
               end;

               if pCO2i(n,i,j)<0
                   pCO2i(n,i,j)=0;
               end;

               T=T2(n,i,j);
               Ta=Tair(n,i,j);
%                Tavg=(T+Tair(n,i,j))/2;
%                T=Tavg; %p4 commented this to match 2nd part
               if Ta<T
                   Tavg=(T+Ta)/2;
               else
                   Tavg=T;
               end;

               rho_dry = .55*(101325/(Rdry*Ta))+.45*(.2348); %kg/m3 modification using density
vapor at 650 C

                if pO2i(n,i,j)>0
```

```
                    %O2+C reaction
                    RO21=(7.2*10^10)*((exp(-16140/(Tavg))))*(pO2i(n,i,j));
                    RO22=770*(v^.65)*(Tavg^.34)*(pO2i(n,i,j));
                    ReactO2=(((7.2*10^10)*((exp(-16140/(Tavg))))*(pO2i(n,i,j)))^(-
1)+(770*(v^.65)*(Tavg^.34)*(pO2i(n,i,j)))^(-1))^(-1); %mg/cm2-h
                    %#not general
                    %p5- E/2
                    ReactO2ts=ReactO2*ts/3600; %mg/cm2-ts
                    RO2mol=ReactO2ts*(100*100*Asurfts(n,i))/12000;%mol/ts, 12000 mg C/mol C

                    A=K1*(exp(-E1/(R*Tavg)));
                    dO2=-RO2mol*(0.5*A+1)/(A+1);

%                     %control to avoid reacting more than avail oxygen.
%                     if abs(dO2)>(rho_dry*Volts(i)*pO2i(n,i,j)/.032)
%                     %(kg/m3*m3/(kg/mol)) 32g O2 /mol
%                         dO2=-rho_dry*Volts(i)*pO2i(n,i,j)/.032; %p4 to1 added -
%                         RO2mol=dO2*(A+1)/(0.5*A+1);
%                         ReactO2=(RO2mol/((100*100*Asurfts(n,i))/12000))/(ts/3600);
%                     end;

                    dmolCO2=RO2mol*(1/(1+A)); %mol increase in CO2 with ts from O reaction
                    dCO2=dmolCO2/(101325*Volts(i)*por(i)/(8.314*Ta)); %p7 changed all T to Ta for
species calcs
                    dmolCO=RO2mol*(A/(A+1)); %mol increase in CO with ts from O reaction
                    dCO=dmolCO/(101325*Volts(i)*por(i)/(8.314*Ta));

                    %CO+0.5*O2-> CO2 has large exothermic.  (eqn from takeda)
                    %VOLUMETRIC
                    if pCOi(n,i,j)>0

                        K2=1.3*(10^8); %m^3/mol-s
                        E2=126000; %J/mol

                        RCOnO2=K2*((exp(-
E2/(R*Ta))))*(pCOi(n,i,j))*((pO2i(n,i,j))^.5)*((pCO2i(n,i,j))^.5); % mol/m3-s
                        molCOnO2=RCOnO2*Volts(i)*por(i)*ts; %mol/ts
                        QCOnO2(n,i,j)=molCOnO2*283000; %J/ts

                        %this is produced IN the gas, so the heat produced will be
                        %considered perfectly distributed, with the heat conducted
                        %to the wall by the same equation

                        dCO_1=-molCOnO2/(101325*Volts(i)*por(i)/(8.314*Ta));
                        dCO2_1=molCOnO2/(101325*Volts(i)*por(i)/(8.314*Ta));
                        dO2_1=-0.5*molCOnO2/(101325*Volts(i)*por(i)/(8.314*Ta));
```

```
    else
        pCOi(n,i,j)=0;
        dCO_1=0;
        dCO2_1=0;
        dO2_1=0;
        QCOnO2(n,i,j)=0;
    end;

    if RO2mol>0 %(molCOnO2/2)
    QOtoCO(n,i,j)=(A/(A+1))*(RO2mol)*111000; %ratio*mol/ts*111000 J/mol
    QOtoCO2(n,i,j)=(1/(1+A))*(RO2mol)*394000; %(1-ratio)*mol/ts*394000 J/mol
    %not considering changes in ratio due to other reactions
    %because negligible
    else
    QOtoCO(n,i,j)=0.0000;
    QOtoCO2(n,i,j)=0.0000;
    end;

else
    ReactO2=0;
    ReactO2ts=0;
    RO2mol=0;
    dCO=0;
    dCO2=0;
    dO2=0;
    dCO_1=0;
    dCO2_1=0;
    dO2_1=0;
    RCOnO2=0;
    molCOnO2=0; %mol/ts
    QCOnO2(n,i,j)=0;
end;

%CO2+C ->2CO endothermic, surface area.  (eqn from moorman)
K3=2220; %
E3=-30635; %

%here, the limiting agent will be CO2 but in our experiment it
%never got large enough to affect the eqn significantly.

if pCO2i(n,i,j)>0
    RCO2nC=K3*((exp(E3/Tavg))); % mol C/m2-s
    molCO2nC=RCO2nC*Asurfts(n,i)*ts; %mol/ts
    dmolCO=molCO2nC; %mol increase in CO and decrease in CO2
    dCO_2=molCO2nC/(101325*Volts(i)*por(i)/(8.314*Ta));
    dCO2_2=-molCO2nC/(101325*Volts(i)*por(i)/(8.314*Ta));
```

```
                QCO2nC(n,i,j)=molCO2nC*-172000; %J/ts
            else
                RCO2nC=0;
                QCO2nC(n,i,j)=0.0000;
                dCO_2=0;
                dCO2_2=0;
            end;

            kond=(1.5207*10^(-11))*(Tair(n,i,j)^3)-(4.8574*10^(-
8))*(Tair(n,i,j)^2)+(1.0184*10^(-4))*(Tair(n,i,j))-(3.9333*10^(-4)); %(.45*(.093/.07)+.55)*
            %W/m-K

            %calculate Q lost by air cooling or air heating of graphite
            %approximate Tair increased as result of only COnO2 (although
            %nonlinear and affected by other heat)

            %Qtoair is formulated to be positive if Q is lost to air
            if por(i)<1
                Qtoair1=a*(Asurfts(n,i))*kond*(24/11)*(T-Tair(n,i,j))*ts/CLair(i); %eqn 10-31
T&K
            else
                Qtoair1=0; %#p4div2 in the case of just a wall, heat transfer considered
below
            end;

             Qtoair2=QCOnO2(n,i,j);

             B=5.67*(10^(-8)); % W/m2-K4
             emissair=.35*.55+.6*.45;
             Qtoair3=arada*Asurfts(n,i)*(emissair)*B*((Tavg^4)-((Tair(n,i,j))^4))*ts; %p7 chg
from (emissair/(emissair+1+emissair*1) to just emissair

                Qtoair(n,i,j)=(Qtoair1+Qtoair2+Qtoair3);
                Qmax=((2308.4*.45+1150*.55)*rho_dry*Volts(i))*(T-Tair(n,i,j))*ts; %kJ/kg-
K*kg/m3*m3*K

                if abs(Qtoair(n,i,j))>abs(Qmax)
                    Qtoair(n,i,j)=Qmax; %p6 #Qmax *.5
                    Qmaxcount=Qtoair(n,i,j)-Qmax;
                end;

             %heat transfer from walls (not graphite)
             Twall=650+273;

                 if Asurfts(n,i)==0
                 Axs=.3*.3;
```

```
                    Pw=4*.3; %"wetted" perimeter
                    CL=4*Axs/Pw;
                    Awall=4*.3*zi(i);
                    Qfromwall(n,i,j)=a*(Awall)*kond*(24/11)*(Twall-Tair(n,i,j))*ts/CL;
%v3:TairRCO to Tair%eqn 10-31 T&K
                    end;

                Qtot=a*(QOtoCO(n,i,j)+QOtoCO2(n,i,j)+QCO2nC(n,i,j)); %J/ts %note, QCOnO2
incorporated into air T

                a1=1; %CONDIN/OUT RELAXATION $v3: changed a1 from .1 to .2 v4: .2 to .3 v6:.3-
>.5 v7->.7 v8:->1

%                  %CALCULATING HEAT CONDUCTED/RADIATED IN AND OUT OF NODES
%                  if por(i)<1
%                     if n>1
%                         if j>1
%                             if j<curii
%                                 Qcondin=a1*kondgra*(1-por(i))*CXA*(T2(n,i,j-1)-
T2(n,i,j))*ts/(zi(i)/curii); %assume
%                                  %                     assume contact between graphite blocks
%                                  %                     as approx by ratio of porosity also
%                                  %                     small ts that
%                                  %                     previous temps relevant.
%                                 Qcondout=a1*kondgra*(1-por(i))*CXA*(T2(n-1,i,j+1)-T2(n-
1,i,j))*ts/((zi(i))/curii);
%                                 Qtot3(n,i,j)=Qtot-Qtoair(n,i,j)+Qcondin+Qcondout;
%                             else %if j=ii..
%                                 Qcondin=a1*kondgra*(1-por(i))*(T2(n,i,j-1)-
T2(n,i,j))*ts/(zi(i)/curii);
%                                 if i<k
%                                     if por(i+1)<1
%                                      Qcondout=a1*kondgra*(1-por(i))*CXA*(T2(n-1,i+1,1)-T2(n-
1,i,j))*ts/(.5*(zi(i)/curii))+.5*(zi(i+1)/ii(1,i+1));
%                                     else
%                                         if i<k-1
%                                             if por(i+2)<1
%                                             Qcondout=arad*CXA*(1-por(i))*B*(((T2(n-
1,i+2,1))^4)-((T2(n-1,i,j))^4))*ts;
%                                             %v3: (1-por(i+2)) instead of
%                                             %just (por(i+2))
%                                             %#v10: chg por(i+2) ->
%                                             %por(i)
%                                             else
%                                             Qcondout=0;
%                                             end;
```

```
%                                       else
%                                       Qcondout=0;
%                                       end;
%                                   end;
%                               else
%                                   Qcondout=0;
%                               end;
%                               Qtot3(n,i,j)=Qtot-Qtoair(n,i,j)+Qcondin+Qcondout;
%                           end;
%                       else %if j=1
%                           if i>1
%                               if por(i-1)<1
%                                Qcondin=a1*kondgra*(1-por(i))*CXA*(T2(n,i-1,previi)-
T2(n,i,j))*ts/(.5*(zi(i)/curii)+.5*(zi(i-1)/ii(1,i-1))); %assume
%                                % assume contact between graphite blocks
%                                % as approx by ratio of porosity also
%                                % small ts that previous temps relevant.
%                               else
%                                 if i>2
%                                   if por(i-2)<1
%                                   Qcondin=arad*CXA*(1-por(i))*B*(((T2(n,i-2,prev2ii))^4)-
((T2(n,i,j))^4))*ts;
%                                   else
%                                   Qcondin=0;
%                                   end;
%                                 else
%                                   Qcondin=0;
%                                 end;
%                               end;
%                           else
%                               Qcondin=0;
%                           end;
%                           Qcondout=a1*kondgra*(1-por(i))*CXA*(T2(n-1,i,j+1)-T2(n-
1,i,j))*ts/(zi(i)/curii);
%                           Qtot3(n,i,j)=Qtot-Qtoair(n,i,j)+Qcondin+Qcondout;
%                       end;
%                   else
%                       Qcondin=0;
%                       Qcondout=0;
%                       Qtot3(n,i,j)=Qtot-Qtoair(n,i,j)+Qcondin+Qcondout;
%                   end;
%               else
                Qcondin=0;
                Qcondout=0;
                Qtot3(n,i,j)=Qtot-Qtoair(n,i,j)+Qcondin+Qcondout;
%               end;
```

```
Qcondinout(n,i,j)=Qcondin + Qcondout;
Qcondout1(n,i,j)=Qcondout;

%calculate new T as result of Q in.
rho_C=2240; %kg/m3
Cp_C=710; %J/kg-K
Cp_air=1.2;
m_C=(1-por(i))*Volts(i)*rho_C;
if por(i)==1 %redundant?
    Tnew=T;
else
    Tnew = T + (Qtot3(n,i,j)+SQ*zi(i))/(Cp_C*m_C); %p6 added SQ
end;



Tair2=Tair(n,i,j)+(Qtoair(n,i,j)+Qfromwall(n,i,j))/((2308.4*.45+1150*.55)*rho_dry*Volts(i)*por(i)
);
 %v3:TairRCO to Tair
if Tair2<300
   Tair2=300;
end;


%UPDATING GAS SPECIES CONCENTRATIONS
delO2=(dO2+dO2_1)/(101325*Volts(i)*por(i)/(8.314*Ta));
if j<curii
    if pO2i(n,i,j)+delO2>0
    pO2i(n+1,i,j+1)=pO2i(n,i,j)+delO2;
        if pO2i(n+1,i,j+1)<0 %redundant intention
        pO2i(n+1,i,j+1)=0;
        end;
    else
        pO2i(n+1,i,j+1)=0;
    end;
    delCO=dCO+dCO_1+dCO_2;
    delCO2=dCO2+dCO2_1+dCO2_2;
    pCOi(n+1,i,j+1)=pCOi(n,i,j)+delCO;
    pCO2i(n+1,i,j+1)=pCO2i(n,i,j)+delCO2;
else  % j=curii
    if i<k+1
        if pO2i(n,i,j)+delO2>0
        pO2i(n+1,i+1,1)=pO2i(n,i,j)+delO2;
            if pO2i(n+1,i+1,1)<0
            pO2i(n+1,i+1,1)=0;
```

```
                    end;
                else
                    pO2i(n+1,i+1,1)=0;
                end;
                delCO=dCO+dCO_1+dCO_2;
                delCO2=dCO2+dCO2_1+dCO2_2;
                pCOi(n+1,i+1,1)=pCOi(n,i,j)+delCO;
                pCO2i(n+1,i+1,1)=pCO2i(n,i,j)+delCO2;
            else %for last slice last section
                pO2i(n+1,i,j)=pO2i(n,i,j)+delO2;
                delCO=dCO+dCO_1+dCO_2;
                delCO2=dCO2+dCO2_1+dCO2_2;
                pCOi(n+1,i,j)=pCOi(n,i,j)+delCO;
                pCO2i(n+1,i,j)=pCO2i(n,i,j)+delCO2;
            end;
        end;

        if pCO2i(n,i,j)<0
            pCO2i(n,i,j)=0;
        end;

        if pCOi(n,i,j)<0
            pCOi(n,i,j)=0;
        end;

        if pO2i(n,i,j)<0
            pO2i(n,i,j)=0;
        end;

        %CORRECTING HEAT ERROR
        errorg(n,i,j)=-(m_C*Cp_C*(Tnew-T))-
Qtoair(n,i,j)+QOtoCO(n,i,j)+QOtoCO2(n,i,j)+QCO2nC(n,i,j)+Qcondin+Qcondout;
        errora(n,i,j)=-((2308.4*.45+1150*.55)*rho_dry*Volts(i)*por(i)*(Tair2-
Tair(n,i,j)))+Qfromwall(n,i,j)+Qtoair(n,i,j);
        ae=0.1; %$heat error relaxation

        %GRAPHITE HEAT ERROR
        if errorg(n,i,j)==0
        else
          if por(i)==1
             Tnew=T;
          else
             Tnew = T + (Qtot3(n,i,j)-ae*errorg(n,i,j))/(Cp_C*m_C);
          end;
         T2(n,i,j)=Tnew;
        end;
```

```
                %GAS HEAT ERROR
                if errora(n,i,j)==0
                else
                    Tair2=Tair(n,i,j)+(Qtoair(n,i,j)+Qfromwall(n,i,j)-
ae*errora(n,i,j))/((2308.4*.45+1150*.55)*rho_dry*Volts(i)*por(i));
                    if Tair2<300
                        Tair2=300;
                    end;
                end;
                %s

               if Tnew<300%923
                   Tnew=300;%#$923;
               end;

               if Tair2<300
                   Tair2=300;
               end;

                %counter Tmax
                if Tnew>Tmax
                    Tmax=Tnew;
                    nmax=n;
                    imax=i;
                    jmax=j;
                end;

                %Tmax for timestep
                if Tnew>Tmaxn
                    Tmaxn=Tnew;
                end;

                %counter Tairmax
                if Tair2>Tairmax
                    Tairmax=Tair2;
                    namax=n;
                    iamax=i;
                    jamax=j;
                end;

               %air cannot heat hotter than geometry by factor 1.001
                if Tair2>(1.001)*Tmaxn
                    Tair2=(1.001)*Tmaxn;
                end;
```

```
%CALCULATING NEW GAS AND GRAPHITE TEMPERATURES

    if n<(h*(3600/ts))
        if Asurfts(n,i)==0
            T2(n+1,i,j)=650+273; %set wall temp
        else
            T2(n+1,i,j)=Tnew;
        end;

        %counter max O2 at pebble height (section 9)
        if pO2i(n,9,j)>pO2i(n,9,j)
            pO2maxpeb=pO2i(n,9,j);
        end;
        if j<curii
            Tair(n+1,i,j+1)=Tair2;
        else
            if i<k+1
                Tair(n+1,i+1,1)=Tair2;
            end;
        end;
    else %patch for last time step
        if j<curii
        T2(n,i,j+1)=Tnew;
        Tair(n,i,j+1)=Tair2;
        else
            if i<k+1
                if Asurfts(i+1)==0
                T2(n,i+1,1)=650+273; %set wall temp
                else
                T2(n,i+1,1)=Tnew;
                end;
                Tair(n,i+1,1)=Tair2;
            end;
        end;
    end;

%v9: fill in values by height
T2Ch(n,c2)=T2(n,i,j)-273;
TairCh(n,c2)=Tair(n,i,j)-273;
pO2ih(n,c2)=pO2i(n,i,j);
pCOih(n,c2)=pCOi(n,i,j);
pCO2ih(n,c2)=pCO2i(n,i,j);

c=c-1;
if c==0
    j=1;
```

```
                break
            end;

        end;

        %v3: added mean values for volumes
        T2m(n,i)=mean(T2(n,i,1:curii));
        Tairm(n,i)=mean(Tair(n,i,1:curii));
        pO2im(n,i)=mean(pO2i(n,i,1:curii));
        pCOim(n,i)=mean(pCOi(n,i,1:curii));
        pCO2im(n,i)=mean(pCO2i(n,i,1:curii));
        QCOnO2m(n,i)=mean(QCOnO2(n,i,1:curii));
        QOtoCOm(n,i)=mean(QOtoCO(n,i,1:curii));
        QOtoCO2m(n,i)=mean(QOtoCO2(n,i,1:curii));
        QCO2nCm(n,i)=mean(QCO2nC(n,i,1:curii));
        Qtoairm(n,i)=mean(Qtoair(n,i,1:curii));
        Qfromwallm(n,i)=mean(Qfromwall(n,i,1:curii));
        Qtot3m(n,i)=mean(Qtot3(n,i,1:curii));
        Qcondinoutm(n,i)=mean(Qcondinout(n,i,1:curii));
        Qcondoutm(n,i)=mean(Qcondout1(n,i,1:curii));
        errorgm(n,i)=mean(errorg(n,i,1:curii));
        erroram(n,i)=mean(errora(n,i,1:curii));

        if c>0
            continue
        else
            break
        end;



    end;
end;

%CONTINUATION-  TRANSIENT
for n=(sum(ii)+1):(h*(3600/ts)) %calculate for remainder of h hours
    c=n;
    c2=0;
    %Tmax for timestep reset
    Tmaxn=650;
    for i=1:k; %(each i is a section)
        %#v3: added velocity per section
        v=mdot/(por(i)*CXA);
%         nn=nn+c2
        %v11p4 adding some sort of burnoff increase in surface area
        Asurfts(n,i)=Reffts(i)*Asurfpz(i)/zi(i);
```

```
        %v15 commented below; n is greater than 1
%         if n>1
% %             if n>nn% && n>1
%               if (sum(QOtoCO(n-1,i,:))+sum(QOtoCO2(n-1,i,:)))>0
%                Asurfts(n,i)=ainc*Asurfts(n-1,i);
%               end;
% %             end;
%         end;

        Vol(i)=CXA*zi(i);
        Reffts(i)=((zi(i)/(ts*v))^-1);
        Volts(i)=(Reffts(i))*Vol(i); %v6 took out *por(i) which led to bad graphite calcs...
assume both vol and surf A have same cross sections with height.

         if i>1
         previi=ii(1,i-1);
         end;
         if i>2
         prev2ii=ii(1,i-2);
         end;
         curii=ii(1,i);

        for j=1:ii(1,i)
            c2=c2+1;
            %for s=1:it

               if pCOi(n,i,j)<0
                   pCOi(n,i,j)=0; %p4 to1 dbstop out...
%                    delCO
%                    dbstop
               end;
               if T2(n,i,j)>4000
                   Tnew
                   dbstop
               end;

               if T2(n,i,j)<300
                   T2(n,i,j)=300;
               end;

               if pCO2i(n,i,j)<0
                   pCO2i(n,i,j)=0;
               end;

               T=T2(n,i,j);
```

```
                Ta=Tair(n,i,j);
%                 Tavg=(T+Tair(n,i,j))/2;
%                 T=Tavg; %p4 commented this to match 2nd part

%                commented v16 because too low...
%                 if Ta<T
%                     Tavg=(T+Ta)/2;
%                 else
                    Tavg=T;
%                 end;

               rho_dry = .55*(101325/(Rdry*Ta))+.45*(.2348); %kg/m3 modification using density
vapor at 650 C

                if pO2i(n,i,j)>0
                    RO21=(7.2*10^10)*((exp(-16140/(Tavg))))*(pO2i(n,i,j));
                    RO22=770*(v^.65)*(Tavg^.34)*(pO2i(n,i,j));
                    ReactO2=(((7.2*10^10)*((exp(-16140/(Tavg))))*(pO2i(n,i,j)))^(-
1)+(770*(v^.65)*(Tavg^.34)*(pO2i(n,i,j)))^(-1))^(-1); %mg/cm2-h
                    %#not general
                    %p5- E/2
                    ReactO2ts=ReactO2*ts/3600; %mg/cm2-ts
                    RO2mol=ReactO2ts*(100*100*Asurfts(n,i))/12000;%mol/ts, 12000 mg C/mol C

                    A=K1*(exp(-E1/(R*Tavg)));
                    dO2=-RO2mol*(0.5*A+1)/(A+1);

%                     %control to avoid reacting more than avail oxygen.
%                     if abs(dO2)>(rho_dry*Volts(i)*pO2i(n,i,j)/.032)
%                     %(kg/m3*m3/(kg/mol)) 32g O2 /mol
%                         dO2=-rho_dry*Volts(i)*pO2i(n,i,j)/.032; %p4 to1 added -
%                         RO2mol=dO2*(A+1)/(0.5*A+1);
%                         ReactO2=(RO2mol/((100*100*Asurfts(n,i))/12000))/(ts/3600);
%                     end;

                    dmolCO2=RO2mol*(1/(1+A)); %mol increase in CO2 with ts from O reaction
                    dCO2=dmolCO2/(101325*Volts(i)*por(i)/(8.314*Ta)); %p7 changed all T to Ta for
species calcs
                    dmolCO=RO2mol*(A/(A+1)); %mol increase in CO with ts from O reaction
                    dCO=dmolCO/(101325*Volts(i)*por(i)/(8.314*Ta));

                    %CO+0.5*O2-> CO2 has large exothermic.  (eqn from takeda)
                    %VOLUMETRIC
                    if pCOi(n,i,j)>0

                        K2=1.3*(10^8); %m^3/mol-s
```

```
                    E2=126000; %J/mol

                    RCOnO2=K2*((exp(-
E2/(R*Ta))))*(pCOi(n,i,j))*((pO2i(n,i,j))^.5)*((pCO2i(n,i,j))^.5); % mol/m3-s
                    molCOnO2=RCOnO2*Volts(i)*por(i)*ts; %mol/ts
                    QCOnO2(n,i,j)=molCOnO2*283000; %J/ts

                    %this is produced IN the gas, so the heat produced will be
                    %considered perfectly distributed, with the heat conducted
                    %to the wall by the same equation

                    dCO_1=-molCOnO2/(101325*Volts(i)*por(i)/(8.314*Ta));
                    dCO2_1=molCOnO2/(101325*Volts(i)*por(i)/(8.314*Ta));
                    dO2_1=-0.5*molCOnO2/(101325*Volts(i)*por(i)/(8.314*Ta));
                else
                    pCOi(n,i,j)=0;
                    dCO_1=0;
                    dCO2_1=0;
                    dO2_1=0;
                    QCOnO2(n,i,j)=0;
                end;

                if RO2mol>0 %(molCOnO2/2)
                QOtoCO(n,i,j)=(A/(A+1))*(RO2mol)*111000; %ratio*mol/ts*111000 J/mol
                QOtoCO2(n,i,j)=(1/(1+A))*(RO2mol)*394000; %(1-ratio)*mol/ts*394000 J/mol
                %not considering changes in ratio due to other reactions
                %because negligible
                else
                QOtoCO(n,i,j)=0.0000;
                QOtoCO2(n,i,j)=0.0000;
                end;

            else
                ReactO2=0;
                ReactO2ts=0;
                RO2mol=0;
                dCO=0;
                dCO2=0;
                dO2=0;
                dCO_1=0;
                dCO2_1=0;
                dO2_1=0;
                RCOnO2=0;
                molCOnO2=0; %mol/ts
                QCOnO2(n,i,j)=0;
            end;
```

```
%CO2+C ->2CO endothermic, surface area.  (eqn from moorman)
K3=2220; %
E3=-30635; %

%here, the limiting agent will be CO2 but in our experiment it
%never got large enough to affect the eqn significantly.

if pCO2i(n,i,j)>0
    RCO2nC=K3*((exp(E3/Tavg))); % mol C/m2-s
    molCO2nC=RCO2nC*Asurfts(n,i)*ts; %mol/ts
    dmolCO=molCO2nC; %mol increase in CO and decrease in CO2
    dCO_2=molCO2nC/(101325*Volts(i)*por(i)/(8.314*Ta));
    dCO2_2=-molCO2nC/(101325*Volts(i)*por(i)/(8.314*Ta));
    QCO2nC(n,i,j)=molCO2nC*-172000; %J/ts
else
    RCO2nC=0;
    QCO2nC(n,i,j)=0.0000;
    dCO_2=0;
    dCO2_2=0;
end;

kond=(1.5207*10^(-11))*(Tair(n,i,j)^3)-(4.8574*10^(-
8))*(Tair(n,i,j)^2)+(1.0184*10^(-4))*(Tair(n,i,j))-(3.9333*10^(-4)); %(.45*(.093/.07)+.55)*
%W/m-K


 %Qtoair is formulated to be positive if heat is
 %transferred from graphite to air
if por(i)<1
    Qtoair1=a*(Asurfts(n,i))*kond*(24/11)*(T-Tair(n,i,j))*ts/CLair(i); %eqn 10-31
T&K

else
    Qtoair1=0; %#p4div2 in the case of just a wall, heat transfer considered
below
    %Qtoair3=0; %#p4div2 in the case of just a wall, heat transfer considered
below
end;

Qtoair2=QCOnO2(n,i,j);

B=5.67*(10^(-8)); % W/m2-K4
emissair=.35*.55+.6*.45;
Qtoair3=arada*Asurfts(n,i)*(emissair)*B*((Tavg^4)-((Tair(n,i,j))^4))*ts; %p7 chg
from (emissair/(emissair+1+emissair*1) to just emissair
```

```
                Qtoair(n,i,j)=(Qtoair1+Qtoair2+Qtoair3);
                Qmax=((2308.4*.45+1150*.55)*rho_dry*Volts(i))*(T-Tair(n,i,j))*ts; %W/kg-
K*kg/m3*m3*K

%                 if abs(Qtoair(n,i,j))>abs(Qmax)
%                     Qtoair(n,i,j)=Qmax; %p6 #Qmax *.5
%                     Qmaxcount=Qtoair(n,i,j)-Qmax;
%                 end;

                 %heat transfer from walls (not graphite)
                 Twall=650+273;

                 %positive if wall is hotter than air
                 if Asurfts(n,i)==0
                 Axs=.3*.3;
                 Pw=4*.3; %"wetted" perimeter
                 CL=4*Axs/Pw;
                 Awall=4*.3*zi(i);
                 Qfromwall(n,i,j)=a*(Awall)*kond*(24/11)*(Twall-Tair(n,i,j))*ts/CL; %v3:TairRCO
to Tair%eqn 10-31 T&K
                 end;

                 Qairtot=Qtoair(n,i,j)+Qfromwall(n,i,j);

                 %v23
                if abs(Qairtot)>abs(Qmax)
                        Qairtot=Qmax; %p6 #Qmax *.5
                end;

                 %v14 commented
%                   if T>Tair(n,i,j)&&Qairtot>Qmax1 %took out abs, added temp cond
%                      Qmaxcount=Qtoair(n,i,j)+Qfromwall(n,i,j)-Qmax1;
%                      Qtoair(n,i,j)=Qmax1-Qfromwall(n,i,j); %p6 #Qmax *.5
%                  else
% %                       if T<Tair(n,i,j)&&abs(Qairtot)>Qmax2
% %                       Qtoair(n,i,j)=Qmax2-Qfromwall(n,i,j);
% %                       Qmaxcount=0;
% %                       end;
%                  end;

                 Qtot=a*(QOtoCO(n,i,j)+QOtoCO2(n,i,j)+QCO2nC(n,i,j)); %J/ts %note, QCOnO2
incorporated into air T
```

```
                a1=1; %CONDIN/OUT RELAXATION $v3: changed a1 from .1 to .2 v4: .2 to .3 v6:.3-
>.5 v7->.7 v8:->1

% %                  %CALCULATING HEAT CONDUCTED/RADIATED IN AND OUT OF NODES
                if por(i)<1
                   if n>1
                       if j>1
                           if j<curii
                               Qcondin=a1*kondgra*(1-por(i))*CXA*(T2(n,i,j-1)-
T2(n,i,j))*ts/(zi(i)/curii); %assume
                                %                       assume contact between graphite blocks
                                %                       as approx by ratio of porosity also
                                %                       small ts that
                                %                       previous temps relevant.
                               Qcondout=a1*kondgra*(1-por(i))*CXA*(T2(n-1,i,j+1)-T2(n-
1,i,j))*ts/((zi(i))/curii);
                               Qtot3(n,i,j)=Qtot-Qtoair(n,i,j)+Qcondin+Qcondout;
                           else %if j=ii..
                               Qcondin=a1*kondgra*(1-por(i))*(T2(n,i,j-1)-
T2(n,i,j))*ts/(zi(i)/curii);
                               if i<k
                                   if por(i+1)<1
                                    Qcondout=a1*kondgra*(1-por(i))*CXA*(T2(n-1,i+1,1)-T2(n-
1,i,j))*ts/(.5*(zi(i)/curii))+.5*(zi(i+1)/ii(1,i+1));
                                   else
                                       if i<k-1
                                           if por(i+2)<1
                                           Qcondout=arad*CXA*(1-por(i))*B*(((T2(n-1,i+2,1))^4)-
((T2(n-1,i,j))^4))*ts;

                                           %v3: (1-por(i+2)) instead of
                                           %just (por(i+2))
                                           %#v10: chg por(i+2) ->
                                           %por(i)
                                           else
                                           Qcondout=0;
                                           end;
                                       else
                                       Qcondout=0;
                                       end;
                                   end;
                               else
                                   Qcondout=0;
                               end;
                               Qtot3(n,i,j)=Qtot-Qtoair(n,i,j)+Qcondin+Qcondout;
                           end;
                       else %if j=1
```

```
                        if i>1
                            if por(i-1)<1
                             Qcondin=a1*kondgra*(1-por(i))*CXA*(T2(n,i-1,previi)-
T2(n,i,j))*ts/(.5*(zi(i)/curii)+.5*(zi(i-1)/ii(1,i-1))); %assume
                             %                        assume contact between graphite blocks
                             %                        as approx by ratio of porosity also
                             %                        small ts that previous temps relevant.
                            else
                              if i>2
                                if por(i-2)<1
                                Qcondin=arad*CXA*(1-por(i))*B*(((T2(n,i-2,prev2ii))^4)-
((T2(n,i,j))^4))*ts;

                                else
                                Qcondin=0;
                                end;
                              else
                                Qcondin=0;
                              end;
                            end;
                        else
                            Qcondin=0;
                        end;
                        Qcondout=a1*kondgra*(1-por(i))*CXA*(T2(n-1,i,j+1)-T2(n-
1,i,j))*ts/(zi(i)/curii);
                        Qtot3(n,i,j)=Qtot-Qtoair(n,i,j)+Qcondin+Qcondout;
                    end;
                else
                    Qcondin=0;
                    Qcondout=0;
                    Qtot3(n,i,j)=Qtot-Qtoair(n,i,j)+Qcondin+Qcondout;
                end;
            else
            Qcondin=0;
            Qcondout=0;
            Qtot3(n,i,j)=Qtot-Qtoair(n,i,j)+Qcondin+Qcondout;
            end;

            Qcondinout(n,i,j)=Qcondin + Qcondout;
            Qcondout1(n,i,j)=Qcondout;

            %calculate new T as result of Q in.
            rho_C=2240; %kg/m3
            Cp_C=710; %J/kg-K
            Cp_air=1.2;
            m_C=(1-por(i))*Volts(i)*rho_C;
            if por(i)==1 %redundant?
```

```
        Tnew=T;
    else
        Tnew = T + (Qtot3(n,i,j)+SQ*zi(i))/(Cp_C*m_C); %p6 added SQ
    end;


Tair2=Tair(n,i,j)+(Qairtot)/((2308.4*.45+1150*.55)*rho_dry*Volts(i)*por(i));

%v14 commented below #
%       v3:TairRCO to Tair
%      if Tair2<300
%          Tair2=300;
%      end;
%      if Qmaxcount>0
%          if Tair2<T
%              Tair2=T;
%          end;
%      end;
%      if Tair2>T
%          Tair2=T;
%      end;


 %UPDATING GAS SPECIES CONCENTRATIONS
 delO2=(dO2+dO2_1)/(101325*Volts(i)*por(i)/(8.314*Ta));
 if j<curii
     if pO2i(n,i,j)+delO2>0
     pO2i(n+1,i,j+1)=pO2i(n,i,j)+delO2;
         if pO2i(n+1,i,j+1)<0 %redundant intention
         pO2i(n+1,i,j+1)=0;
         end;
     else
         pO2i(n+1,i,j+1)=0;
     end;
     delCO=dCO+dCO_1+dCO_2;
     delCO2=dCO2+dCO2_1+dCO2_2;
     pCOi(n+1,i,j+1)=pCOi(n,i,j)+delCO;
     pCO2i(n+1,i,j+1)=pCO2i(n,i,j)+delCO2;
 else  % j=curii
     if i<k+1
         if pO2i(n,i,j)+delO2>0
         pO2i(n+1,i+1,1)=pO2i(n,i,j)+delO2;
             if pO2i(n+1,i+1,1)<0
             pO2i(n+1,i+1,1)=0;
             end;
         else
```

```
                    pO2i(n+1,i+1,1)=0;
                end;
                delCO=dCO+dCO_1+dCO_2;
                delCO2=dCO2+dCO2_1+dCO2_2;
                pCOi(n+1,i+1,1)=pCOi(n,i,j)+delCO;
                pCO2i(n+1,i+1,1)=pCO2i(n,i,j)+delCO2;
            else %for last slice last section
                pO2i(n+1,i,j)=pO2i(n,i,j)+delO2;
                delCO=dCO+dCO_1+dCO_2;
                delCO2=dCO2+dCO2_1+dCO2_2;
                pCOi(n+1,i,j)=pCOi(n,i,j)+delCO;
                pCO2i(n+1,i,j)=pCO2i(n,i,j)+delCO2;
            end;
        end;

        if pCO2i(n,i,j)<0
            pCO2i(n,i,j)=0;
        end;

        if pCOi(n,i,j)<0
            pCOi(n,i,j)=0;
        end;

        if pO2i(n,i,j)<0
            pO2i(n,i,j)=0;
        end;

        %CORRECTING HEAT ERROR
        errorg(n,i,j)=-(m_C*Cp_C*(Tnew-T))-
Qtoair(n,i,j)+QOtoCO(n,i,j)+QOtoCO2(n,i,j)+QCO2nC(n,i,j)+Qcondin+Qcondout;
        errora(n,i,j)=-((2308.4*.45+1150*.55)*rho_dry*Volts(i)*por(i)*(Tair2-
Tair(n,i,j)))+Qfromwall(n,i,j)+Qtoair(n,i,j);
        ae=0.01; %$heat error relaxation %v24 .1->.01

        %GRAPHITE HEAT ERROR
        if errorg(n,i,j)==0
        else
          if por(i)==1
             Tnew=T;
          else
             Tnew = T + (Qtot3(n,i,j)-ae*errorg(n,i,j))/(Cp_C*m_C);
          end;
         T2(n,i,j)=Tnew;
        end;

        %GAS HEAT ERROR
```

```
                if errora(n,i,j)==0
                else
                    Tair2=Tair(n,i,j)+(Qairtot-
ae*errora(n,i,j))/((2308.4*.45+1150*.55)*rho_dry*Volts(i)*por(i));
                    if Tair2<300
                        Tair2=300;
                    end;
                end;
                %s

               %v15 back to 923 instead of 300
               if Tnew<300;%v23 923
                   Tnew=300;%v23 923;
               end;

%                if Tair2<300
%                    Tair2=300;
%                end;


                %counter max O2 at pebble height (section 9)
                if pO2i(n,9,j)>pO2i(n,9,j)
                    pO2maxpeb=pO2i(n,9,j);
                end;

                %counter Tmax
                if Tnew>Tmax
                    Tmax=Tnew;
                    nmax=n;
                    imax=i;
                    jmax=j;
                end;

                %Tmax for flow
                if Tnew>Tmaxn
                    Tmaxn=Tnew;
                end;

                %counter Tairmax
                if Tair2>Tairmax
                    Tairmax=Tair2;
                    namax=n;
                    iamax=i;
                    jamax=j;
                end;
```

```
%air cannot heat hotter than geometry by factor 1.001
 if Tair2>(1+.001)*Tmaxn
     Tair2=(1+.001)*Tmaxn;
 end;

%    %air cannot be cooled more than geometry %v15
%    if Tair2<Tair(n,i,j)&&T2m(n-1,i)>Tair2
%        Tair2=T2m(n-1,i);
%    end;

 %CALCULATING NEW GAS AND GRAPHITE TEMPERATURES

     if n<(h*(3600/ts))
         if Asurfts(n,i)==0
             T2(n+1,i,j)=650+273; %set wall temp
         else
             T2(n+1,i,j)=Tnew;
         end;



         if j<curii
             Tair(n+1,i,j+1)=Tair2;
         else
             if i<k+1
                 Tair(n+1,i+1,1)=Tair2;
             end;
         end;
     else %patch for last time step
         if j<curii
         T2(n,i,j+1)=Tnew;
         Tair(n,i,j+1)=Tair2;
         else
             if i<k+1
                 if Asurfts(i+1)==0
                 T2(n,i+1,1)=650+273; %set wall temp
                 else
                 T2(n,i+1,1)=Tnew;
                 end;
                 Tair(n,i+1,1)=Tair2;
             end;
         end;
     end;
```

```
                %v9: fill in values by height
                T2Ch(n,c2)=T2(n,i,j)-273;
                TairCh(n,c2)=Tair(n,i,j)-273;
                pO2ih(n,c2)=pO2i(n,i,j);
                pCOih(n,c2)=pCOi(n,i,j);
                pCO2ih(n,c2)=pCO2i(n,i,j);

%                 c=c-1;
%                 if c==0
%                     j=1;
%                     break
%                 end;

        end;

        %v3: added mean values for volumes
        T2m(n,i)=mean(T2(n,i,1:curii));
        Tairm(n,i)=mean(Tair(n,i,1:curii));
        pO2im(n,i)=mean(pO2i(n,i,1:curii));
        pCOim(n,i)=mean(pCOi(n,i,1:curii));
        pCO2im(n,i)=mean(pCO2i(n,i,1:curii));
        QCOnO2m(n,i)=mean(QCOnO2(n,i,1:curii));
        QOtoCOm(n,i)=mean(QOtoCO(n,i,1:curii));
        QOtoCO2m(n,i)=mean(QOtoCO2(n,i,1:curii));
        QCO2nCm(n,i)=mean(QCO2nC(n,i,1:curii));
        Qtoairm(n,i)=mean(Qtoair(n,i,1:curii));
        Qfromwallm(n,i)=mean(Qfromwall(n,i,1:curii));
        Qtot3m(n,i)=mean(Qtot3(n,i,1:curii));
        Qcondinoutm(n,i)=mean(Qcondinout(n,i,1:curii));
        Qcondoutm(n,i)=mean(Qcondout1(n,i,1:curii));
        errorgm(n,i)=mean(errorg(n,i,1:curii));
        erroram(n,i)=mean(errora(n,i,1:curii));

%         if c>0
%             continue
%         else
%             break
%         end;



    end;

end;
%%
```

```
%EXPORT TO EXCEL
            s1=(2*sum(ii)+1):60*2:n; %every 60s (if ts=.5s)
            it=1;
            x=1:n;
            f=1:2*sum(ii);
            s=cat(2,f,s1);
%             s=1:1:(n+1);

            height=cat(2,0,cumsum(zi));
            t=0;

            T2Cm=T2m-273;
            TairCm=Tairm-273;
%             T2C=T2-273;
%             TairC=Tair-273;

            %v2:added errora

D=cat(3,T2Cm(s,:),TairCm(s,:),QCOnO2m(s,:),QOtoCOm(s,:),QOtoCO2m(s,:),QCO2nCm(s,:),Qtoairm(s,:),Q
fromwallm(s,:),Qtot3m(s,:),Qtot3m(s,:),Qcondinoutm(s,:),Qcondoutm(s,:),pO2im(s,:),pCOim(s,:),pCO2
im(s,:),errorgm(s,:),erroram(s,:));

sheet=char('T2C','TairC','QCOnO2','QOtoCO','QOtoCO2','QCO2nC','Qtoair','Qfromwall','Qtot2','Qtot3
','Qcondinout','Qcondout','pO2i','pCOi','pCO2i','errorg','errora');
            warning off MATLAB:xlswrite:AddSheet
            t=0;

            for j=1:17
                xlswrite('dataplotz2v27.xls', [t,height;x(s)',D(:,:,j)], sheet(j,:));
            end;
            xlsread('dataplotz2v27.xls', -1);
            %%

            %v9 added below xlsread and Ecat
            E=cat(3,T2Ch(s,:),TairCh(s,:),pO2ih(s,:),pCOih(s,:),pCO2ih(s,:));
            sheet=char('T2C wrt z','TairC wrt z','pO2i wrt z','pCOi wrt z','pCO2i wrt z');
            warning off MATLAB:xlswrite:AddSheet
            for j=1:5
                xlswrite('dataplotz2wrtzv27.xls', [t,heightj;x(s)',E(:,:,j)], sheet(j,:));
            end;
            xlsread('dataplotz2wrtzv27.xls', -1);

u%%
%           PLOTS in MATLAB
```

```
            subplot(2,3,1), plot(x, T2Cm(1:n,1), x, T2Cm(1:n,9),x, TairCm(1:n,1), x,
TairCm(1:n,(k+1)))
            set(gca,'XTick',60*60:60*60:h*3600/ts)
            set(gca,'XTickLabel',{'h'})

            subplot(2,3,2), plot(x, T2Cm(1:n,1), x, T2Cm(1:n,2),  x, T2Cm(1:n,3), x,
T2Cm(1:n,4),x, T2Cm(1:n,5),x, T2Cm(1:n,6),x, T2Cm(1:n,7))
            set(gca,'XTick',60*60:60*60:h*3600/ts)
            set(gca,'XTickLabel',{'h'})

            subplot(2,3,3), plot(x, TairCm(1:n,1), x, TairCm(1:n,2),  x, TairCm(1:n,3), x,
TairCm(1:n,4),x, TairCm(1:n,5),x, TairCm(1:n,6),x, TairCm(1:n,7))
            set(gca,'XTick',60*60:60*60:h*3600/ts)
            set(gca,'XTickLabel',{'h'})

            subplot(2,3,4), plot(x, pO2im(1:n,1), x, pO2im(1:n,(k+1)))
            set(gca,'XTick',60*60:60*60:h*3600/ts)
            set(gca,'XTickLabel',{'h'})

            subplot(2,3,5), plot(x, pCO2im(1:n,1), x, pCO2im(1:n,(k+1)))
            set(gca,'XTick',60*60:60*60:h*3600/ts)
            set(gca,'XTickLabel',{'h'})

            subplot(2,3,6), plot(x, pCOim(1:n,1), x, pCOim(1:n,(k+1)))
            set(gca,'XTick',60*60:60*60:h*3600/ts)
            set(gca,'XTickLabel',{'h'})

%%
it=10;
T2C=T2-273;
TairC=Tair-273;
x=1:n;
hrsarray=(0:h)';
% time1=strvcat('h', 'h 15 min', 'h 30 min', 'h 45 min');
% time2=strvcat('h', 'h 30 min');
% time3=('h');
% Time1=[time1, hrsarray];
height=cat(2,0,cumsum(zi));

% function time_string=secs2hms(h*(3600/ts))
%     time_string='';
%     nhours = 0;
%     nmins = 0;
%     if time_in_secs >= 3600
%         nhours = floor(h*(3600/ts)/3600);
%         if nhours > 1
```

```
%             hour_string = ' hrs, ';
%         else
%             hour_string = ' hr, ';
%         end;
%         time_string = [num2str(nhours) hour_string];
%     end;
%     if time_in_secs >= 60
%         nmins = floor((h*(3600/ts) - 3600*nhours)/60);
%         if nmins > 1
%             minute_string = ' mins, ';
%         else
%             minute_string = ' min, ';
%         end;
%         time_string = [time_string num2str(nmins) minute_string];
%     end;
%     %nsecs = time_in_secs - 3600*nhours - 60*nmins;
%     %time_string = [time_string sprintf('%2.1f', nsecs) ' secs'];

%if n<(2*3600)
    %sample data output.
    s=1:30:n; %every 30s

%D1(:,:,1:15)=cat(2,x(s),T2C(s,:),TairC(s,:),TairRCO(s,:),QCOnO2(s,:),QOtoCO(s,:),QOtoCO2(s,:),QC
O2nC(s,:),Qtoair(s,:),Qfromwall(s,:),Qtot3(s,:),pO2i(s,:),pCOi(s,:),pCO2i(s,:),errorg(s,:));

D=cat(3,T2C(s,:,it),TairC(s,:,it),TairRCO(s,:,it),QCOnO2(s,:,it),QOtoCO(s,:,it),QOtoCO2(s,:,it),Q
CO2nC(s,:,it),Qtoair(s,:,it),Qfromwall(s,:,it),Qtot3(s,:,it),pO2i(s,:,it),pCOi(s,:,it),pCO2i(s,:,
it),errorg(s,:,it));
        %D=[height; x(s),height; T2C(s,:),height; TairC(s,:),height; TairRCO(s,:),height;
QCOnO2(s,:),height; QOtoCO(s,:),height; QOtoCO2(s,:),height; QCO2nC(s,:),height;
Qtoair(s,:),height; Qfromwall(s,:),height; Qtot3(s,:),height; pO2i(s,:),height; pCOi(s,:),height;
pCO2i(s,:),height; errorg(s,:)];
        %D=cat(3, height x(s),height T2C(s,:),height TairC(s,:),height TairRCO(s,:),height
QCOnO2(s,:),height QOtoCO(s,:),height QOtoCO2(s,:),height QCO2nC(s,:),height Qtoair(s,:),height
Qfromwall(s,:),height Qtot3(s,:),height pO2i(s,:),height pCOi(s,:),height pCO2i(s,:),height
errorg(s,:));

sheet=char('T2C','TairC','TairRCO','QCOnO2','QOtoCO','QOtoCO2','QCO2nC','Qtoair','Qfromwall','Qto
t3','pO2i','pCOi','pCO2i','errorg');
        warning off MATLAB:xlswrite:AddSheet
        t=0;
        for j=1:14
            xlswrite('dataplotz2.xls', [t,height;x(s)',D(:,:,j)], sheet(j,:,it));
        end;
        xlsread('dataplotz2.xls', -1);
```

```
subplot(2,3,1), plot(x, T2C(1:n,1,it), x, T2C(1:n,(k+1),it), x, TairC(1:n,1,it), x,
TairC(1:n,(k+1),it));
set(gca,'XTick',15*60:15*60:h*3600/ts)
set(gca,'XTickLabel',{1:h*'h 15 min', 'h 30 min','h 45 min'})

subplot(2,3,2), plot(x, TairC(1:n,1,it), x, TairC(1:n,(k+1),it))
set(gca,'XTick',15*60:15*60:h*3600/ts)
set(gca,'XTickLabel',{'15 min', '30 min','45 min','h'})

subplot(2,3,3), plot(height, T2C(n,(k+1),it), height, TairC(n,(k+1),it),height,
T2C(n/2,(k+1),it), height, TairC(n/2,(k+1),it), height, T2C(n/4,(k+1),it), height,
TairC(n/4,(k+1),it))
% set(gca,'XTick',height((k+1)))
% set(gca,'XTickLabel',{'m'})

subplot(2,3,4), plot(x, pO2i(1:n,1,it), x, pO2i(1:n,(k+1),it))
set(gca,'XTick',15*60:15*60:h*3600/ts)
set(gca,'XTickLabel',{'15 min', '30 min','45 min','h'})

subplot(2,3,5), plot(x, pCO2i(1:n,1,it), x, pCO2i(1:n,(k+1),it))
set(gca,'XTick',15*60:15*60:h*3600/ts)
set(gca,'XTickLabel',{'15 min', '30 min','45 min','h'})

subplot(2,3,6), plot(x, pCOi(1:n,1,it), x, pCOi(1:n,(k+1),it))
set(gca,'XTick',15*60:15*60:h*3600/ts)
set(gca,'XTickLabel',{'15 min', '30 min','45 min','h'})
%else

    %if n<(4*3600)
 %sample data output.
    s=1:60:h*3600/ts; %every 60s

%D1(:,:,1:15)=cat(2,x(s),T2C(s,:,it),TairC(s,:,it),TairRCO(s,:,it),QCOnO2(s,:,it),QOtoCO(s,:,it),
QOtoCO2(s,:,it),QCO2nC(s,:,it),Qtoair(s,:,it),Qfromwall(s,:,it),Qtot3(s,:,it),pO2i(s,:,it),pCOi(s
,:,it),pCO2i(s,:,it),errorg(s,:,it));

D=cat(3,T2C(s,:,it),TairC(s,:,it),TairRCO(s,:,it),QCOnO2(s,:,it),QOtoCO(s,:,it),QOtoCO2(s,:,it),Q
CO2nC(s,:,it),Qtoair(s,:,it),Qfromwall(s,:,it),Qtot3(s,:,it),pO2i(s,:,it),pCOi(s,:,it),pCO2i(s,:,
it),errorg(s,:,it));
        %D=[height; x(s),height; T2C(s,:,it),height; TairC(s,:,it),height;
TairRCO(s,:,it),height; QCOnO2(s,:,it),height; QOtoCO(s,:,it),height; QOtoCO2(s,:,it),height;
QCO2nC(s,:,it),height; Qtoair(s,:,it),height; Qfromwall(s,:,it),height; Qtot3(s,:,it),height;
pO2i(s,:,it),height; pCOi(s,:,it),height; pCO2i(s,:,it),height; errorg(s,:,it)];
        %D=cat(3, height x(s),height T2C(s,:,it),height TairC(s,:,it),height
TairRCO(s,:,it),height QCOnO2(s,:,it),height QOtoCO(s,:,it),height QOtoCO2(s,:,it),height
```

```
QCO2nC(s,:,it),height Qtoair(s,:,it),height Qfromwall(s,:,it),height Qtot3(s,:,it),height
pO2i(s,:,it),height pCOi(s,:,it),height pCO2i(s,:,it),height errorg(s,:,it));

sheet=char('T2C','TairC','TairRCO','QCOnO2','QOtoCO','QOtoCO2','QCO2nC','Qtoair','Qfromwall','Qto
t3','pO2i','pCOi','pCO2i','errorg');
        warning off MATLAB:xlswrite:AddSheet
        t=0;
        for j=1:14
            xlswrite('dataplotz2.xls', [t,height;x(s)',D(:,:,j)], sheet(j,:,it));
        end;
        xlsread('dataplotz2.xls', -1);

    subplot(2,3,1), plot(x, T2C(1:n,1,it), x, T2C(1:n,(k+1),it),x, TairC(1:n,1,it), x,
TairC(1:n,(k+1),it))
    set(gca,'XTick',30*60:30*60:h*3600/ts)
    set(gca,'XTickLabel',{'30 min', 'h'})

    subplot(2,3,2), plot(x, TairC(1:n,1,it), x, TairC(1:n,(k+1),it))
    set(gca,'XTick',30*60:30*60:h*3600/ts)
    set(gca,'XTickLabel',{'30 min', 'h'})

    subplot(2,3,4), plot(x, pO2i(1:n,1,it), x, pO2i(1:n,(k+1),it))
    set(gca,'XTick',30*60:30*60:h*3600/ts)
    set(gca,'XTickLabel',{'30 min', 'h'})

    subplot(2,3,5), plot(x, pCO2i(1:n,1,it), x, pCO2i(1:n,(k+1),it))
    set(gca,'XTick',30*60:30*60:h*3600/ts)
    set(gca,'XTickLabel',{'30 min', 'h'})

    subplot(2,3,6), plot(x, pCOi(1:n,1,it), x, pCOi(1:n,(k+1),it))
    set(gca,'XTick',30*60:30*60:h*3600/ts)
    set(gca,'XTickLabel',{'30 min', 'h'})
    %else

%%
        %if n>(4*3600)
     %sample data output.
            s=1:60*5:n; %every 30s
            it=1;
            x=1:n;
            height=cat(2,0,cumsum(zi));

            T2Cm=T2m-273;
            TairCm=Tairm-273;
            T2C=T2-273;
            TairC=Tair-273;
```

```
            %v2:added errora

%D1(:,:,1:15)=cat(2,x(s),T2C(s,:,it),TairC(s,:,it),TairRCO(s,:,it),QCOnO2(s,:,it),QOtoCO(s,:,it),
QOtoCO2(s,:,it),QCO2nC(s,:,it),Qtoair(s,:,it),Qfromwall(s,:,it),Qtot3(s,:,it),pO2i(s,:,it),pCOi(s
,:,it),pCO2i(s,:,it),errorg(s,:,it));

D=cat(3,T2Cm(s,:),TairCm(s,:),TairRCOm(s,:),QCOnO2m(s,:),QOtoCOm(s,:),QOtoCO2m(s,:),QCO2nCm(s,:),
Qtoairm(s,:),Qfromwallm(s,:),Qtot3m(s,:),Qcondinoutm(s,:),pO2im(s,:),pCOim(s,:),pCO2im(s,:),error
gm(s,:),erroram(s,:));
            %D=[height; x(s),height; T2C(s,:,it),height; TairC(s,:,it),height;
TairRCO(s,:,it),height; QCOnO2(s,:,it),height; QOtoCO(s,:,it),height; QOtoCO2(s,:,it),height;
QCO2nC(s,:,it),height; Qtoair(s,:,it),height; Qfromwall(s,:,it),height; Qtot3(s,:,it),height;
pO2i(s,:,it),height; pCOi(s,:,it),height; pCO2i(s,:,it),height; errorg(s,:,it)];
            %D=cat(3, height x(s),height T2C(s,:,it),height TairC(s,:,it),height
TairRCO(s,:,it),height QCOnO2(s,:,it),height QOtoCO(s,:,it),height QOtoCO2(s,:,it),height
QCO2nC(s,:,it),height Qtoair(s,:,it),height Qfromwall(s,:,it),height Qtot3(s,:,it),height
pO2i(s,:,it),height pCOi(s,:,it),height pCO2i(s,:,it),height errorg(s,:,it));

sheet=char('T2C','TairC','TairRCO','QCOnO2','QOtoCO','QOtoCO2','QCO2nC','Qtoair','Qfromwall','Qto
t3','Qcondinout','pO2i','pCOi','pCO2i','errorg','errora');
            warning off MATLAB:xlswrite:AddSheet
            t=0;

            for j=1:16
                xlswrite('dataplotz2v83.xls', [t,height;x(s)',D(:,:,j)], sheet(j,:));
            end;
            xlsread('dataplotz2v83.xls', -1);

            subplot(2,3,1), plot(x, T2Cm(1:n,1), x, T2Cm(1:n,9),x, TairCm(1:n,1), x,
TairCm(1:n,(k+1)))
            set(gca,'XTick',60*60:60*60:h*3600/ts)
            set(gca,'XTickLabel',{'h'})

            subplot(2,3,2), plot(x, T2Cm(1:n,1), x, T2Cm(1:n,2),  x, T2Cm(1:n,3), x,
T2Cm(1:n,4),x, T2Cm(1:n,5),x, T2Cm(1:n,6),x, T2Cm(1:n,7))
            set(gca,'XTick',60*60:60*60:h*3600/ts)
            set(gca,'XTickLabel',{'h'})

            subplot(2,3,3), plot(x, TairCm(1:n,1), x, TairCm(1:n,2),  x, TairCm(1:n,3), x,
TairCm(1:n,4),x, TairCm(1:n,5),x, TairCm(1:n,6),x, TairCm(1:n,7))
            set(gca,'XTick',60*60:60*60:h*3600/ts)
            set(gca,'XTickLabel',{'h'})

            subplot(2,3,4), plot(x, pO2im(1:n,1), x, pO2im(1:n,(k+1)))
            set(gca,'XTick',60*60:60*60:h*3600/ts)
```

```
            set(gca,'XTickLabel',{'h'})

            subplot(2,3,5), plot(x, pCO2im(1:n,1), x, pCO2im(1:n,(k+1)))
            set(gca,'XTick',60*60:60*60:h*3600/ts)
            set(gca,'XTickLabel',{'h'})

            subplot(2,3,6), plot(x, pCOim(1:n,1), x, pCOim(1:n,(k+1)))
            set(gca,'XTick',60*60:60*60:h*3600/ts)
            set(gca,'XTickLabel',{'h'})
        %end;
    %end;

%end;
```

# APPENDIX C: 2D FLUENT DECK

Note that the steady state and transient models used the same basic inputs.

FLUENT
Version: 2d, dp, pbns, spe, lam (2d, double precision, pressure-based, species, laminar)
Release: 6.3.26
Title:

Models
---

| Model | Settings |
|---|---|
| Space | 2D |
| Time | Steady |
| Viscous | Laminar |
| Heat Transfer | Enabled |
| Solidification and Melting | Disabled |
| Radiation | None |
| Species Transport | Reacting (5 species) |
| Coupled Dispersed Phase | Disabled |
| Pollutants | Disabled |
| Pollutants | Disabled |
| Soot | Disabled |

Boundary Conditions
---

Zones

| name | id | type |
|---|---|---|
| tall_chimney | 27 | fluid |
| peb2 | 28 | fluid |
| peb1topeb2 | 29 | fluid |
| peb1 | 30 | fluid |
| ref2toref3 | 31 | fluid |
| ref1toref2 | 32 | fluid |
| entry_face_collection_chamber | 33 | fluid |
| inlet_pipe | 34 | fluid |
| r1chs | 35 | fluid |
| r2chs | 36 | fluid |
| r3chs | 37 | fluid |
| r3gs | 38 | solid |
| r2gs | 39 | solid |
| r1gs | 40 | solid |
| outlet_vent.87.1.1 | 22 | outflow |
| pressure_inlet.86.1.1 | 23 | mass-flow-inlet |
| solidfluidwalls.1.1-shadow | 90 | wall |
| solidfluidwalls:041-shadow | 89 | wall |
| solidfluidwalls:042-shadow | 88 | wall |
| solidfluidwalls:043-shadow | 87 | wall |
| solidfluidwalls:044-shadow | 86 | wall |
| solidfluidwalls:045-shadow | 85 | wall |
| solidfluidwalls:046-shadow | 84 | wall |
| solidfluidwalls:047-shadow | 83 | wall |
| solidfluidwalls:048-shadow | 82 | wall |
| solidfluidwalls.1.1 | 24 | wall |
| outer_wall.1.1 | 25 | wall |
| default-interior.1.1 | 26 | interior |
| solidfluidwalls:041 | 41 | wall |
| solidfluidwalls:042 | 42 | wall |

| | | |
|---|---|---|
| solidfluidwalls:043 | 43 | wall |
| solidfluidwalls:044 | 44 | wall |
| solidfluidwalls:045 | 45 | wall |
| solidfluidwalls:046 | 46 | wall |
| solidfluidwalls:047 | 47 | wall |
| solidfluidwalls:048 | 48 | wall |
| outer_wall:049 | 49 | wall |
| outer_wall:050 | 50 | wall |
| outer_wall:051 | 51 | wall |
| outer_wall:052 | 52 | wall |
| outer_wall:053 | 53 | wall |
| outer_wall:054 | 54 | wall |
| outer_wall:055 | 55 | wall |
| outer_wall:056 | 56 | wall |
| outer_wall:057 | 57 | wall |
| outer_wall:058 | 58 | wall |
| default-interior:059 | 59 | interior |
| default-interior:060 | 60 | interior |
| default-interior:061 | 61 | interior |
| default-interior:062 | 62 | interior |
| default-interior:063 | 63 | interior |
| default-interior:064 | 64 | interior |
| default-interior:065 | 65 | interior |
| default-interior:066 | 66 | interior |
| default-interior:067 | 67 | interior |
| default-interior:068 | 68 | interior |
| default-interior:069 | 69 | interior |
| default-interior:070 | 70 | interior |
| default-interior:071 | 71 | interior |
| default-interior:072 | 72 | interior |
| default-interior:073 | 73 | interior |
| default-interior:074 | 74 | interior |
| default-interior:075 | 75 | interior |
| default-interior:076 | 76 | interior |
| default-interior:077 | 77 | interior |
| default-interior:078 | 78 | interior |
| default-interior:079 | 79 | interior |
| default-interior:080 | 80 | interior |
| default-interior:081 | 81 | interior |

Boundary Conditions

tall_chimney

| Condition | Value |
|---|---|
| Material Name | mixture-template |
| Specify source terms? | no |
| Source Terms | ((mass) (x-momentum) (y-momentum) (species-0) (species-1) (species-2) (species-3) (energy) (p1)) |
| Specify fixed values? | no |
| Fixed Values | ((x-velocity (inactive . #f) (constant . 0) (profile )) (y-velocity (inactive . #f) (constant . 0) (profile )) (species-0 (inactive . #f) (constant . 0) (profile )) (species-1 (inactive . #f) (constant . 0) (profile )) (species-2 (inactive . #f) (constant . 0) (profile )) (species-3 (inactive . #f) (constant . 0) (profile )) (temperature (inactive . #f) (constant . 0) (profile ))) |
| Motion Type | 0 |
| X-Velocity Of Zone (m/s) | 0 |
| Y-Velocity Of Zone (m/s) | 0 |
| Rotation speed (rad/s) | 0 |
| X-Origin of Rotation-Axis (m) | 0 |
| Y-Origin of Rotation-Axis (m) | 0 |
| Deactivated Thread | no |
| Porous zone? | no |
| X-Component of Direction-1 Vector | 1 |
| Y-Component of Direction-1 Vector | 0 |
| Relative Velocity Resistance Formulation? | yes |

Direction-1 Viscous Resistance (1/m2) 0
Direction-2 Viscous Resistance (1/m2) 0
Choose alternative formulation for inertial resistance? no
Direction-1 Inertial Resistance (1/m) 0
Direction-2 Inertial Resistance (1/m) 0
C0 Coefficient for Power-Law 0
C1 Coefficient for Power-Law 0
Porosity 1
Solid Material Name graphite-south-africa
Reaction Mechanism 0
Activate reaction mechanisms? yes
Surface-Volume-Ratio (1/m) 0

peb2

Condition Value

---

Material Name mixture-template
Specify source terms? no
Source Terms ((mass) (x-momentum) (y-momentum) (species-0) (species-1) (species-2) (species-3) (energy) (p1))
Specify fixed values? no
Fixed Values ((x-velocity (inactive . #f) (constant . 0) (profile )) (y-velocity (inactive . #f) (constant . 0) (profile )) (species-0 (inactive . #f) (constant . 0) (profile )) (species-1 (inactive . #f) (constant . 0) (profile )) (species-2 (inactive . #f) (constant . 0) (profile )) (species-3 (inactive . #f) (constant . 0) (profile )) (temperature (inactive . #f) (constant . 0) (profile )))
Motion Type 0
X-Velocity Of Zone (m/s) 0
Y-Velocity Of Zone (m/s) 0
Rotation speed (rad/s) 0
X-Origin of Rotation-Axis (m) 0
Y-Origin of Rotation-Axis (m) 0
Deactivated Thread no
Porous zone? yes
X-Component of Direction-1 Vector 1
Y-Component of Direction-1 Vector 0
Relative Velocity Resistance Formulation? yes
Direction-1 Viscous Resistance (1/m2) 0
Direction-2 Viscous Resistance (1/m2) 0
Choose alternative formulation for inertial resistance? no
Direction-1 Inertial Resistance (1/m) 0
Direction-2 Inertial Resistance (1/m) 0
C0 Coefficient for Power-Law 340
C1 Coefficient for Power-Law 1.6107
Porosity 0.39500001
Solid Material Name graphite-south-africa
Reaction Mechanism 0
Activate reaction mechanisms? yes
Surface-Volume-Ratio (1/m) 0

peb1topeb2

Condition Value

---

Material Name mixture-template
Specify source terms? no
Source Terms ((mass) (x-momentum) (y-momentum) (species-0) (species-1) (species-2) (species-3) (energy) (p1))
Specify fixed values? no
Fixed Values ((x-velocity (inactive . #f) (constant . 0) (profile )) (y-velocity (inactive . #f) (constant . 0) (profile )) (species-0 (inactive . #f) (constant . 0) (profile )) (species-1 (inactive . #f) (constant . 0) (profile )) (species-2 (inactive . #f) (constant . 0) (profile )) (species-3 (inactive . #f) (constant . 0) (profile )) (temperature (inactive . #f) (constant . 0) (profile )))
Motion Type 0
X-Velocity Of Zone (m/s) 0

| | |
|---|---|
| Y-Velocity Of Zone (m/s) | 0 |
| Rotation speed (rad/s) | 0 |
| X-Origin of Rotation-Axis (m) | 0 |
| Y-Origin of Rotation-Axis (m) | 0 |
| Deactivated Thread | no |
| Porous zone? | no |
| X-Component of Direction-1 Vector | 1 |
| Y-Component of Direction-1 Vector | 0 |
| Relative Velocity Resistance Formulation? | yes |
| Direction-1 Viscous Resistance (1/m2) | 0 |
| Direction-2 Viscous Resistance (1/m2) | 0 |
| Choose alternative formulation for inertial resistance? | no |
| Direction-1 Inertial Resistance (1/m) | 0 |
| Direction-2 Inertial Resistance (1/m) | 0 |
| C0 Coefficient for Power-Law | 0 |
| C1 Coefficient for Power-Law | 0 |
| Porosity | 1 |
| Solid Material Name | graphite-south-africa |
| Reaction Mechanism | 0 |
| Activate reaction mechanisms? | yes |
| Surface-Volume-Ratio (1/m) | 0 |

peb1

| Condition | Value |
|---|---|
| Material Name | mixture-template |
| Specify source terms? | no |
| Source Terms | ((mass) (x-momentum) (y-momentum) (species-0) (species-1) (species-2) (species-3) (energy) (p1)) |
| Specify fixed values? | no |
| Fixed Values | ((x-velocity (inactive . #f) (constant . 0) (profile )) (y-velocity (inactive . #f) (constant . 0) (profile )) (species-0 (inactive . #f) (constant . 0) (profile )) (species-1 (inactive . #f) (constant . 0) (profile )) (species-2 (inactive . #f) (constant . 0) (profile )) (species-3 (inactive . #f) (constant . 0) (profile )) (temperature (inactive . #f) (constant . 0) (profile ))) |
| Motion Type | 0 |
| X-Velocity Of Zone (m/s) | 0 |
| Y-Velocity Of Zone (m/s) | 0 |
| Rotation speed (rad/s) | 0 |
| X-Origin of Rotation-Axis (m) | 0 |
| Y-Origin of Rotation-Axis (m) | 0 |
| Deactivated Thread | no |
| Porous zone? | yes |
| X-Component of Direction-1 Vector | 1 |
| Y-Component of Direction-1 Vector | 0 |
| Relative Velocity Resistance Formulation? | yes |
| Direction-1 Viscous Resistance (1/m2) | 0 |
| Direction-2 Viscous Resistance (1/m2) | 0 |
| Choose alternative formulation for inertial resistance? | no |
| Direction-1 Inertial Resistance (1/m) | 0 |
| Direction-2 Inertial Resistance (1/m) | 0 |
| C0 Coefficient for Power-Law | 36.688 |
| C1 Coefficient for Power-Law | 1.7599 |
| Porosity | 0.39500001 |
| Solid Material Name | steel |
| Reaction Mechanism | 0 |
| Activate reaction mechanisms? | yes |
| Surface-Volume-Ratio (1/m) | 0 |

ref2toref3

| Condition | Value |
|---|---|
| Material Name | mixture-template |

Specify source terms? no
Source Terms ((mass) (x-momentum) (y-momentum) (species-0) (species-1) (species-2) (species-3) (energy) (p1))
Specify fixed values? no
Fixed Values ((x-velocity (inactive . #f) (constant . 0) (profile )) (y-velocity (inactive . #f) (constant . 0) (profile )) (species-0 (inactive . #f) (constant . 0) (profile )) (species-1 (inactive . #f) (constant . 0) (profile )) (species-2 (inactive . #f) (constant . 0) (profile )) (species-3 (inactive . #f) (constant . 0) (profile )) (temperature (inactive . #f) (constant . 0) (profile )))
Motion Type 0
X-Velocity Of Zone (m/s) 0
Y-Velocity Of Zone (m/s) 0
Rotation speed (rad/s) 0
X-Origin of Rotation-Axis (m) 0
Y-Origin of Rotation-Axis (m) 0
Deactivated Thread no
Porous zone? no
X-Component of Direction-1 Vector 1
Y-Component of Direction-1 Vector 0
Relative Velocity Resistance Formulation? yes
Direction-1 Viscous Resistance (1/m2) 0
Direction-2 Viscous Resistance (1/m2) 0
Choose alternative formulation for inertial resistance? no
Direction-1 Inertial Resistance (1/m) 0
Direction-2 Inertial Resistance (1/m) 0
C0 Coefficient for Power-Law 0
C1 Coefficient for Power-Law 0
Porosity 1
Solid Material Name graphite-south-africa
Reaction Mechanism 0
Activate reaction mechanisms? yes
Surface-Volume-Ratio (1/m) 0

ref1toref2

Condition Value

---

Material Name mixture-template
Specify source terms? no
Source Terms ((mass) (x-momentum) (y-momentum) (species-0) (species-1) (species-2) (species-3) (energy) (p1))
Specify fixed values? no
Fixed Values ((x-velocity (inactive . #f) (constant . 0) (profile )) (y-velocity (inactive . #f) (constant . 0) (profile )) (species-0 (inactive . #f) (constant . 0) (profile )) (species-1 (inactive . #f) (constant . 0) (profile )) (species-2 (inactive . #f) (constant . 0) (profile )) (species-3 (inactive . #f) (constant . 0) (profile )) (temperature (inactive . #f) (constant . 0) (profile )))
Motion Type 0
X-Velocity Of Zone (m/s) 0
Y-Velocity Of Zone (m/s) 0
Rotation speed (rad/s) 0
X-Origin of Rotation-Axis (m) 0
Y-Origin of Rotation-Axis (m) 0
Deactivated Thread no
Porous zone? no
X-Component of Direction-1 Vector 1
Y-Component of Direction-1 Vector 0
Relative Velocity Resistance Formulation? yes
Direction-1 Viscous Resistance (1/m2) 0
Direction-2 Viscous Resistance (1/m2) 0
Choose alternative formulation for inertial resistance? no
Direction-1 Inertial Resistance (1/m) 0
Direction-2 Inertial Resistance (1/m) 0
C0 Coefficient for Power-Law 0
C1 Coefficient for Power-Law 0
Porosity 1
Solid Material Name graphite-south-africa
Reaction Mechanism 0
Activate reaction mechanisms? yes

Surface-Volume-Ratio (1/m) 0

entry_face_collection_chamber

Condition Value

---

---

---

Material Name mixture-template
Specify source terms? no
Source Terms ((mass) (x-momentum) (y-momentum) (species-0) (species-1) (species-2) (species-3) (energy) (p1))
Specify fixed values? no
Fixed Values ((x-velocity (inactive . #f) (constant . 0) (profile )) (y-velocity (inactive . #f) (constant . 0) (profile )) (species-0 (inactive . #f) (constant . 0) (profile )) (species-1 (inactive . #f) (constant . 0) (profile )) (species-2 (inactive . #f) (constant . 0) (profile )) (species-3 (inactive . #f) (constant . 0) (profile )) (temperature (inactive . #f) (constant . 0) (profile )))
Motion Type 0
X-Velocity Of Zone (m/s) 0
Y-Velocity Of Zone (m/s) 0
Rotation speed (rad/s) 0
X-Origin of Rotation-Axis (m) 0
Y-Origin of Rotation-Axis (m) 0
Deactivated Thread no
Porous zone? no
X-Component of Direction-1 Vector 1
Y-Component of Direction-1 Vector 0
Relative Velocity Resistance Formulation? yes
Direction-1 Viscous Resistance (1/m2) 0
Direction-2 Viscous Resistance (1/m2) 0
Choose alternative formulation for inertial resistance? no
Direction-1 Inertial Resistance (1/m) 0
Direction-2 Inertial Resistance (1/m) 0
C0 Coefficient for Power-Law 0
C1 Coefficient for Power-Law 0
Porosity 1
Solid Material Name graphite-south-africa
Reaction Mechanism 0
Activate reaction mechanisms? yes
Surface-Volume-Ratio (1/m) 0

inlet_pipe

Condition Value

---

---

---

Material Name mixture-template
Specify source terms? no
Source Terms ((mass) (x-momentum) (y-momentum) (species-0) (species-1) (species-2) (species-3) (energy) (p1))
Specify fixed values? no
Fixed Values ((x-velocity (inactive . #f) (constant . 0) (profile )) (y-velocity (inactive . #f) (constant . 0) (profile )) (species-0 (inactive . #f) (constant . 0) (profile )) (species-1 (inactive . #f) (constant . 0) (profile )) (species-2 (inactive . #f) (constant . 0) (profile )) (species-3 (inactive . #f) (constant . 0) (profile )) (temperature (inactive . #f) (constant . 0) (profile )))
Motion Type 0
X-Velocity Of Zone (m/s) 0
Y-Velocity Of Zone (m/s) 0
Rotation speed (rad/s) 0
X-Origin of Rotation-Axis (m) 0
Y-Origin of Rotation-Axis (m) 0
Deactivated Thread no
Porous zone? no
X-Component of Direction-1 Vector 1
Y-Component of Direction-1 Vector 0
Relative Velocity Resistance Formulation? yes
Direction-1 Viscous Resistance (1/m2) 0
Direction-2 Viscous Resistance (1/m2) 0

Choose alternative formulation for inertial resistance? no
Direction-1 Inertial Resistance (1/m) 0
Direction-2 Inertial Resistance (1/m) 0
C0 Coefficient for Power-Law 0
C1 Coefficient for Power-Law 0
Porosity 1
Solid Material Name graphite-south-africa
Reaction Mechanism 0
Activate reaction mechanisms? yes
Surface-Volume-Ratio (1/m) 0

r1chs

Condition Value

---

---

---

Material Name mixture-template
Specify source terms? no
Source Terms ((mass) (x-momentum) (y-momentum) (species-0) (species-1) (species-2) (species-3) (energy) (p1))
Specify fixed values? no
Fixed Values ((x-velocity (inactive . #f) (constant . 0) (profile )) (y-velocity (inactive . #f) (constant . 0) (profile )) (species-0 (inactive . #f) (constant . 0) (profile )) (species-1 (inactive . #f) (constant . 0) (profile )) (species-2 (inactive . #f) (constant . 0) (profile )) (species-3 (inactive . #f) (constant . 0) (profile )) (temperature (inactive . #f) (constant . 0) (profile )))
Motion Type 0
X-Velocity Of Zone (m/s) 0
Y-Velocity Of Zone (m/s) 0
Rotation speed (rad/s) 0
X-Origin of Rotation-Axis (m) 0
Y-Origin of Rotation-Axis (m) 0
Deactivated Thread no
Porous zone? no
X-Component of Direction-1 Vector 1
Y-Component of Direction-1 Vector 0
Relative Velocity Resistance Formulation? yes
Direction-1 Viscous Resistance (1/m2) 0
Direction-2 Viscous Resistance (1/m2) 0
Choose alternative formulation for inertial resistance? no
Direction-1 Inertial Resistance (1/m) 0
Direction-2 Inertial Resistance (1/m) 0
C0 Coefficient for Power-Law 0
C1 Coefficient for Power-Law 0
Porosity 1
Solid Material Name graphite-south-africa
Reaction Mechanism 0
Activate reaction mechanisms? yes
Surface-Volume-Ratio (1/m) 0

r2chs

Condition Value

---

---

---

Material Name mixture-template
Specify source terms? no
Source Terms ((mass) (x-momentum) (y-momentum) (species-0) (species-1) (species-2) (species-3) (energy) (p1))
Specify fixed values? no
Fixed Values ((x-velocity (inactive . #f) (constant . 0) (profile )) (y-velocity (inactive . #f) (constant . 0) (profile )) (species-0 (inactive . #f) (constant . 0) (profile )) (species-1 (inactive . #f) (constant . 0) (profile )) (species-2 (inactive . #f) (constant . 0) (profile )) (species-3 (inactive . #f) (constant . 0) (profile )) (temperature (inactive . #f) (constant . 0) (profile )))
Motion Type 0
X-Velocity Of Zone (m/s) 0
Y-Velocity Of Zone (m/s) 0
Rotation speed (rad/s) 0

X-Origin of Rotation-Axis (m) 0
Y-Origin of Rotation-Axis (m) 0
Deactivated Thread no
Porous zone? no
X-Component of Direction-1 Vector 1
Y-Component of Direction-1 Vector 0
Relative Velocity Resistance Formulation? yes
Direction-1 Viscous Resistance (1/m2) 0
Direction-2 Viscous Resistance (1/m2) 0
Choose alternative formulation for inertial resistance? no
Direction-1 Inertial Resistance (1/m) 0
Direction-2 Inertial Resistance (1/m) 0
C0 Coefficient for Power-Law 0
C1 Coefficient for Power-Law 0
Porosity 1
Solid Material Name graphite-south-africa
Reaction Mechanism 0
Activate reaction mechanisms? yes
Surface-Volume-Ratio (1/m) 0

r3chs

Condition Value

---

---

---

Material Name mixture-template
Specify source terms? no
Source Terms ((mass) (x-momentum) (y-momentum) (species-0) (species-1) (species-2) (species-3) (energy) (p1))
Specify fixed values? no
Fixed Values ((x-velocity (inactive . #f) (constant . 0) (profile )) (y-velocity (inactive . #f) (constant . 0) (profile )) (species-0 (inactive . #f) (constant . 0) (profile )) (species-1 (inactive . #f) (constant . 0) (profile )) (species-2 (inactive . #f) (constant . 0) (profile )) (species-3 (inactive . #f) (constant . 0) (profile )) (temperature (inactive . #f) (constant . 0) (profile )))
Motion Type 0
X-Velocity Of Zone (m/s) 0
Y-Velocity Of Zone (m/s) 0
Rotation speed (rad/s) 0
X-Origin of Rotation-Axis (m) 0
Y-Origin of Rotation-Axis (m) 0
Deactivated Thread no
Porous zone? no
X-Component of Direction-1 Vector 1
Y-Component of Direction-1 Vector 0
Relative Velocity Resistance Formulation? yes
Direction-1 Viscous Resistance (1/m2) 0
Direction-2 Viscous Resistance (1/m2) 0
Choose alternative formulation for inertial resistance? no
Direction-1 Inertial Resistance (1/m) 0
Direction-2 Inertial Resistance (1/m) 0
C0 Coefficient for Power-Law 0
C1 Coefficient for Power-Law 0
Porosity 1
Solid Material Name graphite-south-africa
Reaction Mechanism 0
Activate reaction mechanisms? yes
Surface-Volume-Ratio (1/m) 0

r3gs

Condition Value

---

Material Name graphite-south-africa
Specify source terms? no
Source Terms ()
Specify fixed values? no
Fixed Values ()

Motion Type 0
X-Velocity Of Zone (m/s) 0
Y-Velocity Of Zone (m/s) 0
Rotation speed (rad/s) 0
X-Origin of Rotation-Axis (m) 0
Y-Origin of Rotation-Axis (m) 0
Deactivated Thread no

r2gs

| Condition | Value |
|---|---|
| Material Name | graphite-south-africa |
| Specify source terms? | no |
| Source Terms | ((energy)) |
| Specify fixed values? | no |
| Fixed Values | ((temperature (inactive . #f) (constant . 0) (profile ))) |
| Motion Type | 0 |
| X-Velocity Of Zone (m/s) | 0 |
| Y-Velocity Of Zone (m/s) | 0 |
| Rotation speed (rad/s) | 0 |
| X-Origin of Rotation-Axis (m) | 0 |
| Y-Origin of Rotation-Axis (m) | 0 |
| Deactivated Thread | no |

r1gs

| Condition | Value |
|---|---|
| Material Name | graphite-south-africa |
| Specify source terms? | no |
| Source Terms | ((energy)) |
| Specify fixed values? | no |
| Fixed Values | ((temperature (inactive . #f) (constant . 0) (profile ))) |
| Motion Type | 0 |
| X-Velocity Of Zone (m/s) | 0 |
| Y-Velocity Of Zone (m/s) | 0 |
| Rotation speed (rad/s) | 0 |
| X-Origin of Rotation-Axis (m) | 0 |
| Y-Origin of Rotation-Axis (m) | 0 |
| Deactivated Thread | no |

outlet_vent.87.1.1

| Condition | Value |
|---|---|
| Flow rate weighting | 1 |

pressure_inlet.86.1.1

| Condition | Value |
|---|---|
| Mass Flow Specification Method | 0 |
| Mass Flow-Rate (kg/s) | 0.003 |
| Mass Flux (kg/m2-s) | 1 |
| Average Mass Flux (kg/m2-s) | 1 |
| Upstream Torque Integral (n-m) | 1 |
| Upstream Total Enthalpy Integral (w/m2) | 1 |
| Total Temperature (k) | 300 |
| Supersonic/Initial Gauge Pressure (pascal) | 0 |
| Direction Specification Method | 1 |
| Reference Frame | 0 |
| X-Component of Flow Direction | 1 |
| Y-Component of Flow Direction | 0 |
| X-Component of Axis Direction | 1 |
| Y-Component of Axis Direction | 0 |

Z-Component of Axis Direction 0
X-Coordinate of Axis Origin (m) 0
Y-Coordinate of Axis Origin (m) 0
Z-Coordinate of Axis Origin (m) 0
(((constant . 9.9999997e-06) (profile )) ((constant . 0.00056000001) (profile )) ((constant . 0.208) (profile )) ((constant . 0.090000004) (profile )))
is zone used in mixing-plane model? no

solidfluidwalls.1.1-shadow

| Condition | Value |
|---|---|
| Wall Thickness (m) | 0 |
| Heat Generation Rate (w/m3) | 0 |
| Material Name | graphite-south-africa |
| Thermal BC Type | 3 |
| Temperature (k) | 300 |
| Heat Flux (w/m2) | 0 |
| Convective Heat Transfer Coefficient (w/m2-k) | 0 |
| Free Stream Temperature (k) | 300 |
| Wall Motion | 0 |
| Shear Boundary Condition | 0 |
| Define wall motion relative to adjacent cell zone? | yes |
| Apply a rotational velocity to this wall? | no |
| Velocity Magnitude (m/s) | 0 |
| X-Component of Wall Translation | 1 |
| Y-Component of Wall Translation | 0 |
| Define wall velocity components? | no |
| X-Component of Wall Translation (m/s) | 0 |
| Y-Component of Wall Translation (m/s) | 0 |
| External Emissivity | 1 |
| External Radiation Temperature (k) | 300 |
| Activate Reaction Mechanisms | yes |
| Rotation Speed (rad/s) | 0 |
| X-Position of Rotation-Axis Origin (m) | 0 |
| Y-Position of Rotation-Axis Origin (m) | 0 |
| X-component of shear stress (pascal) | 0 |
| Y-component of shear stress (pascal) | 0 |
| Surface tension gradient (n/m-k) | 0 |
| Reaction Mechanisms | 0 |
| Specularity Coefficient | 0 |

solidfluidwalls:041-shadow

| Condition | Value |
|---|---|
| Wall Thickness (m) | 0 |
| Heat Generation Rate (w/m3) | 0 |
| Material Name | graphite-south-africa |
| Thermal BC Type | 3 |
| Temperature (k) | 300 |
| Heat Flux (w/m2) | 0 |
| Convective Heat Transfer Coefficient (w/m2-k) | 0 |
| Free Stream Temperature (k) | 300 |
| Wall Motion | 0 |
| Shear Boundary Condition | 0 |
| Define wall motion relative to adjacent cell zone? | yes |
| Apply a rotational velocity to this wall? | no |
| Velocity Magnitude (m/s) | 0 |
| X-Component of Wall Translation | 1 |
| Y-Component of Wall Translation | 0 |
| Define wall velocity components? | no |
| X-Component of Wall Translation (m/s) | 0 |
| Y-Component of Wall Translation (m/s) | 0 |
| External Emissivity | 1 |
| External Radiation Temperature (k) | 300 |
| Activate Reaction Mechanisms | yes |

| | |
|---|---|
| Rotation Speed (rad/s) | 0 |
| X-Position of Rotation-Axis Origin (m) | 0 |
| Y-Position of Rotation-Axis Origin (m) | 0 |
| X-component of shear stress (pascal) | 0 |
| Y-component of shear stress (pascal) | 0 |
| Surface tension gradient (n/m-k) | 0 |
| Reaction Mechanisms | 0 |
| Specularity Coefficient | 0 |

solidfluidwalls:042-shadow

| Condition | Value |
|---|---|
| Wall Thickness (m) | 0 |
| Heat Generation Rate (w/m3) | 0 |
| Material Name | graphite-south-africa |
| Thermal BC Type | 3 |
| Temperature (k) | 300 |
| Heat Flux (w/m2) | 0 |
| Convective Heat Transfer Coefficient (w/m2-k) | 0 |
| Free Stream Temperature (k) | 300 |
| Wall Motion | 0 |
| Shear Boundary Condition | 0 |
| Define wall motion relative to adjacent cell zone? | yes |
| Apply a rotational velocity to this wall? | no |
| Velocity Magnitude (m/s) | 0 |
| X-Component of Wall Translation | 1 |
| Y-Component of Wall Translation | 0 |
| Define wall velocity components? | no |
| X-Component of Wall Translation (m/s) | 0 |
| Y-Component of Wall Translation (m/s) | 0 |
| External Emissivity | 1 |
| External Radiation Temperature (k) | 300 |
| Activate Reaction Mechanisms | yes |
| Rotation Speed (rad/s) | 0 |
| X-Position of Rotation-Axis Origin (m) | 0 |
| Y-Position of Rotation-Axis Origin (m) | 0 |
| X-component of shear stress (pascal) | 0 |
| Y-component of shear stress (pascal) | 0 |
| Surface tension gradient (n/m-k) | 0 |
| Reaction Mechanisms | 0 |
| Specularity Coefficient | 0 |

solidfluidwalls:043-shadow

| Condition | Value |
|---|---|
| Wall Thickness (m) | 0 |
| Heat Generation Rate (w/m3) | 0 |
| Material Name | graphite-south-africa |
| Thermal BC Type | 3 |
| Temperature (k) | 300 |
| Heat Flux (w/m2) | 0 |
| Convective Heat Transfer Coefficient (w/m2-k) | 0 |
| Free Stream Temperature (k) | 300 |
| Wall Motion | 0 |
| Shear Boundary Condition | 0 |
| Define wall motion relative to adjacent cell zone? | yes |
| Apply a rotational velocity to this wall? | no |
| Velocity Magnitude (m/s) | 0 |
| X-Component of Wall Translation | 1 |
| Y-Component of Wall Translation | 0 |
| Define wall velocity components? | no |
| X-Component of Wall Translation (m/s) | 0 |
| Y-Component of Wall Translation (m/s) | 0 |
| External Emissivity | 1 |
| External Radiation Temperature (k) | 300 |

| | |
|---|---|
| Activate Reaction Mechanisms | yes |
| Rotation Speed (rad/s) | 0 |
| X-Position of Rotation-Axis Origin (m) | 0 |
| Y-Position of Rotation-Axis Origin (m) | 0 |
| X-component of shear stress (pascal) | 0 |
| Y-component of shear stress (pascal) | 0 |
| Surface tension gradient (n/m-k) | 0 |
| Reaction Mechanisms | 0 |
| Specularity Coefficient | 0 |

solidfluidwalls:044-shadow

| Condition | Value |
|---|---|
| Wall Thickness (m) | 0 |
| Heat Generation Rate (w/m3) | 0 |
| Material Name | graphite-south-africa |
| Thermal BC Type | 3 |
| Temperature (k) | 300 |
| Heat Flux (w/m2) | 0 |
| Convective Heat Transfer Coefficient (w/m2-k) | 0 |
| Free Stream Temperature (k) | 300 |
| Wall Motion | 0 |
| Shear Boundary Condition | 0 |
| Define wall motion relative to adjacent cell zone? | yes |
| Apply a rotational velocity to this wall? | no |
| Velocity Magnitude (m/s) | 0 |
| X-Component of Wall Translation | 1 |
| Y-Component of Wall Translation | 0 |
| Define wall velocity components? | no |
| X-Component of Wall Translation (m/s) | 0 |
| Y-Component of Wall Translation (m/s) | 0 |
| External Emissivity | 1 |
| External Radiation Temperature (k) | 300 |
| Activate Reaction Mechanisms | yes |
| | (0 0 0 0) |
| | (((constant . 0) (profile )) ((constant . 0) (profile )) ((constant . 0) (profile )) ((constant . 0) (profile ))) |
| Rotation Speed (rad/s) | 0 |
| X-Position of Rotation-Axis Origin (m) | 0 |
| Y-Position of Rotation-Axis Origin (m) | 0 |
| X-component of shear stress (pascal) | 0 |
| Y-component of shear stress (pascal) | 0 |
| Surface tension gradient (n/m-k) | 0 |
| Reaction Mechanisms | 0 |
| Specularity Coefficient | 0 |

solidfluidwalls:045-shadow

| Condition | Value |
|---|---|
| Wall Thickness (m) | 0 |
| Heat Generation Rate (w/m3) | 0 |
| Material Name | graphite-south-africa |
| Thermal BC Type | 3 |
| Temperature (k) | 300 |
| Heat Flux (w/m2) | 0 |
| Convective Heat Transfer Coefficient (w/m2-k) | 0 |
| Free Stream Temperature (k) | 300 |
| Wall Motion | 0 |
| Shear Boundary Condition | 0 |
| Define wall motion relative to adjacent cell zone? | yes |
| Apply a rotational velocity to this wall? | no |
| Velocity Magnitude (m/s) | 0 |
| X-Component of Wall Translation | 1 |
| Y-Component of Wall Translation | 0 |
| Define wall velocity components? | no |

| | |
|---|---|
| X-Component of Wall Translation (m/s) | 0 |
| Y-Component of Wall Translation (m/s) | 0 |
| External Emissivity | 1 |
| External Radiation Temperature (k) | 300 |
| Activate Reaction Mechanisms | yes |
| Rotation Speed (rad/s) | 0 |
| X-Position of Rotation-Axis Origin (m) | 0 |
| Y-Position of Rotation-Axis Origin (m) | 0 |
| X-component of shear stress (pascal) | 0 |
| Y-component of shear stress (pascal) | 0 |
| Surface tension gradient (n/m-k) | 0 |
| Reaction Mechanisms | 0 |
| Specularity Coefficient | 0 |

solidfluidwalls:046-shadow

| Condition | Value |
|---|---|
| Wall Thickness (m) | 0 |
| Heat Generation Rate (w/m3) | 0 |
| Material Name | graphite-south-africa |
| Thermal BC Type | 3 |
| Temperature (k) | 300 |
| Heat Flux (w/m2) | 0 |
| Convective Heat Transfer Coefficient (w/m2-k) | 0 |
| Free Stream Temperature (k) | 300 |
| Wall Motion | 0 |
| Shear Boundary Condition | 0 |
| Define wall motion relative to adjacent cell zone? | yes |
| Apply a rotational velocity to this wall? | no |
| Velocity Magnitude (m/s) | 0 |
| X-Component of Wall Translation | 1 |
| Y-Component of Wall Translation | 0 |
| Define wall velocity components? | no |
| X-Component of Wall Translation (m/s) | 0 |
| Y-Component of Wall Translation (m/s) | 0 |
| External Emissivity | 1 |
| External Radiation Temperature (k) | 300 |
| Activate Reaction Mechanisms | yes |
| Rotation Speed (rad/s) | 0 |
| X-Position of Rotation-Axis Origin (m) | 0 |
| Y-Position of Rotation-Axis Origin (m) | 0 |
| X-component of shear stress (pascal) | 0 |
| Y-component of shear stress (pascal) | 0 |
| Surface tension gradient (n/m-k) | 0 |
| Reaction Mechanisms | 0 |
| Specularity Coefficient | 0 |

solidfluidwalls:047-shadow

| Condition | Value |
|---|---|
| Wall Thickness (m) | 0 |
| Heat Generation Rate (w/m3) | 0 |
| Material Name | graphite-south-africa |
| Thermal BC Type | 3 |
| Temperature (k) | 300 |
| Heat Flux (w/m2) | 0 |
| Convective Heat Transfer Coefficient (w/m2-k) | 0 |
| Free Stream Temperature (k) | 300 |
| Wall Motion | 0 |
| Shear Boundary Condition | 0 |
| Define wall motion relative to adjacent cell zone? | yes |
| Apply a rotational velocity to this wall? | no |
| Velocity Magnitude (m/s) | 0 |
| X-Component of Wall Translation | 1 |
| Y-Component of Wall Translation | 0 |

| | |
|---|---|
| Define wall velocity components? | no |
| X-Component of Wall Translation (m/s) | 0 |
| Y-Component of Wall Translation (m/s) | 0 |
| External Emissivity | 1 |
| External Radiation Temperature (k) | 300 |
| Activate Reaction Mechanisms | yes |
| Rotation Speed (rad/s) | 0 |
| X-Position of Rotation-Axis Origin (m) | 0 |
| Y-Position of Rotation-Axis Origin (m) | 0 |
| X-component of shear stress (pascal) | 0 |
| Y-component of shear stress (pascal) | 0 |
| Surface tension gradient (n/m-k) | 0 |
| Reaction Mechanisms | 0 |
| Specularity Coefficient | 0 |

solidfluidwalls:048-shadow

| Condition | Value |
|---|---|
| Wall Thickness (m) | 0 |
| Heat Generation Rate (w/m3) | 0 |
| Material Name | graphite-south-africa |
| Thermal BC Type | 3 |
| Temperature (k) | 300 |
| Heat Flux (w/m2) | 0 |
| Convective Heat Transfer Coefficient (w/m2-k) | 0 |
| Free Stream Temperature (k) | 300 |
| Wall Motion | 0 |
| Shear Boundary Condition | 0 |
| Define wall motion relative to adjacent cell zone? | yes |
| Apply a rotational velocity to this wall? | no |
| Velocity Magnitude (m/s) | 0 |
| X-Component of Wall Translation | 1 |
| Y-Component of Wall Translation | 0 |
| Define wall velocity components? | no |
| X-Component of Wall Translation (m/s) | 0 |
| Y-Component of Wall Translation (m/s) | 0 |
| External Emissivity | 1 |
| External Radiation Temperature (k) | 300 |
| Activate Reaction Mechanisms | yes |
| Rotation Speed (rad/s) | 0 |
| X-Position of Rotation-Axis Origin (m) | 0 |
| Y-Position of Rotation-Axis Origin (m) | 0 |
| X-component of shear stress (pascal) | 0 |
| Y-component of shear stress (pascal) | 0 |
| Surface tension gradient (n/m-k) | 0 |
| Reaction Mechanisms | 0 |
| Specularity Coefficient | 0 |

solidfluidwalls.1.1

| Condition | Value |
|---|---|
| Wall Thickness (m) | 0 |
| Heat Generation Rate (w/m3) | 0 |
| Material Name | graphite-south-africa |
| Thermal BC Type | 3 |
| Temperature (k) | 300 |
| Heat Flux (w/m2) | 0 |
| Convective Heat Transfer Coefficient (w/m2-k) | 0 |
| Free Stream Temperature (k) | 300 |
| Wall Motion | 0 |
| Shear Boundary Condition | 0 |
| Define wall motion relative to adjacent cell zone? | yes |
| Apply a rotational velocity to this wall? | no |
| Velocity Magnitude (m/s) | 0 |

X-Component of Wall Translation 1
Y-Component of Wall Translation 0
Define wall velocity components? no
X-Component of Wall Translation (m/s) 0
Y-Component of Wall Translation (m/s) 0
External Emissivity 1
External Radiation Temperature (k) 300
Activate Reaction Mechanisms yes
(0 0 0 0)
(((constant . 0) (profile )) ((constant . 0) (profile )) ((constant . 0) (profile )) ((constant . 0) (profile )))
Rotation Speed (rad/s) 0
X-Position of Rotation-Axis Origin (m) 0
Y-Position of Rotation-Axis Origin (m) 0
X-component of shear stress (pascal) 0
Y-component of shear stress (pascal) 0
Surface tension gradient (n/m-k) 0
Reaction Mechanisms 0
Specularity Coefficient 0

outer_wall.1.1

Condition Value
---
--
Wall Thickness (m) 0.0099999998
Heat Generation Rate (w/m3) 0
Material Name steel
Thermal BC Type 5
Temperature (k) 300
Heat Flux (w/m2) 0
Convective Heat Transfer Coefficient (w/m2-k) 19
Free Stream Temperature (k) 923.15002
Wall Motion 0
Shear Boundary Condition 0
Define wall motion relative to adjacent cell zone? yes
Apply a rotational velocity to this wall? no
Velocity Magnitude (m/s) 0
X-Component of Wall Translation 1
Y-Component of Wall Translation 0
Define wall velocity components? no
X-Component of Wall Translation (m/s) 0
Y-Component of Wall Translation (m/s) 0
External Emissivity 1
External Radiation Temperature (k) 923.15002
Activate Reaction Mechanisms no
(0 0 0 0)
(((constant . 0) (profile )) ((constant . 0) (profile )) ((constant . 0) (profile )) ((constant . 0) (profile )))
Rotation Speed (rad/s) 0
X-Position of Rotation-Axis Origin (m) 0
Y-Position of Rotation-Axis Origin (m) 0
X-component of shear stress (pascal) 0
Y-component of shear stress (pascal) 0
Surface tension gradient (n/m-k) 0
Reaction Mechanisms 0
Specularity Coefficient 0

default-interior.1.1

Condition Value
---

solidfluidwalls:041

Condition Value
---
--
Wall Thickness (m) 0

```
Heat Generation Rate (w/m3)                  0
Material Name                                graphite-south-africa
Thermal BC Type                              3
Temperature (k)                              300
Heat Flux (w/m2)                             0
Convective Heat Transfer Coefficient (w/m2-k)      0
Free Stream Temperature (k)                  300
Wall Motion                                  0
Shear Boundary Condition                     0
Define wall motion relative to adjacent cell zone?   yes
Apply a rotational velocity to this wall?    no
Velocity Magnitude (m/s)                     0
X-Component of Wall Translation              1
Y-Component of Wall Translation              0
Define wall velocity components?             no
X-Component of Wall Translation (m/s)        0
Y-Component of Wall Translation (m/s)        0
External Emissivity                          1
External Radiation Temperature (k)           300
Activate Reaction Mechanisms                 yes
                                             (0 0 0 0)
                                             (((constant . 0) (profile )) ((constant . 0) (profile )) ((constant . 0) (profile )) ((constant . 0) (profile )))
Rotation Speed (rad/s)                       0
X-Position of Rotation-Axis Origin (m)       0
Y-Position of Rotation-Axis Origin (m)       0
X-component of shear stress (pascal)         0
Y-component of shear stress (pascal)         0
Surface tension gradient (n/m-k)             0
Reaction Mechanisms                          0
Specularity Coefficient                      0

solidfluidwalls:042

Condition                                    Value
-------------------------------------------------------------------------------------------------------------------------------------------------------------
--
Wall Thickness (m)                           0
Heat Generation Rate (w/m3)                  0
Material Name                                graphite-south-africa
Thermal BC Type                              3
Temperature (k)                              300
Heat Flux (w/m2)                             0
Convective Heat Transfer Coefficient (w/m2-k)      0
Free Stream Temperature (k)                  300
Wall Motion                                  0
Shear Boundary Condition                     0
Define wall motion relative to adjacent cell zone?   yes
Apply a rotational velocity to this wall?    no
Velocity Magnitude (m/s)                     0
X-Component of Wall Translation              1
Y-Component of Wall Translation              0
Define wall velocity components?             no
X-Component of Wall Translation (m/s)        0
Y-Component of Wall Translation (m/s)        0
External Emissivity                          1
External Radiation Temperature (k)           300
Activate Reaction Mechanisms                 yes
                                             (0 0 0 0)
                                             (((constant . 0) (profile )) ((constant . 0) (profile )) ((constant . 0) (profile )) ((constant . 0) (profile )))
Rotation Speed (rad/s)                       0
X-Position of Rotation-Axis Origin (m)       0
Y-Position of Rotation-Axis Origin (m)       0
X-component of shear stress (pascal)         0
Y-component of shear stress (pascal)         0
Surface tension gradient (n/m-k)             0
Reaction Mechanisms                          0
Specularity Coefficient                      0
```

solidfluidwalls:043

| Condition | Value |
|---|---|
| Wall Thickness (m) | 0 |
| Heat Generation Rate (w/m3) | 0 |
| Material Name | graphite-south-africa |
| Thermal BC Type | 3 |
| Temperature (k) | 300 |
| Heat Flux (w/m2) | 0 |
| Convective Heat Transfer Coefficient (w/m2-k) | 0 |
| Free Stream Temperature (k) | 300 |
| Wall Motion | 0 |
| Shear Boundary Condition | 0 |
| Define wall motion relative to adjacent cell zone? | yes |
| Apply a rotational velocity to this wall? | no |
| Velocity Magnitude (m/s) | 0 |
| X-Component of Wall Translation | 1 |
| Y-Component of Wall Translation | 0 |
| Define wall velocity components? | no |
| X-Component of Wall Translation (m/s) | 0 |
| Y-Component of Wall Translation (m/s) | 0 |
| External Emissivity | 1 |
| External Radiation Temperature (k) | 300 |
| Activate Reaction Mechanisms | yes |
| | (0 0 0 0) |
| | (((constant . 0) (profile )) ((constant . 0) (profile )) ((constant . 0) (profile )) ((constant . 0) (profile ))) |
| Rotation Speed (rad/s) | 0 |
| X-Position of Rotation-Axis Origin (m) | 0 |
| Y-Position of Rotation-Axis Origin (m) | 0 |
| X-component of shear stress (pascal) | 0 |
| Y-component of shear stress (pascal) | 0 |
| Surface tension gradient (n/m-k) | 0 |
| Reaction Mechanisms | 0 |
| Specularity Coefficient | 0 |

solidfluidwalls:044

| Condition | Value |
|---|---|
| Wall Thickness (m) | 0 |
| Heat Generation Rate (w/m3) | 0 |
| Material Name | graphite-south-africa |
| Thermal BC Type | 3 |
| Temperature (k) | 300 |
| Heat Flux (w/m2) | 0 |
| Convective Heat Transfer Coefficient (w/m2-k) | 0 |
| Free Stream Temperature (k) | 300 |
| Wall Motion | 0 |
| Shear Boundary Condition | 0 |
| Define wall motion relative to adjacent cell zone? | yes |
| Apply a rotational velocity to this wall? | no |
| Velocity Magnitude (m/s) | 0 |
| X-Component of Wall Translation | 1 |
| Y-Component of Wall Translation | 0 |
| Define wall velocity components? | no |
| X-Component of Wall Translation (m/s) | 0 |
| Y-Component of Wall Translation (m/s) | 0 |
| External Emissivity | 1 |
| External Radiation Temperature (k) | 300 |
| Activate Reaction Mechanisms | yes |
| Rotation Speed (rad/s) | 0 |
| X-Position of Rotation-Axis Origin (m) | 0 |
| Y-Position of Rotation-Axis Origin (m) | 0 |
| X-component of shear stress (pascal) | 0 |

| | |
|---|---|
| Y-component of shear stress (pascal) | 0 |
| Surface tension gradient (n/m-k) | 0 |
| Reaction Mechanisms | 0 |
| Specularity Coefficient | 0 |

solidfluidwalls:045

| Condition | Value |
|---|---|
| Wall Thickness (m) | 0 |
| Heat Generation Rate (w/m3) | 0 |
| Material Name | graphite-south-africa |
| Thermal BC Type | 3 |
| Temperature (k) | 300 |
| Heat Flux (w/m2) | 0 |
| Convective Heat Transfer Coefficient (w/m2-k) | 0 |
| Free Stream Temperature (k) | 300 |
| Wall Motion | 0 |
| Shear Boundary Condition | 0 |
| Define wall motion relative to adjacent cell zone? | yes |
| Apply a rotational velocity to this wall? | no |
| Velocity Magnitude (m/s) | 0 |
| X-Component of Wall Translation | 1 |
| Y-Component of Wall Translation | 0 |
| Define wall velocity components? | no |
| X-Component of Wall Translation (m/s) | 0 |
| Y-Component of Wall Translation (m/s) | 0 |
| External Emissivity | 1 |
| External Radiation Temperature (k) | 300 |
| Activate Reaction Mechanisms | yes |
| | (0 0 0 0) |
| | (((constant . 0) (profile )) ((constant . 0) (profile )) ((constant . 0) (profile )) ((constant . 0) (profile ))) |
| Rotation Speed (rad/s) | 0 |
| X-Position of Rotation-Axis Origin (m) | 0 |
| Y-Position of Rotation-Axis Origin (m) | 0 |
| X-component of shear stress (pascal) | 0 |
| Y-component of shear stress (pascal) | 0 |
| Surface tension gradient (n/m-k) | 0 |
| Reaction Mechanisms | 0 |
| Specularity Coefficient | 0 |

solidfluidwalls:046

| Condition | Value |
|---|---|
| Wall Thickness (m) | 0 |
| Heat Generation Rate (w/m3) | 0 |
| Material Name | graphite-south-africa |
| Thermal BC Type | 3 |
| Temperature (k) | 300 |
| Heat Flux (w/m2) | 0 |
| Convective Heat Transfer Coefficient (w/m2-k) | 0 |
| Free Stream Temperature (k) | 300 |
| Wall Motion | 0 |
| Shear Boundary Condition | 0 |
| Define wall motion relative to adjacent cell zone? | yes |
| Apply a rotational velocity to this wall? | no |
| Velocity Magnitude (m/s) | 0 |
| X-Component of Wall Translation | 1 |
| Y-Component of Wall Translation | 0 |
| Define wall velocity components? | no |
| X-Component of Wall Translation (m/s) | 0 |
| Y-Component of Wall Translation (m/s) | 0 |
| External Emissivity | 1 |
| External Radiation Temperature (k) | 300 |

Activate Reaction Mechanisms yes
(0 0 0 0)
(((constant . 0) (profile )) ((constant . 0) (profile )) ((constant . 0) (profile )) ((constant . 0) (profile )))
Rotation Speed (rad/s) 0
X-Position of Rotation-Axis Origin (m) 0
Y-Position of Rotation-Axis Origin (m) 0
X-component of shear stress (pascal) 0
Y-component of shear stress (pascal) 0
Surface tension gradient (n/m-k) 0
Reaction Mechanisms 0
Specularity Coefficient 0

solidfluidwalls:047

Condition Value
---

--
Wall Thickness (m) 0
Heat Generation Rate (w/m3) 0
Material Name graphite-south-africa
Thermal BC Type 3
Temperature (k) 300
Heat Flux (w/m2) 0
Convective Heat Transfer Coefficient (w/m2-k) 0
Free Stream Temperature (k) 300
Wall Motion 0
Shear Boundary Condition 0
Define wall motion relative to adjacent cell zone? yes
Apply a rotational velocity to this wall? no
Velocity Magnitude (m/s) 0
X-Component of Wall Translation 1
Y-Component of Wall Translation 0
Define wall velocity components? no
X-Component of Wall Translation (m/s) 0
Y-Component of Wall Translation (m/s) 0
External Emissivity 1
External Radiation Temperature (k) 300
Activate Reaction Mechanisms yes
(0 0 0 0)
(((constant . 0) (profile )) ((constant . 0) (profile )) ((constant . 0) (profile )) ((constant . 0) (profile )))
Rotation Speed (rad/s) 0
X-Position of Rotation-Axis Origin (m) 0
Y-Position of Rotation-Axis Origin (m) 0
X-component of shear stress (pascal) 0
Y-component of shear stress (pascal) 0
Surface tension gradient (n/m-k) 0
Reaction Mechanisms 0
Specularity Coefficient 0

solidfluidwalls:048

Condition Value
---

--
Wall Thickness (m) 0
Heat Generation Rate (w/m3) 0
Material Name graphite-south-africa
Thermal BC Type 3
Temperature (k) 300
Heat Flux (w/m2) 0
Convective Heat Transfer Coefficient (w/m2-k) 0
Free Stream Temperature (k) 300
Wall Motion 0
Shear Boundary Condition 0
Define wall motion relative to adjacent cell zone? yes
Apply a rotational velocity to this wall? no
Velocity Magnitude (m/s) 0

X-Component of Wall Translation 1
Y-Component of Wall Translation 0
Define wall velocity components? no
X-Component of Wall Translation (m/s) 0
Y-Component of Wall Translation (m/s) 0
External Emissivity 1
External Radiation Temperature (k) 300
Activate Reaction Mechanisms yes
(0 0 0 0)
(((constant . 0) (profile )) ((constant . 0) (profile )) ((constant . 0) (profile )) ((constant . 0) (profile )))
Rotation Speed (rad/s) 0
X-Position of Rotation-Axis Origin (m) 0
Y-Position of Rotation-Axis Origin (m) 0
X-component of shear stress (pascal) 0
Y-component of shear stress (pascal) 0
Surface tension gradient (n/m-k) 0
Reaction Mechanisms 0
Specularity Coefficient 0

outer_wall:049

Condition Value

--

Wall Thickness (m) 0.0099999998
Heat Generation Rate (w/m3) 0
Material Name steel
Thermal BC Type 5
Temperature (k) 300
Heat Flux (w/m2) 0
Convective Heat Transfer Coefficient (w/m2-k) 19
Free Stream Temperature (k) 923.15002
Wall Motion 0
Shear Boundary Condition 0
Define wall motion relative to adjacent cell zone? yes
Apply a rotational velocity to this wall? no
Velocity Magnitude (m/s) 0
X-Component of Wall Translation 1
Y-Component of Wall Translation 0
Define wall velocity components? no
X-Component of Wall Translation (m/s) 0
Y-Component of Wall Translation (m/s) 0
External Emissivity 1
External Radiation Temperature (k) 923.15002
Activate Reaction Mechanisms no
(0 0 0 0)
(((constant . 0) (profile )) ((constant . 0) (profile )) ((constant . 0) (profile )) ((constant . 0) (profile )))
Rotation Speed (rad/s) 0
X-Position of Rotation-Axis Origin (m) 0
Y-Position of Rotation-Axis Origin (m) 0
X-component of shear stress (pascal) 0
Y-component of shear stress (pascal) 0
Surface tension gradient (n/m-k) 0
Reaction Mechanisms 0
Specularity Coefficient 0

outer_wall:050

Condition Value

Wall Thickness (m) 0.0099999998
Heat Generation Rate (w/m3) 0
Material Name steel
Thermal BC Type 5
Temperature (k) 300
Heat Flux (w/m2) 0
Convective Heat Transfer Coefficient (w/m2-k) 19

| | |
|---|---|
| Free Stream Temperature (k) | 923.15002 |
| Wall Motion | 0 |
| Shear Boundary Condition | 0 |
| Define wall motion relative to adjacent cell zone? | yes |
| Apply a rotational velocity to this wall? | no |
| Velocity Magnitude (m/s) | 0 |
| X-Component of Wall Translation | 1 |
| Y-Component of Wall Translation | 0 |
| Define wall velocity components? | no |
| X-Component of Wall Translation (m/s) | 0 |
| Y-Component of Wall Translation (m/s) | 0 |
| External Emissivity | 1 |
| External Radiation Temperature (k) | 923.15002 |
| Activate Reaction Mechanisms | no |
| Rotation Speed (rad/s) | 0 |
| X-Position of Rotation-Axis Origin (m) | 0 |
| Y-Position of Rotation-Axis Origin (m) | 0 |
| X-component of shear stress (pascal) | 0 |
| Y-component of shear stress (pascal) | 0 |
| Surface tension gradient (n/m-k) | 0 |
| Reaction Mechanisms | 0 |
| Specularity Coefficient | 0 |

outer_wall:051

| Condition | Value |
|---|---|
| Wall Thickness (m) | 0.0099999998 |
| Heat Generation Rate (w/m3) | 0 |
| Material Name | steel |
| Thermal BC Type | 5 |
| Temperature (k) | 300 |
| Heat Flux (w/m2) | 0 |
| Convective Heat Transfer Coefficient (w/m2-k) | 19 |
| Free Stream Temperature (k) | 923.15002 |
| Wall Motion | 0 |
| Shear Boundary Condition | 0 |
| Define wall motion relative to adjacent cell zone? | yes |
| Apply a rotational velocity to this wall? | no |
| Velocity Magnitude (m/s) | 0 |
| X-Component of Wall Translation | 1 |
| Y-Component of Wall Translation | 0 |
| Define wall velocity components? | no |
| X-Component of Wall Translation (m/s) | 0 |
| Y-Component of Wall Translation (m/s) | 0 |
| External Emissivity | 1 |
| External Radiation Temperature (k) | 923.15002 |
| Activate Reaction Mechanisms | no |
| | (0 0 0 0) |
| | (((constant . 0) (profile )) ((constant . 0) (profile )) ((constant . 0) (profile )) ((constant . 0) (profile ))) |
| Rotation Speed (rad/s) | 0 |
| X-Position of Rotation-Axis Origin (m) | 0 |
| Y-Position of Rotation-Axis Origin (m) | 0 |
| X-component of shear stress (pascal) | 0 |
| Y-component of shear stress (pascal) | 0 |
| Surface tension gradient (n/m-k) | 0 |
| Reaction Mechanisms | 0 |
| Specularity Coefficient | 0 |

outer_wall:052

| Condition | Value |
|---|---|
| Wall Thickness (m) | 0.0099999998 |
| Heat Generation Rate (w/m3) | 0 |
| Material Name | steel |

Thermal BC Type 5
Temperature (k) 300
Heat Flux (w/m2) 0
Convective Heat Transfer Coefficient (w/m2-k) 19
Free Stream Temperature (k) 923.15002
Wall Motion 0
Shear Boundary Condition 0
Define wall motion relative to adjacent cell zone? yes
Apply a rotational velocity to this wall? no
Velocity Magnitude (m/s) 0
X-Component of Wall Translation 1
Y-Component of Wall Translation 0
Define wall velocity components? no
X-Component of Wall Translation (m/s) 0
Y-Component of Wall Translation (m/s) 0
External Emissivity 1
External Radiation Temperature (k) 923.15002
Activate Reaction Mechanisms no
Rotation Speed (rad/s) 0
X-Position of Rotation-Axis Origin (m) 0
Y-Position of Rotation-Axis Origin (m) 0
X-component of shear stress (pascal) 0
Y-component of shear stress (pascal) 0
Surface tension gradient (n/m-k) 0
Reaction Mechanisms 0
Specularity Coefficient 0

outer_wall:053

Condition Value

---

--

Wall Thickness (m) 0.0099999998
Heat Generation Rate (w/m3) 0
Material Name steel
Thermal BC Type 5
Temperature (k) 300
Heat Flux (w/m2) 0
Convective Heat Transfer Coefficient (w/m2-k) 19
Free Stream Temperature (k) 923.15002
Wall Motion 0
Shear Boundary Condition 0
Define wall motion relative to adjacent cell zone? yes
Apply a rotational velocity to this wall? no
Velocity Magnitude (m/s) 0
X-Component of Wall Translation 1
Y-Component of Wall Translation 0
Define wall velocity components? no
X-Component of Wall Translation (m/s) 0
Y-Component of Wall Translation (m/s) 0
External Emissivity 1
External Radiation Temperature (k) 923.15002
Activate Reaction Mechanisms no
(0 0 0 0)
(((constant . 0) (profile )) ((constant . 0) (profile )) ((constant . 0) (profile )) ((constant . 0) (profile )))
Rotation Speed (rad/s) 0
X-Position of Rotation-Axis Origin (m) 0
Y-Position of Rotation-Axis Origin (m) 0
X-component of shear stress (pascal) 0
Y-component of shear stress (pascal) 0
Surface tension gradient (n/m-k) 0
Reaction Mechanisms 0
Specularity Coefficient 0

outer_wall:054

Condition Value

```
---------------------------------------------------------------------
Wall Thickness (m)                              0.0099999998
Heat Generation Rate (w/m3)                     0
Material Name                                   steel
Thermal BC Type                                 5
Temperature (k)                                 300
Heat Flux (w/m2)                                0
Convective Heat Transfer Coefficient (w/m2-k)   19
Free Stream Temperature (k)                     923.15002
Wall Motion                                     0
Shear Boundary Condition                        0
Define wall motion relative to adjacent cell zone?  yes
Apply a rotational velocity to this wall?       no
Velocity Magnitude (m/s)                        0
X-Component of Wall Translation                 1
Y-Component of Wall Translation                 0
Define wall velocity components?                no
X-Component of Wall Translation (m/s)           0
Y-Component of Wall Translation (m/s)           0
External Emissivity                             1
External Radiation Temperature (k)              923.15002
Activate Reaction Mechanisms                    no
Rotation Speed (rad/s)                          0
X-Position of Rotation-Axis Origin (m)          0
Y-Position of Rotation-Axis Origin (m)          0
X-component of shear stress (pascal)            0
Y-component of shear stress (pascal)            0
Surface tension gradient (n/m-k)                0
Reaction Mechanisms                             0
Specularity Coefficient                         0

outer_wall:055

Condition                                       Value
---------------------------------------------------------------------------------------------------------------------------------------------------------------
--
Wall Thickness (m)                              0.0099999998
Heat Generation Rate (w/m3)                     0
Material Name                                   steel
Thermal BC Type                                 5
Temperature (k)                                 300
Heat Flux (w/m2)                                0
Convective Heat Transfer Coefficient (w/m2-k)   19
Free Stream Temperature (k)                     923.15002
Wall Motion                                     0
Shear Boundary Condition                        0
Define wall motion relative to adjacent cell zone?  yes
Apply a rotational velocity to this wall?       no
Velocity Magnitude (m/s)                        0
X-Component of Wall Translation                 1
Y-Component of Wall Translation                 0
Define wall velocity components?                no
X-Component of Wall Translation (m/s)           0
Y-Component of Wall Translation (m/s)           0
External Emissivity                             1
External Radiation Temperature (k)              923.15002
Activate Reaction Mechanisms                    no
                                                (0 0 0 0)
                                                (((constant . 0) (profile )) ((constant . 0) (profile )) ((constant . 0) (profile )) ((constant . 0) (profile )))
Rotation Speed (rad/s)                          0
X-Position of Rotation-Axis Origin (m)          0
Y-Position of Rotation-Axis Origin (m)          0
X-component of shear stress (pascal)            0
Y-component of shear stress (pascal)            0
Surface tension gradient (n/m-k)                0
Reaction Mechanisms                             0
Specularity Coefficient                         0
```

outer_wall:056

| Condition | Value |
|---|---|
| Wall Thickness (m) | 0.0099999998 |
| Heat Generation Rate (w/m3) | 0 |
| Material Name | steel |
| Thermal BC Type | 5 |
| Temperature (k) | 300 |
| Heat Flux (w/m2) | 0 |
| Convective Heat Transfer Coefficient (w/m2-k) | 19 |
| Free Stream Temperature (k) | 923.15002 |
| Wall Motion | 0 |
| Shear Boundary Condition | 0 |
| Define wall motion relative to adjacent cell zone? | yes |
| Apply a rotational velocity to this wall? | no |
| Velocity Magnitude (m/s) | 0 |
| X-Component of Wall Translation | 1 |
| Y-Component of Wall Translation | 0 |
| Define wall velocity components? | no |
| X-Component of Wall Translation (m/s) | 0 |
| Y-Component of Wall Translation (m/s) | 0 |
| External Emissivity | 1 |
| External Radiation Temperature (k) | 923.15002 |
| Activate Reaction Mechanisms | no |
| | (0 0 0 0) |
| | (((constant . 0) (profile )) ((constant . 0) (profile )) ((constant . 0) (profile )) ((constant . 0) (profile ))) |
| Rotation Speed (rad/s) | 0 |
| X-Position of Rotation-Axis Origin (m) | 0 |
| Y-Position of Rotation-Axis Origin (m) | 0 |
| X-component of shear stress (pascal) | 0 |
| Y-component of shear stress (pascal) | 0 |
| Surface tension gradient (n/m-k) | 0 |
| Reaction Mechanisms | 0 |
| Specularity Coefficient | 0 |

outer_wall:057

| Condition | Value |
|---|---|
| Wall Thickness (m) | 0.0099999998 |
| Heat Generation Rate (w/m3) | 0 |
| Material Name | steel |
| Thermal BC Type | 5 |
| Temperature (k) | 300 |
| Heat Flux (w/m2) | 0 |
| Convective Heat Transfer Coefficient (w/m2-k) | 19 |
| Free Stream Temperature (k) | 923.15002 |
| Wall Motion | 0 |
| Shear Boundary Condition | 0 |
| Define wall motion relative to adjacent cell zone? | yes |
| Apply a rotational velocity to this wall? | no |
| Velocity Magnitude (m/s) | 0 |
| X-Component of Wall Translation | 1 |
| Y-Component of Wall Translation | 0 |
| Define wall velocity components? | no |
| X-Component of Wall Translation (m/s) | 0 |
| Y-Component of Wall Translation (m/s) | 0 |
| External Emissivity | 1 |
| External Radiation Temperature (k) | 923.15002 |
| Activate Reaction Mechanisms | no |
| | (0 0 0 0) |
| | (((constant . 0) (profile )) ((constant . 0) (profile )) ((constant . 0) (profile )) ((constant . 0) (profile ))) |
| Rotation Speed (rad/s) | 0 |

X-Position of Rotation-Axis Origin (m) 0
Y-Position of Rotation-Axis Origin (m) 0
X-component of shear stress (pascal) 0
Y-component of shear stress (pascal) 0
Surface tension gradient (n/m-k) 0
Reaction Mechanisms 0
Specularity Coefficient 0

outer_wall:058

Condition Value
---
--
Wall Thickness (m) 0.0099999998
Heat Generation Rate (w/m3) 0
Material Name steel
Thermal BC Type 5
Temperature (k) 300
Heat Flux (w/m2) 0
Convective Heat Transfer Coefficient (w/m2-k) 19
Free Stream Temperature (k) 923.15002
Wall Motion 0
Shear Boundary Condition 0
Define wall motion relative to adjacent cell zone? yes
Apply a rotational velocity to this wall? no
Velocity Magnitude (m/s) 0
X-Component of Wall Translation 1
Y-Component of Wall Translation 0
Define wall velocity components? no
X-Component of Wall Translation (m/s) 0
Y-Component of Wall Translation (m/s) 0
External Emissivity 1
External Radiation Temperature (k) 923.15002
Activate Reaction Mechanisms no
(0 0 0 0)
(((constant . 0) (profile )) ((constant . 0) (profile )) ((constant . 0) (profile )) ((constant . 0) (profile )))
Rotation Speed (rad/s) 0
X-Position of Rotation-Axis Origin (m) 0
Y-Position of Rotation-Axis Origin (m) 0
X-component of shear stress (pascal) 0
Y-component of shear stress (pascal) 0
Surface tension gradient (n/m-k) 0
Reaction Mechanisms 0
Specularity Coefficient 0

default-interior:059

Condition Value
---

default-interior:060

Condition Value
---

default-interior:061

Condition Value
---

default-interior:062

Condition Value
---

default-interior:063

Condition Value
---

default-interior:064

Condition Value
---

default-interior:065

Condition Value
---

default-interior:066

Condition Value
---

default-interior:067

Condition Value
---

default-interior:068

Condition Value
---

default-interior:069

Condition Value
---

default-interior:070

Condition Value
---

default-interior:071

Condition Value
---

default-interior:072

Condition Value
---

default-interior:073

Condition Value
---

default-interior:074

Condition Value
---

default-interior:075

Condition Value
---

default-interior:076

Condition Value
---

default-interior:077

| Condition | Value |
|---|---|

default-interior:078

| Condition | Value |
|---|---|

default-interior:079

| Condition | Value |
|---|---|

default-interior:080

| Condition | Value |
|---|---|

default-interior:081

| Condition | Value |
|---|---|

Solver Controls

Equations

| Equation | Solved |
|---|---|
| Flow | yes |
| co | yes |
| co2 | yes |
| o2 | yes |
| h2o | yes |
| Energy | yes |

Numerics

| Numeric | Enabled |
|---|---|
| Absolute Velocity Formulation | yes |

Relaxation

| Variable | Relaxation Factor |
|---|---|
| Pressure | 0.30000001 |
| Density | 1 |
| Body Forces | 1 |
| Momentum | 0.69999999 |
| co | 0.0099999998 |
| co2 | 0.0099999998 |
| o2 | 0.1 |
| h2o | 0.0099999998 |
| Energy | 0.0099999998 |

Linear Solver

| Variable | Solver Type | Termination Criterion | Residual Reduction Tolerance |
|---|---|---|---|
| Pressure | V-Cycle | 0.1 | |
| X-Momentum | Flexible | 0.1 | 0.7 |

| | | | |
|---|---|---|---|
| Y-Momentum | Flexible | 0.1 | 0.7 |
| co | Flexible | 0.1 | 0.7 |
| co2 | Flexible | 0.1 | 0.7 |
| o2 | Flexible | 0.1 | 0.7 |
| h2o | Flexible | 0.1 | 0.7 |
| Energy | Flexible | 0.1 | 0.7 |

Pressure-Velocity Coupling

| Parameter | Value |
|---|---|
| Type | SIMPLE |

Discretization Scheme

| Variable | Scheme |
|---|---|
| Pressure | PRESTO! |
| Momentum | Second Order Upwind |
| co | Second Order Upwind |
| co2 | Second Order Upwind |
| o2 | Second Order Upwind |
| h2o | Second Order Upwind |
| Energy | Second Order Upwind |

Solution Limits

| Quantity | Limit |
|---|---|
| Minimum Absolute Pressure | 1 |
| Maximum Absolute Pressure | 4.9999999e+10 |
| Minimum Temperature | 300 |
| Maximum Temperature | 3000 |

Material Properties

Material: graphite-south-africa (solid)

| Property | Units | Method | Value(s) |
|---|---|---|---|
| Density | kg/m3 | constant | 2240 |
| Cp (Specific Heat) | j/kg-k | constant | 710 |
| Thermal Conductivity | w/m-k | constant | 168 |

Material: nitrogen (fluid)

| Property | Units | Method | Value(s) |
|---|---|---|---|
| Density | kg/m3 | constant | 1.138 |
| Cp (Specific Heat) | j/kg-k | constant | 1040.67 |
| Thermal Conductivity | w/m-k | constant | 0.0242 |
| Viscosity | kg/m-s | constant | 1.663e-05 |
| Molecular Weight | kg/kgmol | constant | 28.0134 |
| Standard State Enthalpy | j/kgmol | constant | 0 |
| Standard State Entropy | j/kgmol-k | constant | 191494.78 |
| Reference Temperature | k | constant | 298.15 |
| L-J Characteristic Length | angstrom | constant | 3.621 |
| L-J Energy Parameter | k | constant | 97.53 |
| Thermal Expansion Coefficient | 1/k | constant | 0 |
| Degrees of Freedom | | constant | 0 |
| Speed of Sound | m/s | none | #f |

Material: carbon-dioxide (fluid)

| Property | Units | Method | Value(s) |
|---|---|---|---|

| | | | |
|---|---|---|---|
| Density | kg/m3 | constant | 1.7878 |
| Cp (Specific Heat) | j/kg-k | constant | 840.37 |
| Thermal Conductivity | w/m-k | constant | 0.0145 |
| Viscosity | kg/m-s | constant | 1.37e-05 |
| Molecular Weight | kg/kgmol | constant | 44.00995 |
| Standard State Enthalpy | j/kgmol | constant | -3.9353235e+08 |
| Standard State Entropy | j/kgmol-k | constant | 213720.2 |
| Reference Temperature | k | constant | 298.15 |
| L-J Characteristic Length | angstrom | constant | 3.941 |
| L-J Energy Parameter | k | constant | 195.2 |
| Thermal Expansion Coefficient | 1/k | constant | 0 |
| Degrees of Freedom | | constant | 0 |
| Speed of Sound | m/s | none | #f |

Material: carbon-monoxide (fluid)

| Property | Units | Method | Value(s) |
|---|---|---|---|
| Density | kg/m3 | constant | 1.1233 |
| Cp (Specific Heat) | j/kg-k | constant | 1043 |
| Thermal Conductivity | w/m-k | constant | 0.025 |
| Viscosity | kg/m-s | constant | 1.75e-05 |
| Molecular Weight | kg/kgmol | constant | 28.01055 |
| Standard State Enthalpy | j/kgmol | constant | -1.1053956e+08 |
| Standard State Entropy | j/kgmol-k | constant | 197531.64 |
| Reference Temperature | k | constant | 298.15 |
| L-J Characteristic Length | angstrom | constant | 0 |
| L-J Energy Parameter | k | constant | 0 |
| Thermal Expansion Coefficient | 1/k | constant | 0 |
| Degrees of Freedom | | constant | 0 |
| Speed of Sound | m/s | none | #f |

Material: water-vapor (fluid)

| Property | Units | Method | Value(s) |
|---|---|---|---|
| Density | kg/m3 | constant | 0.55419999 |
| Cp (Specific Heat) | j/kg-k | constant | 2014 |
| Thermal Conductivity | w/m-k | constant | 0.0261 |
| Viscosity | kg/m-s | constant | 1.34e-05 |
| Molecular Weight | kg/kgmol | constant | 18.01534 |
| Standard State Enthalpy | j/kgmol | constant | -2.418379e+08 |
| Standard State Entropy | j/kgmol-k | constant | 188696.44 |
| Reference Temperature | k | constant | 298.15 |
| L-J Characteristic Length | angstrom | constant | 2.605 |
| L-J Energy Parameter | k | constant | 572.4 |
| Thermal Expansion Coefficient | 1/k | constant | 0 |
| Degrees of Freedom | | constant | 0 |
| Speed of Sound | m/s | none | #f |

Material: steel (solid)

| Property | Units | Method | Value(s) |
|---|---|---|---|
| Density | kg/m3 | constant | 8030 |
| Cp (Specific Heat) | j/kg-k | constant | 502.48001 |
| Thermal Conductivity | w/m-k | constant | 16.27 |

Material: carbon-solid (fluid)

| Property | Units | Method | Value(s) |
|---|---|---|---|
| Density | kg/m3 | constant | 2000 |
| Cp (Specific Heat) | j/kg-k | constant | 1220 |
| Thermal Conductivity | w/m-k | constant | 0.045400001 |
| Viscosity | kg/m-s | constant | 1.72e-05 |
| Molecular Weight | kg/kgmol | constant | 12.01115 |

| | | | |
|---|---|---|---|
| Standard State Enthalpy | j/kgmol | constant | -101.268 |
| Standard State Entropy | j/kgmol-k | constant | 5731.747 |
| Reference Temperature | k | constant | 298 |
| L-J Characteristic Length | angstrom | constant | 0 |
| L-J Energy Parameter | k | constant | 0 |
| Thermal Expansion Coefficient | 1/k | constant | 0 |
| Degrees of Freedom | | constant | 0 |
| Speed of Sound | m/s | none | #f |

Material: (water-vapor . mixture-template) (fluid)

| Property | Units | Method | Value(s) |
|---|---|---|---|
| Cp (Specific Heat) | j/kg-k | constant | 2014 |
| Thermal Conductivity | w/m-k | constant | 0.0261 |
| Viscosity | kg/m-s | constant | 1.34e-05 |
| Molecular Weight | kg/kgmol | constant | 18.01534 |
| Standard State Enthalpy | j/kgmol | constant | -2.418379e+08 |
| Standard State Entropy | j/kgmol-k | constant | 188696.44 |
| Reference Temperature | k | constant | 298.15 |
| L-J Characteristic Length | angstrom | constant | 2.605 |
| L-J Energy Parameter | k | constant | 572.4 |
| Degrees of Freedom | | constant | 0 |
| Speed of Sound | m/s | none | #f |

Material: oxygen (fluid)

| Property | Units | Method | Value(s) |
|---|---|---|---|
| Density | kg/m3 | constant | 1.2999 |
| Cp (Specific Heat) | j/kg-k | constant | 919.31 |
| Thermal Conductivity | w/m-k | constant | 0.0246 |
| Viscosity | kg/m-s | constant | 1.919e-05 |
| Molecular Weight | kg/kgmol | constant | 31.9988 |
| Standard State Enthalpy | j/kgmol | constant | 0 |
| Standard State Entropy | j/kgmol-k | constant | 205026.86 |
| Reference Temperature | k | constant | 298.15 |
| L-J Characteristic Length | angstrom | constant | 3.458 |
| L-J Energy Parameter | k | constant | 107.4 |
| Thermal Expansion Coefficient | 1/k | constant | 0 |
| Degrees of Freedom | | constant | 0 |
| Speed of Sound | m/s | none | #f |

Material: (oxygen . mixture-template) (fluid)

| Property | Units | Method | Value(s) |
|---|---|---|---|
| Cp (Specific Heat) | j/kg-k | constant | 919.31 |
| Thermal Conductivity | w/m-k | constant | 0.0246 |
| Viscosity | kg/m-s | constant | 1.919e-05 |
| Molecular Weight | kg/kgmol | constant | 31.9988 |
| Standard State Enthalpy | j/kgmol | constant | 0 |
| Standard State Entropy | j/kgmol-k | constant | 205026.86 |
| Reference Temperature | k | constant | 298.15 |
| L-J Characteristic Length | angstrom | constant | 3.458 |
| L-J Energy Parameter | k | constant | 107.4 |
| Degrees of Freedom | | constant | 0 |
| Speed of Sound | m/s | none | #f |

Material: (water-vapor . mixture-template) (fluid)

| Property | Units | Method | Value(s) |
|---|---|---|---|
| Cp (Specific Heat) | j/kg-k | constant | 2014 |
| Thermal Conductivity | w/m-k | constant | 0.0261 |
| Viscosity | kg/m-s | constant | 1.34e-05 |
| Molecular Weight | kg/kgmol | constant | 18.01534 |

| | | | |
|---|---|---|---|
| Standard State Enthalpy | j/kgmol | constant | -2.418379e+08 |
| Standard State Entropy | j/kgmol-k | constant | 188696.44 |
| Reference Temperature | k | constant | 298.15 |
| L-J Characteristic Length | angstrom | constant | 2.605 |
| L-J Energy Parameter | k | constant | 572.4 |
| Degrees of Freedom | | constant | 0 |
| Speed of Sound | m/s | none | #f |

Material: (oxygen . mixture-template) (fluid)

| Property | Units | Method | Value(s) |
|---|---|---|---|
| Cp (Specific Heat) | j/kg-k | constant | 919.31 |
| Thermal Conductivity | w/m-k | constant | 0.0246 |
| Viscosity | kg/m-s | constant | 1.919e-05 |
| Molecular Weight | kg/kgmol | constant | 31.9988 |
| Standard State Enthalpy | j/kgmol | constant | 0 |
| Standard State Entropy | j/kgmol-k | constant | 205026.86 |
| Reference Temperature | k | constant | 298.15 |
| L-J Characteristic Length | angstrom | constant | 3.458 |
| L-J Energy Parameter | k | constant | 107.4 |
| Degrees of Freedom | | constant | 0 |
| Speed of Sound | m/s | none | #f |

Material: mixture-template (mixture)

| Property | Units | Method | Value(s) |
|---|---|---|---|
| Mixture Species | | names | ((co co2 o2 h2o c<s>) () ()) |
| Reaction | | finite-rate | ((O2 w C to CO ((o2 0.5 0.5 1) (c<s> 1 1 1)) ((co 1 0.5 1)) ((co2 0 1) (h2o 0 1)) (stoichiometry 0.5o2 + 1c<s> --> 1co) (arrhenius 4e+12 2e+08 0) (mixing-rate 4 0.5) (use-third-body-efficiencies? . #f) (surface-reaction? . #t)) (CO w O2 ((co 1 1 1) (o2 0.5 1 1)) ((co2 1 0 1)) ((h2o 0 1) (c<s> 1 1)) (stoichiometry 1co + 0.5o2 --> 1co2) (arrhenius 2.24e+12 1.674e+08 0) (mixing-rate 4 0.5) (use-third-body-efficiencies? . #f)) (CO2 to CO and O2 ((co2 1 1 1)) ((co 1 0 1) (o2 0.5 0 1)) ((h2o 0 1) (c<s> 1 1)) (stoichiometry 1co2 --> 1co + 0.5o2) (arrhenius 45000000 1.674e+08 0) (mixing-rate 4 0.5) (use-third-body-efficiencies? . #f)) (o2 w C to CO2 ((o2 1 0.5 1) (c<s> 1 1 1)) ((co2 1 0.5 1)) ((co 0 1) (h2o 0 1)) (stoichiometry 1o2 + 1c<s> --> 1co2) (arrhenius 9.9999998e+10 2e+08 0) (mixing-rate 4 0.5) (use-third-body-efficiencies? . #f) (surface-reaction? . #t))) |
| Mechanism | | reaction-mechs | ((mechanism-1 (reaction-type . all) (reaction-list O2 w C to CO CO w O2 CO2 to CO and O2 o2 w C to CO2) (site-info))) |
| Density | kg/m3 | incompressible-ideal-gas | #f |
| Cp (Specific Heat) | j/kg-k | mixing-law | #f |
| Thermal Conductivity | w/m-k | mass-weighted-mixing-law | #f |
| Viscosity | kg/m-s | ideal-gas-mixing-law | #f |
| Mass Diffusivity | m2/s | constant-dilute-appx | (2.8799999e-05) |
| Thermal Diffusion Coefficient | kg/m-s | kinetic-theory | #f |
| Thermal Expansion Coefficient | 1/k | constant | 0 |
| Speed of Sound | m/s | none | #f |

Material: (carbon-monoxide . mixture-template) (fluid)

| Property | Units | Method | Value(s) |
|---|---|---|---|
| Cp (Specific Heat) | j/kg-k | constant | 1043 |
| Thermal Conductivity | w/m-k | constant | 0.025 |
| Viscosity | kg/m-s | constant | 1.75e-05 |
| Molecular Weight | kg/kgmol | constant | 28.01055 |
| Standard State Enthalpy | j/kgmol | constant | -1.1053956e+08 |
| Standard State Entropy | j/kgmol-k | constant | 197531.64 |
| Reference Temperature | k | constant | 298.15 |
| L-J Characteristic Length | angstrom | constant | 0 |
| L-J Energy Parameter | k | constant | 0 |
| Degrees of Freedom | | constant | 0 |
| Speed of Sound | m/s | none | #f |

Material: (carbon-dioxide . mixture-template) (fluid)

| Property | Units | Method | Value(s) |
|---|---|---|---|
| Cp (Specific Heat) | j/kg-k | constant | 840.37 |
| Thermal Conductivity | w/m-k | constant | 0.0145 |
| Viscosity | kg/m-s | constant | 1.37e-05 |
| Molecular Weight | kg/kgmol | constant | 44.00995 |
| Standard State Enthalpy | j/kgmol | constant | -3.9353235e+08 |
| Standard State Entropy | j/kgmol-k | constant | 213720.2 |
| Reference Temperature | k | constant | 298.15 |
| L-J Characteristic Length | angstrom | constant | 3.941 |
| L-J Energy Parameter | k | constant | 195.2 |
| Degrees of Freedom | | constant | 0 |
| Speed of Sound | m/s | none | #f |

Material: (carbon-solid . mixture-template) (fluid)

| Property | Units | Method | Value(s) |
|---|---|---|---|
| Cp (Specific Heat) | j/kg-k | constant | 1220 |
| Thermal Conductivity | w/m-k | constant | 0.045400001 |
| Viscosity | kg/m-s | constant | 1.72e-05 |
| Molecular Weight | kg/kgmol | constant | 12.01115 |
| Standard State Enthalpy | j/kgmol | constant | -101.268 |
| Standard State Entropy | j/kgmol-k | constant | 5731.747 |
| Reference Temperature | k | constant | 298 |
| L-J Characteristic Length | angstrom | constant | 0 |
| L-J Energy Parameter | k | constant | 0 |
| Degrees of Freedom | | constant | 0 |
| Speed of Sound | m/s | none | #f |

Material: aluminum (solid)

| Property | Units | Method | Value(s) |
|---|---|---|---|
| Density | kg/m3 | constant | 2719 |
| Cp (Specific Heat) | j/kg-k | constant | 871 |
| Thermal Conductivity | w/m-k | constant | 202.4 |

Material: air (fluid)

| Property | Units | Method | Value(s) |
|---|---|---|---|
| Density | kg/m3 | constant | 1.225 |
| Cp (Specific Heat) | j/kg-k | constant | 1006.43 |
| Thermal Conductivity | w/m-k | constant | 0.0242 |
| Viscosity | kg/m-s | constant | 1.7894e-05 |
| Molecular Weight | kg/kgmol | constant | 28.966 |
| Standard State Enthalpy | j/kgmol | constant | 0 |
| Standard State Entropy | j/kgmol-k | constant | 0 |
| Reference Temperature | k | constant | 298.15 |
| L-J Characteristic Length | angstrom | constant | 3.711 |
| L-J Energy Parameter | k | constant | 78.6 |
| Thermal Expansion Coefficient | 1/k | constant | 0 |
| Degrees of Freedom | | constant | 0 |
| Speed of Sound | m/s | none | #f |